BOSTON UNIVERSITY

GRADUATE SCHOOL OF ARTS AND SCIENCES

Dissertation

DEVELOPMENT OF A PRACTICAL AND MOBILE BRAIN-COMPUTER COMMUNICATION DEVICE FOR PROFOUNDLY PARALYZED INDIVIDUALS

by

SEAN LORENZ

B.A., Oral Roberts University, 1998
M.T.S., Boston University, 2007

Submitted in partial fulfillment of the

requirements for the degree of

Doctor of Philosophy

2013

© Copyright by
SEAN LORENZ
2012

Approved by

First Reader ______________________________

Frank H. Guenther, PhD
Professor of Speech, Language, and Hearing Sciences
Boston University

Second Reader ______________________________

Jonathan S. Brumberg, PhD
Assistant Professor of Speech-Language-Hearing
University of Kansas

Third Reader ______________________________

Rupal Patel, PhD
Associate Professor of Speech-Language
Pathology and Audiology / Computer and
Information Science
Northeastern University

ACKNOWLEDGEMENTS

The work described in this dissertation would not have been possible without the guidance of my readers: Frank Guenther, Jon Brumberg and Rupal Patel. I want to thank Frank for his vision, Jon for his coding and BCI guidance, and Rupal for her inspiring ideas in context-aware AACs. A number of individuals in the CNS department have also been a great help and support over the past five years. Thank you to the members of the Speech Lab, Tech Lab, and Neuroprosthesis Lab for the great discussions. I'd especially like to thank Byron Galbraith for his code that proved to be an invaluable asset.

I am also humbled and encouraged by the five severely motor-impaired participants and their families from Boston and Duluth, Georgia that were willing to spend time wearing an EEG cap while a light flickered at them for hours.

I'd also like to thank Max Versace and Heather Ames for their continual grad program advice and support. Also, thank you for taking a chance on my ideas and letting me be part of a soon-to-be prosperous and budding company.

Finally, thank you to my best friend and wife, Kelly, for your never-ending love, support, inspiration, and confidence in my capabilities. One marriage, two kids, four homes, and five years later you deserve an end to this degree more than anyone.

The work described in the following dissertation was partly funded by CELEST, an NSF Science of Learning Center.

DEVELOPMENT OF A PRACTICAL AND MOBILE BRAIN-COMPUTER COMMUNICATION DEVICE FOR PROFOUNDLY PARALYZED INDIVIDUALS

(Order No.)

SEAN LORENZ

Boston University Graduate School of Arts and Sciences, 2013

Major Professor: Frank H. Guenther, Professor of Speech, Language,
and Hearing Sciences

ABSTRACT

Brain-computer interface (BCI) technology has seen tremendous growth over the past several decades, with numerous groundbreaking research studies demonstrating technical viability (Sellers et al., 2010; Silvoni et al., 2011). Despite this progress, BCIs have remained primarily in controlled laboratory settings. This dissertation proffers a blueprint for translating research-grade BCI systems into real-world applications that are noninvasive and fully portable, and that employ intelligent user interfaces for communication. The proposed architecture is designed to be used by severely motor-impaired individuals, such as those with locked-in syndrome, while reducing the effort and cognitive load needed to communicate. Such a system requires the merging of two primary research fields: 1) electroencephalography (EEG)-based BCIs and 2) intelligent user interface design.

The EEG-based BCI portion of this dissertation provides a history of the field, details of our software and hardware implementation, and results from an experimental study aimed at verifying the utility of a BCI based on the steady-state visual evoked potential (SSVEP), a robust brain response to visual stimulation at controlled frequencies. The visual stimulation, feature extraction, and classification algorithms for the BCI were specially designed to achieve successful real-time performance on a laptop computer. Also, the BCI was developed in Python, an open-source programming language that combines programming ease with effective handling of hardware and software requirements. The result of this work was *The Unlock Project* app software for BCI development. Using it, a four-choice SSVEP BCI setup was implemented and tested with five severely motor-impaired and fourteen control participants. The system showed a wide range of usability across participants, with classification rates ranging from 25-95%.

The second portion of the dissertation discusses the viability of intelligent user interface design as a method for obtaining a more user-focused vocal output communication aid tailored to motor-impaired individuals. A proposed blueprint of this communication "app" was developed in this dissertation. It would make use of readily available laptop sensors to perform facial recognition, speech-to-text decoding, and geo-location. The ultimate goal is to couple sensor information with natural language processing to construct an intelligent user interface that shapes communication in a practical SSVEP-based BCI.

TABLE OF CONTENTS

LIST OF TABLES

LIST OF FIGURES

LIST OF ABBREVIATIONS

AAC	....	Augmentative and Alternative Communication
ALS	....	Amyotrophic Lateral Sclerosis
ANOVA	....	Analysis Of Variance
API	....	Application Programming Interface
BCI	....	Brain-Computer Interface
BMI	....	Brain-Machine Interface
BOLD	....	Blood-Oxygen-Level-Dependent
CCA	....	Canonical Correlation Analysis
CPU	....	Central Processing Unit
CRT	....	Cathode Ray Tube
CWT	....	Continuous Wavelet Transform
DWT	....	Discrete Fourier Transform
ECoG	....	Electrocorticography
EEG	....	Electroencephalography
EMG	....	Electromyography
EOG	....	Electrooculography
ERP	....	Event-Related Potential
FFT	....	Fast Fourier Transform
fMRI	....	Functional Magnetic Resonance Imaging
fNIRS	....	Functional Near-Infrared Spectroscopy
GPS	....	Global Positioning System

GUI	....	Graphical User Interface
HCI	....	Human-Computer Interaction
HSD	....	Harmonic Sum Decision
Hz	....	Hertz
IUI	....	Intelligent User Interface
LCD	....	Liquid Crystal Display
LDA	....	Linear Discriminant Analysis
LED	....	Light-Emitting Diode
LGN	....	Lateral Geniculate Nucleus
LIS	....	Locked-In Syndrome
MEG	....	Magnetoencephalography
MTM	....	Multi-taper Method
PSD	....	Power Spectral Density
PSP	....	Progressive Supranuclear Palsy
SLIC	....	Stimulus-Locked Inter-trace Correlation
SMR	....	Sensorimotor Rhythm
SNR	....	Signal-To-Noise Ratio
SSVEP	....	Steady-State Visual Evoked Potential
UDP	....	User Datagram Protocol
V1	....	Primary Visual Cortex
VOCA	....	Voice Output Communication Aid

1 Introduction

The primary goal of this dissertation is to develop a practical brain-computer interface (BCI) that can help restore communication to severely motor-impaired individuals. In the book and subsequent film, *The Diving Bell and the Butterfly*, journalist Jean-Dominique Bauby suffered a stroke while driving his car one day. After 20 days in a coma, he woke up and was unable to move his limbs or mouth – Jean-Dominique was “locked-in”. Despite being able to communicate with his mouth, Jean-Dominique was fully cognitively aware and able to answer yes/no questions using only eye blinks. In fact, it was this blinking form of communication that Jean-Dominique used to write his book, describing his struggles as someone with locked-in syndrome.

What if individuals like Mr. Bauby were able to communicate with friends, loved ones, and caregivers in a faster and more efficient manner? The technological advances in this dissertation were designed to address this difficult transition of moving BCI research from the lab to the home. The result of this dissertation research was a fully portable and noninvasive BCI based on user needs in practical use environments. In order to build such a BCI system, two primary research fields needed to be investigated and merged – electroencephalography (EEG)-based BCIs and context-aware computing.

1.1 EEG-based BCIs

The BCI realm can be broken down into two larger categories – invasive and noninvasive. Invasive BCIs have the advantage of penetrating the skull and either resting on the gray matter of the brain or within the cortex itself. This close proximity to neural activity gives a sharper, more accurate representation of cortical activity in various brain regions, yet has the disadvantage of requiring surgery. Noninvasive recording techniques such as EEG, on the other hand, can record neural electrical activity that escapes the skull by placing electrodes over the scalp. EEG equipment has gotten progressively cheaper and more portable over the past century, making EEG a perfect tool for testing BCIs.

Of the numerous BCI paradigms that currently exist, systems based on the steady-state visual evoked potential (SSVEP) have experienced significant advances leading to fast information transfer rates and high classification accuracies (Zhu et al. 2010; Müller-Putz et al. 2005; Wang, Wang, and Jung 2010; Bin et al. 2011). These BCIs are based on prior psychophysical and evoked potential studies of visual cortex in response to steady, driving visual stimuli (Guger, Edlinger, and Krausz 2011; Strasburger, Murray, and Remky 1993; Pollen 1999).

This SSVEP-based BCI research was used as the foundation for building the BCI system discussed in this dissertation. Rather than build new mathematical methods for SSVEP BCIs, the focus here was to create a BCI system that could be used in the home for everyday use by a severely motor-impaired individual. The

Unlock Project, an endeavor created at Boston University to give full BCI "app" systems to profoundly paralyzed users, was formed in order to create such a system. The result of this effort is a fully portable laptop BCI using a wireless EEG cap and a new Python application programming interface built specifically for quick and open-source BCI "app" development.

An experimental study was conducted after finalizing both hardware and software components of the non-invasive, mobile BCI system. The purpose of the study was two-fold, 1) to validate technical capabilities of the BCI system and 2) to assess user performance, both healthy and impaired. Since the target user for such a system would be a severely motor-impaired individual, the system experiment was tested on five paralyzed participants with fourteen control participants for comparison purposes. Control participants showed classification accuracies for the four-direction SSVEP BCI task in the range of 50-95%, whereas individuals with speech-motor impairments performed anywhere from 10-80% per run. Results from this experiment are discussed in greater detail in Section 4.2.

1.2 Context-aware computing

In order to create a BCI that could potentially be used in everyday life, SSVEP BCI systems need to move beyond bit-rates and take into account the user and his or her needs. For this reason, research from human-computer interaction, intelligent user interfacing, context-aware computing, and augmentative and alternative communication were used to shape the model design of a context-aware brain computer communication device called ContextSpeak (see Chapter 5).

Context-aware computing is a new field of study that takes sensor inputs from a device in order to adapt according to a current location, who's around you, who's talking to you, what you've done in the past using that device, and how you've used it in a particular context (Schilit, Adams, and Want 1994). The notion of situated cognition is something that our brain does subconsciously thousands of times a day, yet only recently have computational devices such as laptops or tablets been equipped with the processing power and/or sensors to consider multimodal fusion possibilities.

In this dissertation, current voice output communication aids (VOCAs) are discussed for populations that are unable to communicate normally; this includes individuals with locked-in syndrome, ALS, or other severe motor impairments. A theoretical intelligent user interface model and GUI for future development of a communication device was built based on VOCA principles. Building such a system will require the fusion of sensor data such as GPS location, time of day, built-in camera for facial recognition, and audio input for speech-to-text translation with natural language processing algorithm outputs in a novel way.

1.3 Organization of dissertation

The remainder of this dissertation is organized into four chapters. Chapter 2 gives a broad overview of the brain-computer interface field, covering both invasive and noninvasive recording methodologies. This chapter also goes into detail on the various EEG-based BCI paradigms that currently exist along with the hardware and software necessary to create such systems. Chapter 3 will discuss solely steady-state visual evoked potential (SSVEP) BCIs. This review includes a brief history of SSVEP BCIs, the neurobiology of SSVEPs, stimulus variation considerations, analysis methods and current models in the field. Chapter 4 details the methods and results of the four-choice SSVEP BCI system developed for purposes of this dissertation and the Unlock Project as a whole. Comparisons between control and severe speech and motor impaired groups are discussed along with limitations of this particular SSVEP BCI with respects to in-home use by paralyzed individuals. Chapter 5 discusses the need to move beyond bit-rates for practical BCI systems by taking into account user needs for a communication device. In order to create efficient and fast communication for severely motor-impaired individuals, the notion of context-aware computing and intelligent user interfacing is discussed with relation to laptop sensor input and natural language processing algorithms.. Finally, Chapter 6 concludes the dissertation with a summary of results and findings across the various topics discussed in the prior chapters, and suggests future steps for building a practical context-aware BCI.

2 Brain-Computer Interfaces

2.1 Introduction to BCIs

A search for "brain-computer interface" (BCI) or "brain-machine interface" (BMI) papers from 1980 to 2000 renders 42 results during a PubMed search, whereas from 2000 to 2012 this number increases dramatically – from a mere 42 academic papers written on the topic to an astounding 1310 papers. The ability to translate neural activity into behavioral action has occupied the pages of science fiction for generations, yet only recently have these technological capabilities started to catch up with human creativity. Although commercial BCIs in their current form are confined to novelty gaming add-ons for healthy users, options for the severely motor-impaired are far-reaching, spanning from control of a clickable mouse cursor on a screen to spelling sentences for speech synthesizer output to navigating a wheelchair (Sutter 1992; S. Kim et al. 2007; Wolpaw et al. 2002; Birbaumer 2006; Vanacker et al. 2007).

The main factors that have allowed these BCIs to be constructed include faster, more powerful computers, a better understanding of both the neurobiology and psychophysics of brain function, and a better understanding of what applications would be useful for individuals who benefit most from BCI advancements (Sutter 1992; Kubler and Müller 2007). Another variable accounting for the increase in BCI research has been the number of viable paradigms that researchers have developed in the past few decades for extracting reliable signals from the brain for BCI control. Oscillations and evoked or event-related potentials such as the P300, sensorimotor rhythm (SMR), and steady-state visual evoked potential (SSVEP) have been explored in numerous variations in order to increase classification rates, bit rates, and user speed. Now that affordable and portable computing power for neurofeedback is readily available, learning is also a factor contributing to BCI control. The interaction between man and machine allows for adaptation of both decoders and the user's brain, hopefully increasing performance by the BCI user over time.

This chapter begins by looking at the BCI field from a bird's eye view, discussing the primary bifurcation of invasive versus noninvasive research paradigms. Next, the focus will be honed down to solely EEG-based BCI methods and paradigms, followed by an overview of EEG-based BCI hardware and software. Lastly, this chapter will end with discussion of The Unlock Project – an ongoing effort begun here at Boston University to give full-functioning BCI systems to severely motor-impaired individuals.

In the BCI literature there are two broad fields of research, invasive and noninvasive recordings/acquisition, both attempting to progress a number of different interfaces. These BCI outputs include functions such as mobile robot control, robotic arm control for missing limbs, and restored speech communication. In order to get a full scope of the field, both invasive and noninvasive methods/paradigms will be discussed briefly, with emphasis placed on speech communication BCIs in particular since that research area is the primary focus of this dissertation.

2.2 BCI Recording Types

2.2.1 Invasive

BCIs can record neural activity one of two ways: 1) either noninvasively from the scalp or 2) invasively by recording from inside the skull or the cortex. Both BCI acquisition methods have advantages and disadvantages, so matching the desired behavioral output with the BCI user and their needs will determine whether or not an invasive BCI is the best option. Within the realm of invasive signal acquisition types, there are several categories of neurobiological recording technologies available for human use, as described in a recent review brain-computer interfaces for speech communication (Felleman and Van Essen 1991; Brumberg et al. 2010).

Utay Array

The Utah Array is a wired, percutaneous intracortical electrode array that records from small neuron populations within gray matter (Hendry and Reid 2000; Maynard, Nordhausen, and Normann 1997). Such arrays have been used primarily for simulated arm reaching in humans (Vialatte et al. 2010; Chadwick et al. 2011). Single unit rate measures are a reliable method for population coding, a technique whereby a population vector for a group of neurons within motor regions of humans and primates can be attributed a certain direction of movement (Regan 1966; Georgopoulos, Schwartz, and Kettner 1986).

Neurotrophic Electrode

The Neurotrophic Electrode is a wireless, transcutaneous intracortical electrode system. Unlike the Utah array, which consists of a grid of electrodes, the Neurotrophic Electrode is a small glass cone attached to several gold wires, allowing axons to grow into the cone for electrical recording. This system has been successfully used in a BMI for restoring communication via real-time speech synthesis by implanting the cone in precentral gyrus, more specifically the ventral primary motor cortex known to be the speech articular region of the brain, of an individual with locked-in syndrome (Morgan, Hansen, and Hillyard 1996; Guenther et al. 2009).

Electrocorticogram (ECoG)

Another promising invasive BCI option being heavily researched today involves ECoG, a method by which a surgeon performs a craniotomy in order to open a segment of the skull, exposing the brain surface so that a grid of up to 64 scalp electrodes can surgically implanted (temporarily) on the cortical surface (Clark and Hillyard 1996; Wennberg et al. 1998; Voytek et al. 2009). ECoG surgeries are often performed on patients in order to localize epileptogenic zones, i.e. cortical areas that are known to be the origin of epileptic seizures. While the ECoG electrodes are on the patient's cortex, motor tasks are also sometimes performed in order to gain further insight into invasive BCI control options. These ECoG studies have shown discrimination of individual finger movements (Srinivasan, Bibi, and Nunez 2006; Miller et al. 2009) and even classification of a small set of spoken words (Slotnick et al. 1999; Kellis et al. 2010).

Both Utah Array and Neurotrophic Electrode BCIs have the advantage of acquiring more refined neural responses than electrodes that are not inserted into the cortex, which can be especially important for discrimination between more precise motor control neural signatures, or complex speech/communication representations. The primary disadvantages to these intracortical methods, however, are twofold: 1) implants can damage cells in the region and produce problematic tissue reactions to introduction of a foreign object (Turner et al. 1999) diminishing viable signal over time, and 2) single-unit recording may be too localized for reproduction of cognitive or behavioral tasks. In other words, activity from one neuron may not provide enough information to encode complex movements (e.g. arm or face movements). For this reason, ECoG has become a popular method for acquiring/recording neural signals that reflect the electrical activity of synchronously firing pyramidal cells at a finer spatial resolution than electroencephalography (EEG), yet not so fine that only single neuron spikes are detected. A downside of ECoG recording is the lack of precise neural information. It is also still unknown how long an actual BCI user with an ECoG electrode grid array could successfully keep such a system implanted on the cortical surface.

2.2.2 Noninvasive

EEG

Of all the BCI technology available for recording neural activity to date, the oldest, and still the most popular, recording method is EEG. As opposed to the invasive methods mentioned earlier, noninvasive recording (EEG in particular) is far easier to get up and running because no surgery is necessary, the cost of setting up an EEG system is relatively low, and researchers can quickly obtain precise temporal data for real-time signal acquisition. All of these, among other reasons, make EEG a palatable option for BCI researchers that require a feasible method for running BCI tasks with real-time neurofeedback on human participants. In fact, the idea of reading mental thoughts by observing EEG changes when a subject shifted their attention was noted in the first EEG studies done by Hans Berger. He recorded the first human electroencephalograms in 1924, coining the term EEG for that matter, and published his once-controversial findings later in 1929 (Zhu et al. 2010; Haas 2003).

The EEG signal derives from the summated postsynaptic potentials of millions of pyramidal neurons in the cortex. These neural firings are often observed as different oscillations picked up within the EEG signal. Traditionally, oscillations have been grouped into several frequency bands, including: delta (0 – 4 Hz), theta (5 – 7 Hz), alpha (8 – 12 Hz), beta (13 – 30 Hz), and gamma (36 Hz – 46 Hz) (Davidson, Jackson, and Larson 2000). The gamma range, however, is being modified to include "high gamma" frequencies that are often not seen in EEG signals but have been discussed recently in the ECoG literature (Ray et al. 2008). The ability to extract precise temporal signals and detect frequency bands from EEG makes it a useful tool for BCI researchers. EEG's primary disadvantage is low spatial resolution, which is a result of the amassed electrical signal that passes through the brain, dura, cerebrospinal fluid, skull and finally scalp. With that said, there are numerous methods, such as the frequently used Laplacian of Gaussian function, for obtaining better estimates of the cortical surface potential (Srinivasan 1999).

Magnetoencephalography (MEG)

MEG measures the brain's magnetic activity and is known to provide far better spatial resolution than EEG while adding the benefit of excellent temporal resolution. More specifically, synchronized neural currents induce weak magnetic fields that can be picked up by arrays of superconducting quantum interference devices making up the MEG signal. Due to the orientation of the magnetic field produced from the electrical current, MEG signal is perpendicular to the cortical surface, i.e. largely in the sulci, whereas EEG signal tends to stem from cortical gyri.

In the past decade several research groups have explored the use of MEG signals for predicting two-dimensional cursor movement using a similar drawing task scenario as described in the EEG-based BCI literature (Moratti et al. 2007; McFarland et al. 1997; Wolpaw, McFarland, and Vaughan 2000; Georgopoulos et al. 2005). This study by Georgopoulos et al. did not involve imagined movements, but rather controlled arm movement of a grasped X-Y plane joystick. Lack of imagined motor movements aside, high correlation coefficients between actual and predicted trajectories were reported. This study showed for the first time that MEG signals could be used for real-time, single trial prediction of drawing movement trajectories. The drawback of MEG for BCI use is primarily the machine size and cost, making it untenable for practical use.

Functional magnetic resonance imaging (fMRI)

fMRI, an imaging procedure measuring brain activity by detecting changes in blood flow, has been a cornerstone of cognitive neuroscience research for the past several decades. Changes in the magnetic resonance due to neuronal activity are called the hemodynamic response; further, when a certain brain region is especially active, blood flow to that area increases as well. Variation in blood oxygen dependent contrast, or BOLD signal, is often investigated as being correlated with change in neural activity. Since the replenishment of deoxygenated blood can take up to a few seconds, fMRI's temporal resolution is low but its spatial resolution can be very precise with current scanner technology. The fMRI paradigm mentioned here has been used to investigate everything from empathy (Völlm et al. 2006) to consciousness (Morgan, Hansen, and Hillyard 1996; Morgan, Hansen, and Hillyard 1996; Boly et al. 2008).

fMRI is now used as another BCI tool for neuroscientific research and treatment (Sitaram et al. 2007). The goal of the Sitaram study was to look for abnormal activity in certain brain regions (given an individual's chronic condition), then use an fMRI BCI to modify local neural activity for patient-based psychophysiological treatment. For this particular experiment, the user's task is to self-regulate their BOLD response which is displayed as the feedback display on the video projection. By regulating one's BOLD signal, the participant's goal is to move an animated fish toward a small food item. With time, say the authors, the patient should be able to engage neural plasticity in the affected regions as a means of stroke rehabilitation, treatment of chronic pain, social phobias, or even emotional disorders. Unfortunately, fMRI BCIs suffer from the same drawbacks as MEG. Prohibitive costs and size make them solely research endeavors meant to further understanding of neural processes.

Functional near-infrared spectroscopy (fNIRS)

Lastly, fNIRS is an increasingly popular noninvasive BCI choice due to ease of cap preparation; this is relative to EEG cap preparation that often requires abrasion of the scalp and gelling individual electrodes. fNIRS relies upon the near-infrared portion of the electromagnetic spectrum that consists of the wavelength range of 780-2526 nm. A NIR spectrometer is composed of a light source, a monochromater, a sample holder, and a detector necessary for transmission and reflection measurement (Reich 2005). NIR light is able to penetrate the human skull into the cortex allowing it to pick up changes in oxygenation associated with neural activity via the absorption and scattering of NIR photons. Thus, fNIRS measures the optical changes at specific wavelengths within the NIR band. There is a slow response (5–8s) and a fast (ms) fNIRS response with the latter possibly corresponding to the EEG evoked potential; hence it is known as the Event Related Optical Signal.

One of the first fNIRS BCI studies looked at the slower vascular NIR response since it can be monitored as a real-time motor imagery BCI. Participants were asked to imagine clenching a ball with the hand, and given feedback on the screen with a shrinking or growing circle in response to changing hemoglobin levels. The NIRS optode ("optic electrode") was placed over the 10-20 International EEG electrode placement system (see **Figure 2-1**) equivalent of C3, an area located over the left hemisphere's primary motor cortex. Offline data analysis resulted in a classification accuracy of 75%, which is similar to accuracies seen in sensorimotor rhythm experiments (Coyle et al. 2004). The primary disadvantage with fNIRS as a BCI is the relatively low spatial *and* temporal resolution, yet its ease of preparation makes it a potentially viable practical BCI option.

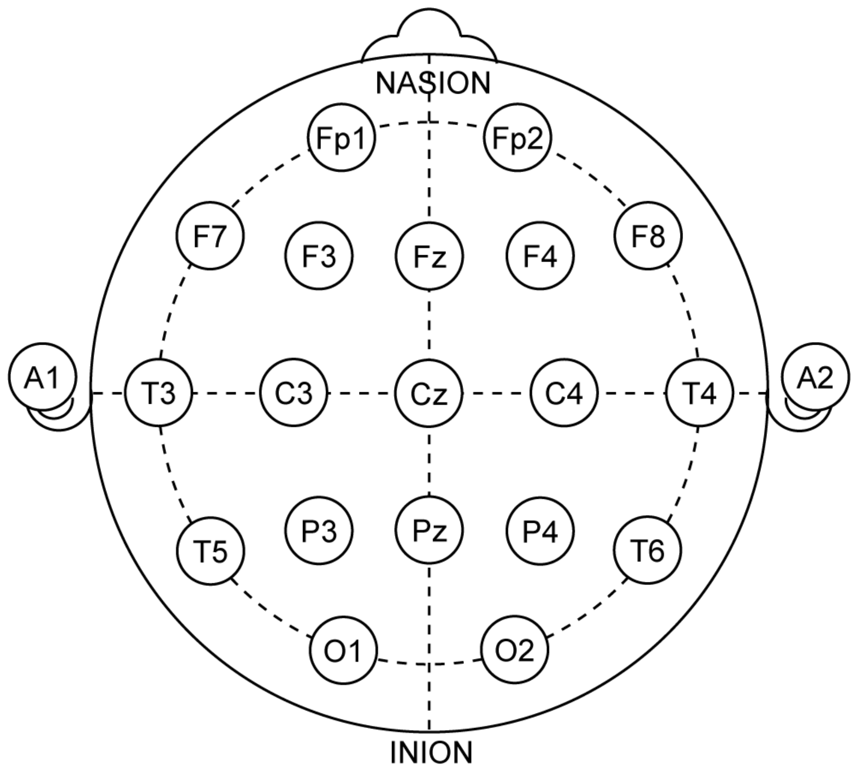

Figure 2-1. Electrode names and locations in the 10-20 International EEG system.

A comparison of all four noninvasive methods is shown below in **Table 2-1**. Each of these four methods has their advantages and disadvantages, yet in the long run EEG continues to be the best choice for BCI use thanks to its relatively low costs and portability. fNIRS is also extremely portable and easy to use but suffers from low temporal and spatial resolution. Both fMRI and MEG show promising results however both of these methods can only be used in a research setting due to the very high costs and large scanners needed.

Method	Advantages	Disadvantages	System Cost	Temporal Resolution	Spatial Resolution
EEG	High temporal resolution; relatively low startup costs; quick preparation time; portability	Low spatial resolution; susceptible to artifacts; need to gel electrodes	~$10K	1ms	~1cm
MEG	High temporal and spatial resolution	Untenable for in-home use; non-portable; expensive	~$2M	1ms	~1mm
fMRI	High spatial resolution	Untenable for in-home use; expensive; low temporal resolution	~$2-3M	1s	<1mm
fNIRS	Ease of use; portability; extended cap use time	Low spatial/temporal resolution	~$30K	10ms	~3cm

Table 2-1. Comparison of noninvasive BCI recording methods. See (Dieters et al. 2011) for a pricing assessment based on fNIRS.

2.3 BCI Paradigms

One question often raised during BCI demos and in news articles is: "Can your EEG cap read my mind?" Despite the hopeful intrigue of science fiction promises over the past century, our limited ability to extract detailed meaning from the spatially crude neural activity estimates picked by EEG in order to translate this signal back into behavior has narrowed the possibilities to a few BCI paradigms. This dissertation will discuss three categories of state-of-the-art EEG-based BCIs – P300 or evoked potential methods, motor imagery, and SSVEP – as shown in Table 2 (Birbaumer and Cohen 2007).

The P300 response

The P300 response is the most common type of event-related potential used with BCIs. This paradigm uses positive amplitude event-related potentials occurring around 300ms after presentation of an infrequent “target” stimulus to identify attended stimuli (Sellers et al. 2006; Krusienski et al. 2008). In one paradigm, users attend to grid locations that yield a P300, or “oddball”, response when flashed. The most recent P300 research has exhibited bit rates upwards of 42.1 bits/min (Fazel-Rezai et al. 2012). One positive aspect of the P300 paradigm is that it requires little training to achieve effective BCI use, yet the low bit rates are problematic. It is also unknown whether or not the P300 response attenuates over prolonged use, or if P300 Spellers depend on eye gaze (P. Brunner et al. 2010). These are issues that concern not only P300 BCI paradigms, but also others such as the SSVEP approach.

Motor imagery

Motor imagery is a paradigm whereby a subject imagines limb movements in order to control a cursor moving on a computer screen. Combinations of hand, arm and foot motor imagery are often used for two-dimensional control (Vaughan et al. 2006; Wolpaw and McFarland 2004). This BCI approach has numerous advantages to P300 or SSVEP paradigms – the primary one being the lack of visual stimulus display. Imagining a limb movement eliminates the need for screen display optimization or flashing unpleasant stimuli at the user for extended lengths of time. Another advantage is that motor imagery is more easily formulated as a continuous BCI method as opposed to a discrete classification system, allowing the user to potentially control a cursor in two dimensions on a screen – or even three-dimensions (Royer et al. 2010).

Overall, mean classification accuracies for recent two-dimensional continuous movement motor imagery studies hover around 75% (Zhang, Li, and Deng 2010; Neuper et al. 2009). It has been shown, however, that this accuracy can start low and increase dramatically when the user receives neurofeedback as to how well they are doing at controlling the BCI (Birbaumer 2006). One promising advance in increased motor imagery classification rates investigates the causal influence of gamma oscillations on the sensorimotor rhythm (Grosse-Wentrup, Schölkopf, and Hill 2011). Much work has been done to understand the mechanisms of gamma oscillations in the brain, and this research has greatly benefitted the BCI community.

SSVEP

Lastly, in the SSVEP paradigm subjects attend to one of *n* flashing stimuli, flickering at a specific frequency resulting in a specific brain response that can be then decoded for classification outputs. Recent SSVEP BCIs studies have shown mean online accuracies upwards of 92% with 96 bits/min at only 2.1 seconds per selection (Bin et al. 2011). In addition to classification accuracies, it is important to note that motor imagery is often asynchronous while P300 and SSVEP are synchronous, i.e., they require an input stimulus that provides key timing information (Brumberg and Guenther 2010).

BCI Method	Advantages	Disadvantages	Citations
P300 Speller	Proven methods; large number of selection outputs; few electrodes needed	Low bit rates; slow spelling of words; not as IUI-friendly	(Sellers et al., 2006; Krusienski et al., 2008; Brunner et al., 2010)
Motor Imagery	Continuous 2D control; relatively high bit rates	Requires much training; more electrodes may be needed; can be difficult to control for some users	Vaughan et al., 2006; Wolpaw & McFarland, 2006;
SSVEP	High bit rates; robust signals; few electrodes needed	Fewer discrete selections; display issues; stimuli can be a nuisance	(Müller-Putz et al. 2008; Zhu et al. 2010; Bin et al. 2011)

Table 2-2. Summary of advantages and disadvantages for popular BCI paradigms.

In the past few years, a new idea of combining the methods mentioned in **Table 2-2** has been proposed. This new breed of BCI is known as the "hybrid BCI". Hybrid BCIs can include combinations of non-neural signals such as eye blinks, residual muscle movements or heart rate with BCI components such as alpha rhythm responses, motor imagery and/or SSVEP. Nonetheless, for an SSVEP/motor imagery hybrid system, the motor imagery element does not add a noticeable increase in accuracy, with the SSVEP component driving much of the performance (Luo and Sullivan 2010; Pfurtscheller et al. 2010; C. Brunner et al. 2011). Hybrid BCI systems combine neural EEG signals with one or more non-neural signals such as: 1) electromyography (EMG) for recording muscle movements, 2) electrooculography (EOG) for recording eye movements, or even 3) electrocardiography (ECG) for recording heart rate fluctuations. For purposes of this dissertation an SSVEP-EOG hybrid system was implemented wherein the EOG signal was used as a mouse click/selection once the subject arrived at the proper grid selection while SSVEP was used to direct movement in the grid. In addition to EOG mouse clicks, the alpha rhythm response that is visible in the power spectrum when a user closes their eyes was also investigated as another possible hybrid BCI alternative.

With SSVEP BCIs producing such high accuracy and bit rate results, this particular paradigm is a top contender for real world BCI use, where high accuracies are required for communication. Translating highly controlled lab results into home BCI solutions is a daunting task that requires a merging of not just engineering skill sets, but also current research in neuroscience, psychophysics, software development, and human-computer interaction. In addition to this list, user-specific needs and tolerances must be addressed in the SSVEP stimulus itself, the BCI algorithm's adaptive capabilities, and user interaction with the voice output communication aid (VOCA) system.

2.4 EEG-Based BCI Hardware & Software

2.4.1 BCI Hardware

Critical hardware and software decisions must be made in order to create a cost-effective, portable BCI. Of these decisions, picking the proper EEG headset is of utmost importance. Typical EEG headsets in a lab setting involve wet electrodes requiring electrolytic gel to be inserted in each electrode at regular intervals in order to retain sufficient EEG impedance values and signal-to-noise ratio. Such a restriction makes wet electrode configurations suboptimal for long-term home BCI use. A number of non-electrolytic gel electrode systems are quickly being introduced to the market, some of which have been tested and compared in the Neural Prosthesis Lab for viability and practicality of in-home BCI use.

Two commercially available EEG headsets have been purchased and considered for use in the lab thus far – the NeuroSky MindBand[1] and the Emotiv Epoc[2]. The NeuroSky MindBand was chosen because it has two dry electrode sensors placed within an elastic band, and also delivers wireless Bluetooth signal for maximal portability. The sensors are normally placed over the forehead in order to obtain prefrontal cortex signal, yet the MindBand, shown on the right in **Figure 2-2**, can also be turned around to be placed near the occipital cortex so that an SSVEP paradigm could theoretically be implemented. By turning the MindBand

---

[1] http://www.neurosky.com/Products/MindBand.aspx
[2] http://www.emotiv.com/store/hardware/epoc-bci/epoc-neuroheadset/

around 180 degrees, the two sensors are approximately positioned to the right and left of Oz in the standard International 10-20 system of EEG electrode placement. The MindBand is advantageous due to its ease of use, yet it lacks practicality when not placed over the forehead due to the flat sensors being difficult to permeate hair in order to make direct contact with the scalp over the back of the head.

Figure 2-2. The Emotiv Epoc EEG headset (left) and NeuroSky MindBand EEG sensor band (right).

The Emotiv Epoc headset, to the left in **Figure 2-2** above, is also a wireless system, transmitting EEG data via Bluetooth. This particular headset is not fully "dry" in the sense that it cannot be placed on the head without some sort of conductive liquid; rather, the Epoc uses sensors that require liquid electrolytic (saline) solution applied to small sponge-like pads making contact directly with each of the cap's sensors. Despite the need for saline application to the sensor pads, affixing the cap to a user's head is remarkably easier than any research-grade EEG cap that requires gelling of each individual electrodes or abrasion of the scalp. The Emotiv Epoc has 14 sensors situated throughout most areas of the head, yet the design of the cap did not take into account 10-20 placements of their sensors, making it difficult to perform BCI tasks such as motor imagery. There are sensors near C3 and C4, situated over the left and right primary motor cortices, yet moving the individual electrode positions is difficult in order to assure BCI-specific placement. The Epoc does, however, contain sensors directly over O1 and O2 in the primary visual cortex, making it an excellent candidate for SSVEP BCI use.

Both the MindBand and Epoc headsets benefit from being commercially available to both the general public and researchers, making both caps cost-effective and valid options for in-home BCI use. The downside of the Epoc system, in particular, is its restrictive application programming interface (API) access that requires expensive licensing in order to get raw data out of the cap. The Neural Prosthesis lab was able to access the Epoc's raw signal via the Emotiv's C API and then import the data using a custom-built wrapper to Python for further processing.

Numerous companies offer research-grade EEG caps, yet one in particular, g.Tec[3], has developed products that are well-suited for BCI research. Two separate g.Tec systems were used in this dissertation – one that is geared towards in-lab BCI development and another that is portable for real-world BCI research. The former

[3] http://www.gtec.at/

g.Tec system mentioned uses three g.USBamps (see the top setup in **Figure 2-3**), high-performance and high-accuracy biosignal amplifiers and acquisition systems for accurate recording of EEG signals. The latter g.Tec system is called the g.MOBIlab+ (see the middle setup in **Figure 2-3**). This particular biosignal acquisition system is both portable and wireless, transmitting up to 8 channels of EEG data via Bluetooth in a similar manner to both the MindBand and Epoc headsets.

Figure 2-3. a) g.Tec research BCI setup; b) g.MOBIlab+ mobile BCI setup; c) Unlock Project custom dry electrode setup.

As is evident in a) and b) of **Figure 2-3**, both g.Tec systems use the same EEG cap, g.GAMMAbox for power supply and electrode driver/interface, as well as the same type of electrodes that can be placed anywhere in the 10-20 compliant cap. The only differences between the research and mobile systems are the type of amplifier and signal send method used for each along with the number of electrodes in each cap – 48 for the research system (a modular setup with increments of 16 channels per amp) and 8 for the mobile system. For the experiments performed in this dissertation, active ring electrodes were used and placed inside the cap and filled with electrolytic gel once placed on the participant's head.

Both g.Tec systems are effective BCI research setups due to the robust signal obtained from active electrodes and easy access of raw data, yet these g.Tec products are prohibitively expensive, costing an order of magnitude more for the g.MOBIlab+ system alone. For this reason, the OpenEEG project[4] was created for hobbyists wanting to build custom-made EEG caps – as was done for the Unlock Project (see Section 2.4.3) – and offer several advantages to both commercially-available and research-grade systems:

1. **10-20 system compliance.** Most commercial EEG headsets available on the market to date are built to appeal to gamers and hobbyists. A custom cap built by BCI researchers, on the other hand, takes into account the

[4] http://openeeg.sourceforge.net/doc/

importance of positioning electrodes strategically according to the 10-20 system names and locations. For example, it is known in the BCI literature that C3 and C4 are spatially optimal for limb motor imagery tasks, Cz and Pz are often used in P300 Spellers, and O1 and O2 render the strongest signal responses for SSVEP BCIs.

2. **Cheaper hardware.** For the first iteration of the Unlock Project EEG cap, three dry electrodes were connected to an "off-the-shelf" amplifier, which then sends filtered data to an Arduino microcontroller board with Bluetooth send capabilities. Other iterations of homemade caps that might be used for the Unlock Project in the future are currently being tested.
3. **Open signal acquisition.** Most EEG systems require purchase of a dedicated API in order to gain access to raw data, whereas the system developed in this dissertation and for the Unlock Project allows users to directly work with EEG signals in Python. With this Arduino-based EEG system, a serial COM port was specified from the Bluetooth-enabled device and then opened directly in Python to grab incoming data from the Arduino device without interfacing with proprietary device libraries.
4. **Functional aesthetics.** The Epoc has a sleek style, yet it is impractical for BCI users that may be locked-in or have ALS. These users are often angled back, resting their heads against a padded wheelchair head mount, making the Epoc design a difficult choice for severely motor-

impaired BCI users. On the opposite end of the spectrum, the g.Tec electrode cap is obviously unappealing from an aesthetic point of view for someone that would be using the BCI at home and/or in public. For this reason, our custom EEG headset attempts to combine both form and function by embedding 10-20 spatially compliant electrodes comfortably into a baseball cap. The initial Unlock Project cap shown in **Figure 2-3** uses homemade electrodes; the newest version uses the wet g.LADYbird active electrodes (Guger Technologies, Graz, AT) in order to compare signal-to-noise ratio (SNR) and classification accuracy across systems.

2.4.2 BCI Software

Choosing the proper software for a brain-computer interface is a difficult task. There are numerous questions that need to be answered first in order to select the system that works best for what is being investigated: What type of BCI paradigm will be used? Will the BCI require real-time neurofeedback? What kind of computing power is necessary to run the BCI? What kind of EEG headset will be used to collect data? What level of coding knowledge is needed to modify the BCI algorithms and stimulus/feedback display? Are there plans to commercialize the BCI? Will proprietary data acquisition and BCI software APIs prohibit this commercialization effort?

One of the first software packages to address many of these questions is called BCI2000 – a general-purpose system for BCI research (Schalk et al. 2004).

BCI2000 was developed at The Wadsworth Institute (Albany, NY) by Gerwin Schalk and colleagues. At the time of BCI2000's arrival, many labs investigating BCI were using similar approaches, yet there was no overarching software API that could be used to more easily handle signal acquisition, digitizing of signal, perform signal processing methods such as feature extraction and algorithm translation, and sending device commands to a user's computer or other device. The original BCI2000 design consisted of four modules that communicate with one another – data source, signal processing, user application, and operator interface – all programmed and maintained using C++ in order to optimize speed and efficiency of data handling. A potential downside of BCI2000 is its reliance on C++, a powerful language that can prolong development time and make it difficult for non-computer scientists to develop applications. For this reason, recent releases of BCI2000 now allow for interaction with software like MATLAB or Python. The software is free for non-profit and educational purposes, but would not be sufficient for commercial aspirations.

BCI2000 has been the predominant choice of many BCI researchers[5] for almost a decade; however, new platforms are being developed that have non-restrictive licensing agreements. One newcomer, OpenViBE, uses a BCI platform that is highly modular, and provides a more graphical user interface (GUI)-based approach to BCI development for non-programmers as displayed in **Figure 2-4**

[5] As of the end of June 2012, the BCI2000 website (http://www.bci2000.org/) states usage by over 600 labs around the world.

(Renard et al. 2010). OpenViBE also provides a number of visualization and virtual reality plug-in tools for various BCI paradigms such as the P300 Speller or motor imagery.

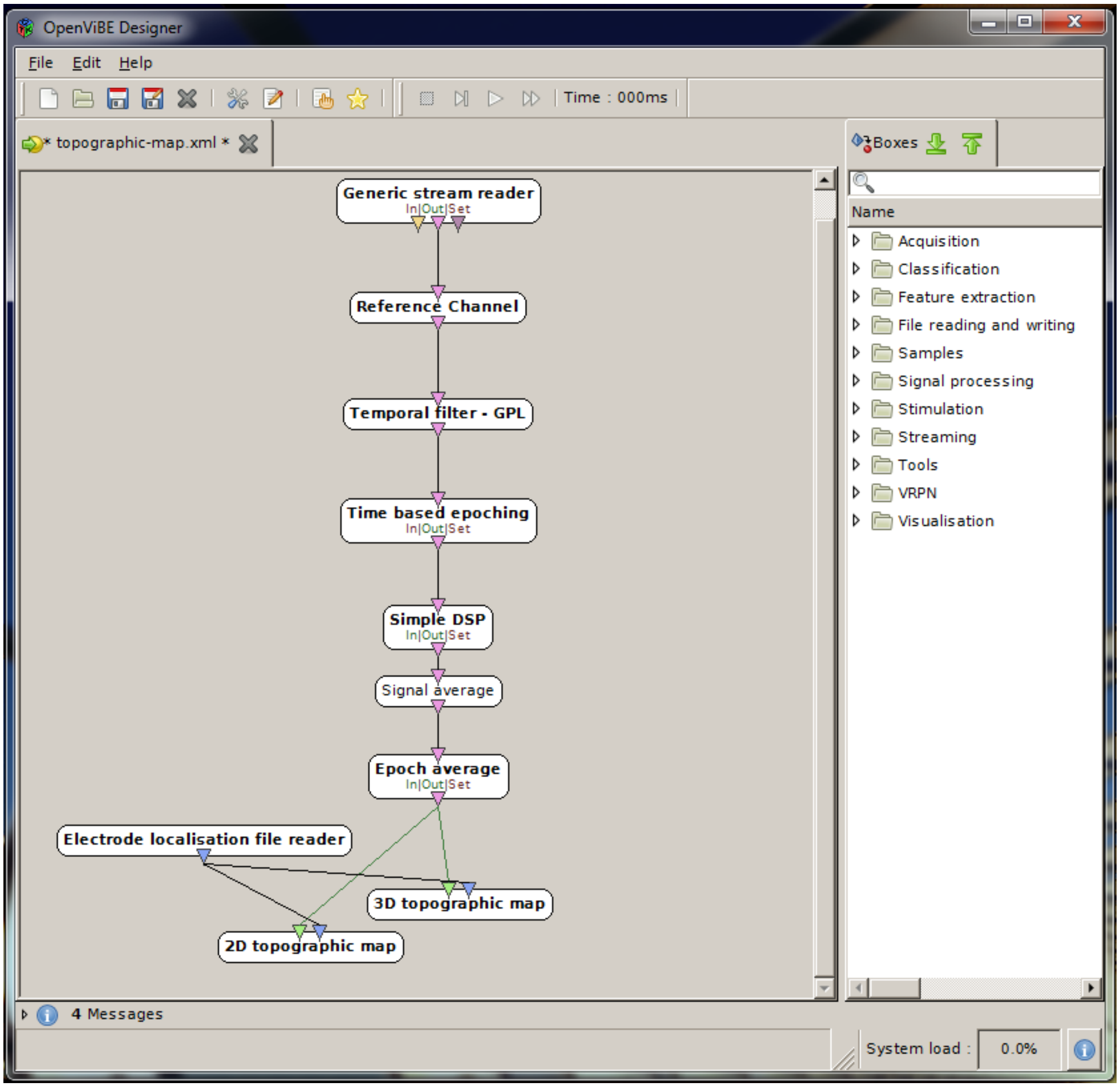

Figure 2-4. The OpenViBE Designer GUI interface for creating a 3D topographic “heat map” of real-time EEG data streams.

OpenViBE was a top candidate for getting started with BCI paradigms due to its several existing samples with drag-and-drop GUI modules. Unfortunately, despite claims of GUI-based modularity, modifying the stimulation and visualization files outside the provided tools became an onerous task. The C++ classes themselves were highly interconnected and required more effort than advantage in constructing BCIs for rapid development, thus a different software direction was pursued.

Since the lab's experimental EEG setup relies on g.Tec electrode caps and amps, g.Tec's g.HIsys software package has been used for the past several years to develop both offline BCI analysis routines as well as a few online BCI feedback paradigms. Like OpenViBE, g.HIsys was developed to ease development time by using Mathworks' MATLAB and Simulink software that allows researchers to create processing-specific modules that can be dragged and dropped into place. G.Tec's choice of MATLAB is no accident, since many neuroscientists and engineers use its many built-in signal processing, statistics, and classification toolboxes on a daily basis (Guger, Edlinger, and Krausz 2011).

Initial pilot studies exploring SSVEP as a robust BCI method used the g.HIsys paradigm to extract and process data directly from either the g.MOBIlab or g.USBamps. Both g.Tec amplifiers (the far left module box in **Figure 2-5**) have an easy to use, configurable dialog box in Simulink that allows users to modify sampling rate, frame length, number of channels, bandpass parameters and other key preprocessing steps. **Figure 2-5** also shows the model developed using g.MOBIlab and g.HIsys to acquire Bluetooth signal from a wireless g.Tec device. The model then preprocesses data, runs the signal processing, and then decodes incoming EEG signals every five seconds.

What is not shown here is any of the visual stimulation used for the initial pilot SSVEP studies. Rather than use g.Tec's provided visual stimulation modules, Psychtoolbox, a popular MATLAB-based psychophysics vision research toolkit, was used to present the SSVEP stimuli. The specifics of SSVEP stimulation techniques are discussed further in Chapter 3. The Simulink SSVEP model receives User Datagram Protocol (UDP) packets telling the program that a new trial has started in the Psychtoolbox script running on a separate machine. In this case, a trial cue was simply the presentation of either "up", "down", "left", or "right" on the center of a 21-inch LCD monitor. Once a UDP cue input packet is received from Psychtoolbox, the Simulink model processes incoming EEG data and makes a classifier decision, and finally sends a UDP packet back to Psychtoolbox to display whether or not the direction was accurately predicted or not.

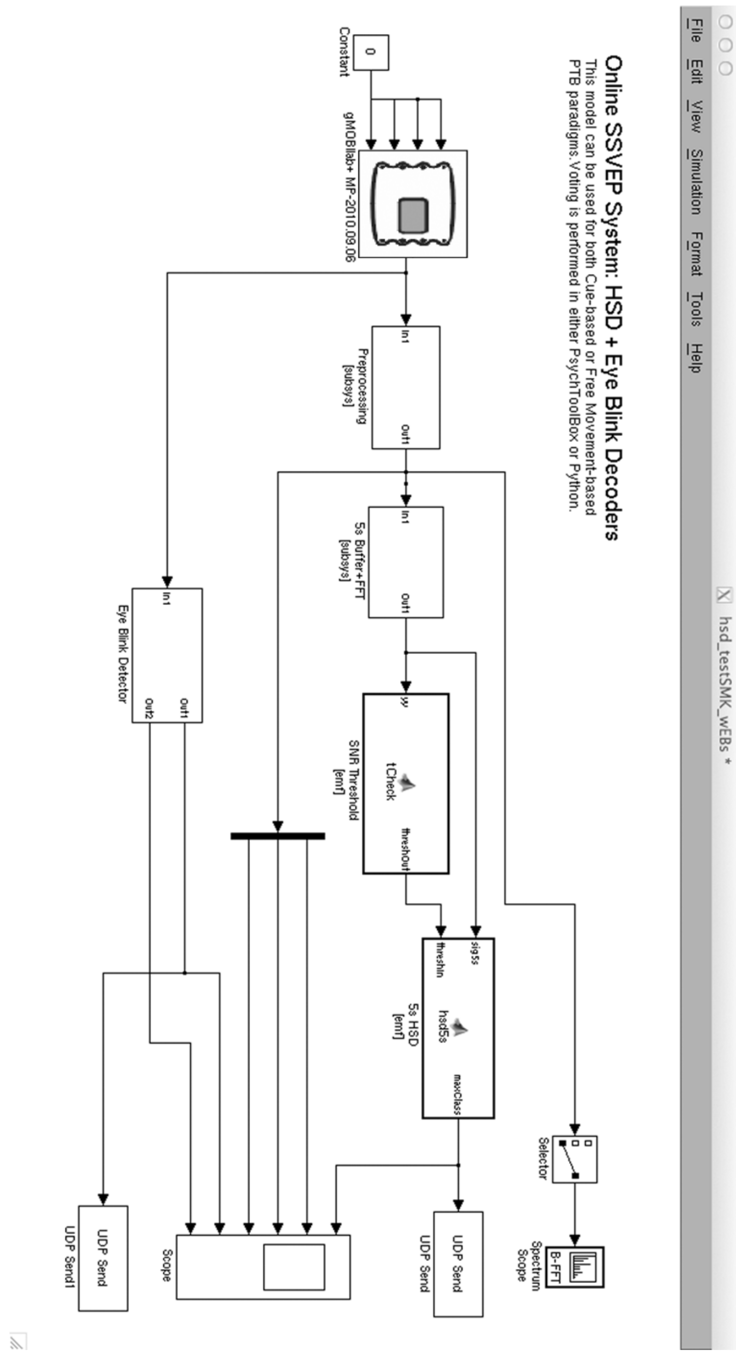

Figure 2-5. Simulink model of online signal acquisition via the g.MOBIlab and SSVEP harmonic sum decision classification with eye blink decoding. HSD=Harmonic Sum Decision; UDP=User Datagram Protocol; emf=Embedded Matlab Function; FFT=Fast Fourier Transform

Once the Simulink model was completed, it rendered comparable classification accuracies to those found in offline data analyses. One major issue with the Simulink framework, however, is its restriction on handling various types of data inputs, i.e. scalars versus vectors of buffered or variable-sized data. Unfortunately, most Simulink blocks/modules are not compatible with variable-sized data using the frame-based, rather than sample-based, sampling mode. If a real-time model in Simulink is required, it is difficult to implement a vector block output that changes with each time step. Working around Simulink limitations such as these added months of development debugging time and led to the decision for developing an intuitive programming environment in Python. Another key reason for moving on from Simulink software had to do with Mathworks' strict licensing agreements which are well-handled and easily dealt with in a research institution, but not an optimal software choice for loading on a single laptop computer for in-home BCI use. The lack of efficient coding practices and capabilities along with closed software distribution prompted a move towards Python – a programming language that allowed for flexibility and speed along with open-source distribution.

2.4.3 Unlock Project

After exploring a few of the more popular BCI software packages such as OpenViBE or Simulink, it became clear that a custom software solution was required in order to build a BCI system that is fast, portable, easy to use, and open-source. The decision to use Python led to construction of a new framework for software development of BCI applications called The Unlock Project. This API focused on development of "apps" that could easily be coded in Python without extensive knowledge, or access to, stimulus presentation packages (such as pygame or pyglet) or the BCI algorithms used to extract classification outputs. By pushing the more detailed BCI and display code "under the hood", developers are able to build apps that can take advantage of a four-option (currently) output to perform tasks such as select from a grid of speech phrases for communication, choose a channel on a laser-controlled remote control, play a game of chess, etc.

The Unlock Project framework borrows themes from existing BCI software but shifts the focus from academic research to practical, in-home BCI app development by individuals who need not be in the academic field. The Unlock Project framework is divided into two high-level modules:

1. The **core backend** that handles data acquisition, system initialization, and intermodule communication.
2. A **developer app API** that, as mentioned earlier, obfuscates the core backend so developers can focus on building an app with a set of defined documentation function.

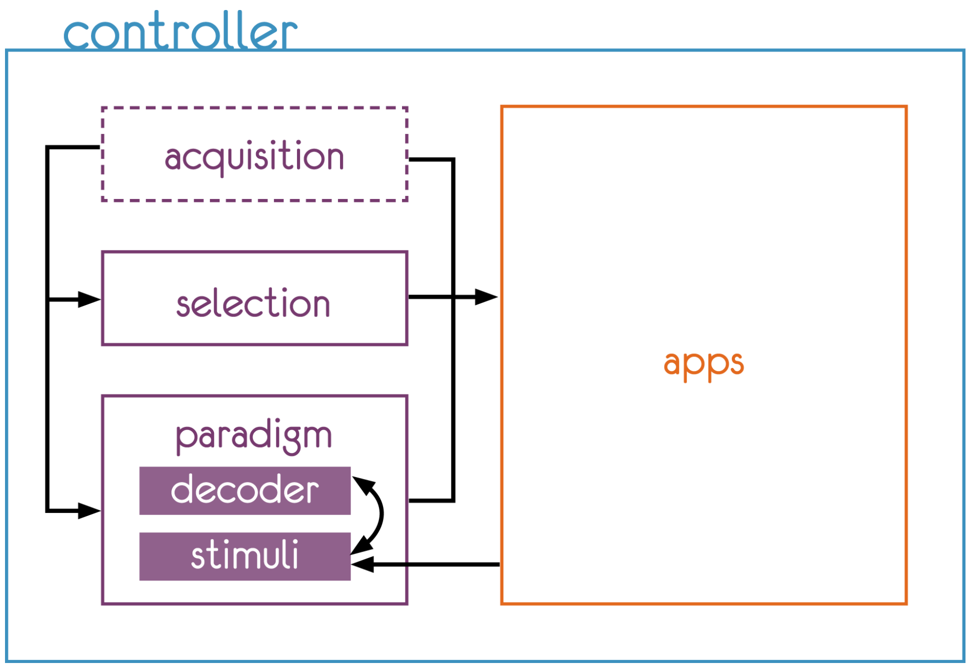

Figure 2-6. A system diagram of the framework processing modules. Arrows indicate lines of communication between processing modules, handled in the background by a master controller. The effort here has been to isolate, as much as possible, the app environment from the remaining modules. This isolation is key for invoking a "crowd-sourcing" paradigm for BCI application development.

Figure 2-6 gives an overview of how these two primary modules interact. The core backend consists of the purple modules to the left, beginning with the acquisition submodule that grabs raw EEG data directly from the amp. Currently, this acquisition submodule supports two types of EEG hardware: 1) the g.Tec MOBIlab and 2) the Emotiv Epoc. A third hardware option supporting custom Arduino Bluetooth data send EEG caps is also possible given that these signals are easily accessible via Python's standard `serial` package. A goal of The Unlock Project is to allow for easy switching of acquisition hardware using a GUI that handles variations in sampling rates, numerical data types, and signal de-multiplexing in order to send comparable buffered data packets to both the selection and paradigm submodules.

Much of the BCI heavy lifting occurs in the paradigm submodule, which consists of a set of decoder and stimulus display classes. Since the BCI prototype discussed in this dissertation deals exclusively with SSVEP-based BCIs, this was the first supported paradigm in The Unlock Project API. After the paradigm submodule has displayed a stimulus for user visualization in conjunction with a decoder decision, the selection submodule sends a decision (ordinal number 1 - 4 for a four-choice SSVEP task) and a selection (a binary blink detection in its current state) to the app. This is where the developer receives this processed information via the `update(decision, selection)` method.

```
def draw():
# Place all drawing or multimodal output
# commands here

def update(choice = None, select = False):
# Updates all methods based on current
# decoding choice
#
# choice: a scalar value part of an
# enumerated type known to both
# decoders and feedback methods
#
# select: a Boolean value indicating
```

```
# whether to "select" or
# act upon the [choice] value
```

Figure 2-7. Code description for `draw()` and `update()` methods required for all app implementations. The update function assumes no choices have been made, and, therefore, should not process any selections.

Now that an input is received, the `draw()` routine is called by the API every loop. It is here that developers have free reign to construct apps that could be useful for severely motor impaired individuals. **Figure 2-7** lays out a simplified code description of these two apps creation routines. The first working app in the Unlock Project framework uses a four-choice SSVEP-based BCI output to navigate a green square up, down, left, or right inside a grid. This app was used for the “static grid” and “hierarchy grid” experiments discussed in Chapter 4.

3 SSVEP-Based BCIs

3.1 A Brief History of SSVEP BCIs

In 1977, Jacques Vidal made the amazing discovery that single EEG epochs, rather than an average of numerous time-locked trials, could be used to classify individual evoked responses in the human brain (Vidal 1977). Not only did Vidal classify over single epochs, but he was also able to use event-related potentials to perform real-time classification for four-directional navigation of a maze displayed on a computer display. Vidal used a red checkerboard pattern flipped 45 degrees (to look like a diamond for up, down, left, right flicker stimulation – see **Figure 3-1**) that emanated from a xenon flash for visual stimulation. A simple linear Bayesian decision rule was calculated over each class (up, down, left, or right) to effectively and efficiently classifies movement direction in the maze.

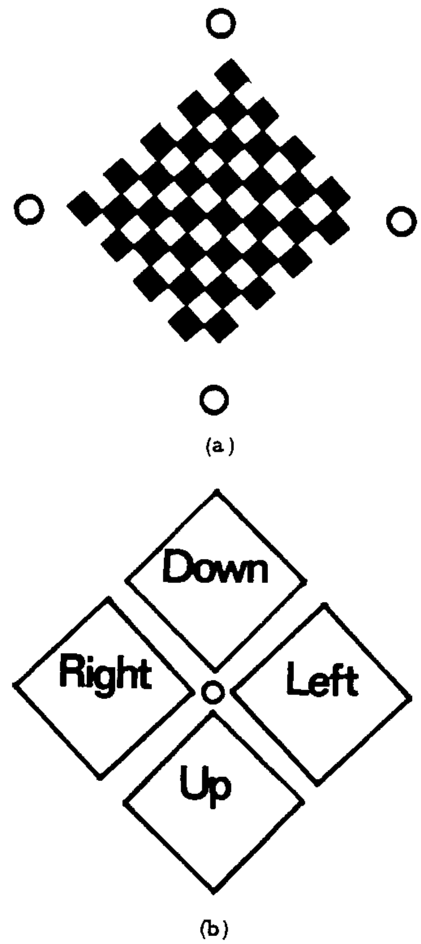

Figure 3-1. Stimulus target in real-time visual ERP experiment (Vidal 1977).

Fifteen years later, Erich Sutter was the first to address the needs of the ALS population using brain signals rather than existing eye tracker systems, which were quite unreliable at the time (Sutter 1992). Sutter developed what he called a "brain response interface" that used SSVEP signals from EEG to select from a grid of letters displayed on a CRT monitor. This pioneering study used white pseudo-random binary sequences, also called m-sequences, to display alternating red/green check patterns on a dedicated stimulus display. A dedicated processor handled the brain response interface algorithm that was simply correlation coefficients of a template SSVEP response compared to the actual EEG response. The output of this system was displayed on the screen for user feedback along with a simultaneous speech synthesizer output of a selected word, letter, or phrase (see **Figure 3-2**).

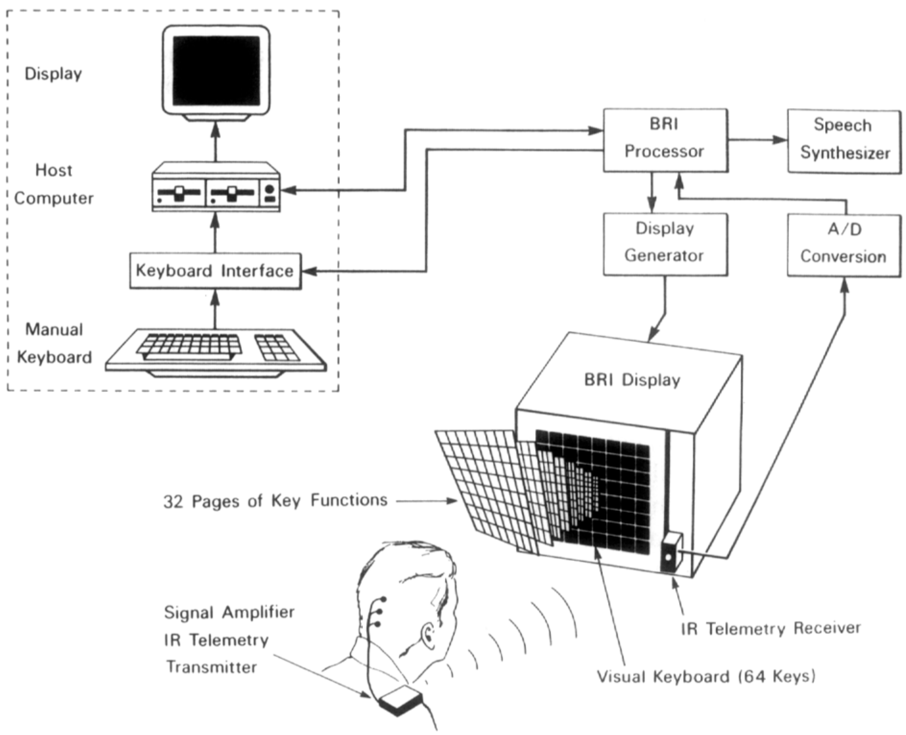

Figure 3-2. Diagram of Sutter's initial "brain response interface" system (Sutter 1992).

This system was run on 70 healthy and 20 severely disabled individuals. One ALS patient even agreed to have a small strip of electrodes chronically implanted in the space between the dura and skull in order to increase signal-to-noise (SNR). Sutter claimed that this patient was able to communicate at rates of 10 to 12 words/minute and make selections on the virtual keyboard once ever 1.2 seconds. No results were reported for the other 79 participants of the study, yet this laid the foundation for countless SSVEP BCI studies to follow.

3.2 The Visual System and SSVEPs

So how was Sutter able to take advantage of the SSVEP for his brain response interface? And how did he know that flashing lights at human participants would work? It turns out that humans have evolved to become extremely visually oriented creatures. Leaning on the visual system to perform a lion's share of neural processing takes a lot of real estate within the brain as is quickly evident when looking at Felleman and Van Essen's famous figure displaying the intricate and complex connective hierarchy of the primate visual system (Felleman and Van Essen 1991). After light hits the eye and makes its way to photoreceptors on the retina, various populations of ganglion cells begin processing visual information such as depth, color and luminance.

This visual scene information is then sent along the optic nerve to the lateral geniculate nucleus (LGN) of the thalamus – an area long known to route information to visual cortical areas for further processing. The LGN is composed of six layers that, grossly speaking, process motion and depth via the magnocellular pathway and color and edges via the parvocellular pathway, passing this information to the primary visual cortex (V1, or striate cortex). It is here that visual cortical processing begins, working its way up, and back down, to extrastriate visual areas such as V2, V3, and V4, then splitting off ventrally down the "what" pathway and dorsally up the "where" pathway. Recently, the koniocellular pathway was added as a third visual processing stream thought to be important for primate color perception (Hendry and Reid 2000). This simplistic schematic of the visual system is constantly undergoing revision and refinement but gives a framework to begin understanding how visual evoked responses are processed in V1 and beyond.

In an excellent review of SSVEP visual processing and its application to BCI systems, Vialatte et al. explain that VEPs differ from SSVEPs in that the former elicit a transient response of the visual system if the stimulus presented is brief and non-repetitive (Vialatte et al. 2010). As for the steady-state VEP, Regan tested an experiment nearly 50 years ago that suggested a response evoked by a sinusoidally modulated xenon arc lamp stimulus presented at a constant repetition frequency and retinal illumination might retain some residual aspect of the original stimulus in V1 (Regan 1966). One EEG electrode was placed 8cm above the inion and a second 5cm to the right of the first, vaguely approximating the Oz and O2 10-20 positions, respectively. After presenting a 10Hz stable VEP of small amplitudes to participants, Regan discovered an initial transient response followed by a steady, synchronous increased change in amplitude from the raw EEG signal. He called this the "steady-state" VEP.

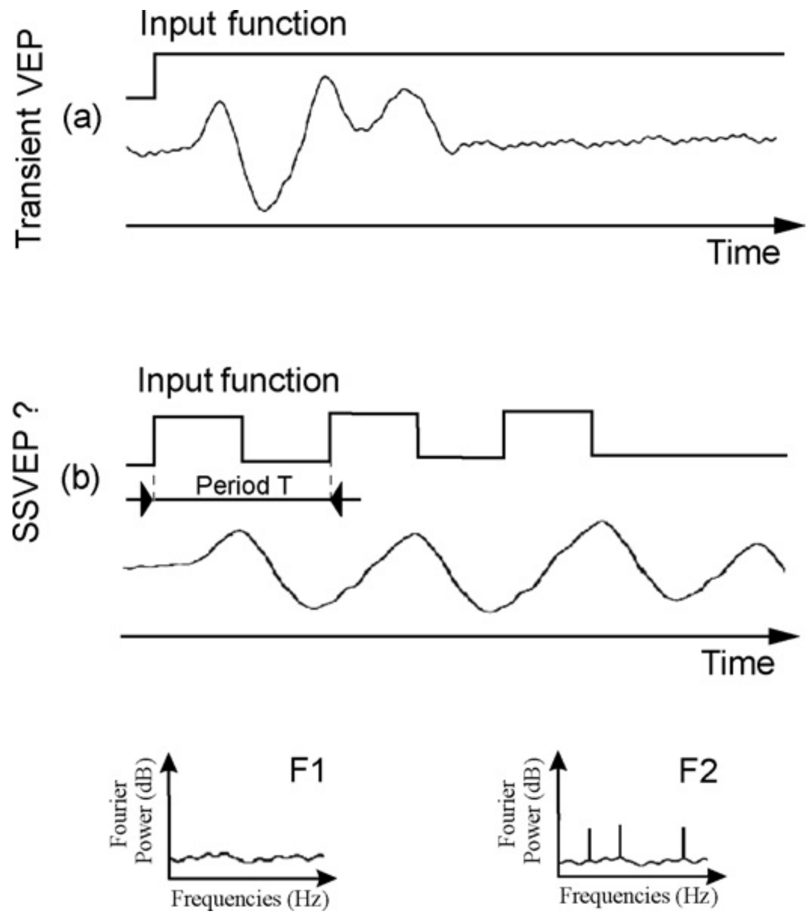

Figure 3-3. A modeled (a) transient VEP vs. (b) SSVEP EEG response over time (Vialatte et al. 2010). Below these two traces are power spectral density plots illustrating the difference between transient VEPs on the left (F1) and SSVEPs at a certain flicker frequency on the right (F2).

Several studies performed in the mid-1990s revealed that selective attention to stimulus location modulates the SSVEP response (Morgan, Hansen, and Hillyard 1996). More specifically, a stimulus presented to an attended location in the visual field elicits larger VEPs in extrastriate cortex from 80-200ms after stimulus onset. Such a cortical response suggests that being in the "spotlight" of visual attention enhances the VEP. This hypothesis was extended to SSVEP stimulus presentation, comparing cortical activation patterns of attended versus unattended flickering alphanumeric character sequences displayed on both the left (12Hz flicker) or right (8.6Hz flicker) sides of a computer screen. Thirteen EEG electrodes were disbursed over each cortical area and the results showed a much larger amplitude response to the attended flicker sequence position. In particular, the amplitude SSVEP of left 12Hz attend-left trials was largest at occipital-temporal areas over the right hemisphere whereas right 8.6Hz attend-right trials were more disbursed across the scalp.

Another study by the same research group also showed that *spatial* selective attention affects early extrastriate but not V1 and V2 components of the VEP (Clark and Hillyard 1996). Small circular checkerboards were randomly flashed on the right and left side of the screen in order to obtain topography of VEPs and attention effects. Using a spatiotemporal dipole model, they discovered that the C1 component of the response was found in V1, whereas the attention-sensitive P1 component resided in extrastriate area 19. It is also believed that low-frequency SSVEPs originate at the LGN.

Striate and extrastriate visual cortices may be the impetus of SSVEP phase-locking to visually attended flicker stimuli, but this is not the cortical stopping point. It has been shown that a Laplacian spatial filter (a technique for comparing current source densities in neighboring electrodes) to SSVEP topographical activations rendered sensitivities to small changes of around 1-2Hz in input frequency at occipital and parietal electrodes (Srinivasan, Bibi, and Nunez 2006). At

10Hz, this change became pronounced across numerous regions including lateral frontal cortex. This same study discussed results where, in upper alpha bands, long-wavelength traveling waves propagated from occipital to prefrontal electrodes, whereas delta and lower alpha bands formed standing-wave patterns over posterior and anterior electrode regions. From these two distinct patterns of activity, one could posit that SSVEP is generated from two localized sources: a stationary source presumably over visual areas and a distributed, traveling wave source over numerous cortical regions. Thus, VEPs may reach their steady-state in a succession of both local and broad dipoles, where the resulting wave propagation is determined by the characteristics of the stimuli themselves. These characteristics will be discussed in detail in the next section.

Neurophysiological studies of the SSVEP response in recent years have focused on spatiotemporal analysis of cortical source and propagation over various frequency range limits. One study continued the work done by Hillyard and colleagues of combining fMRI with EEG recordings and mapping (Slotnick et al. 1999) in order to estimate cortical source locations of pattern reversal SSVEP stimuli (Di Russo et al. 2007). They confirmed the results of studies mentioned earlier that time-varying SSVEPs have two primary cortical sources localized to V1 and V5/MT, an area known to be important for motion processing. Less prominent contributions were also seen in V3 and V4. As for the sequence of this activity progression, the authors believe that both SSVEP and VEP sequences of cortical activation are equivalent.

3.3 SSVEP Stimulus Presentation Variations

From the section above, it becomes clear that there are numerous factors involved in optimally evoking visually induced responses in the human brain that are strong enough to travel through the dura and skull and subsequently be picked up as a robust EEG electrode signal. SSVEP BCI researchers have spent the two decades since Sutter's 1992 study attempting to optimize SNR in the EEG signal by taking into account a number of different stimulus display parameters such as *color*, *flicker frequency*, *pattern shape*, *pattern reversal*, and *flicker hardware*. A recent survey of SSVEP stimulation methods for BCI use compiled results from 57 papers, which was used as a base for work being done in the field (Zhu et al. 2010). All of these parameters have been explored in pilot studies within the Neural Prosthetics lab, and are being investigated further using the recently developed Unlock Project API discussed in Section 2.4.3.

3.3.1 Color

Zhu's survey of SSVEP stimulation methods found that color stimuli, especially green, often performed best among the studies discussed. One study looked at the difference between red/black versus green/black on-off stimuli displayed on a computer monitor (Cheng et al. 2001). One blinking square was shown at a time on the monitor, but its color changed according to the frequency displayed – i.e. 7.23Hz for red/black and 8.01Hz for green/black. If both frequencies were in the "on" state, the stimulus square turned yellow; this was done to detect phase coupling of two stimulus frequencies in the EEG data. Rhythms at the duplicate, sum or difference of these two stimulated frequencies can be evoked by multiple color stimuli.

In our own color variation pilot study a decrease in power was, compared to white, observed for most colors presented (red, green, blue, yellow, cyan, magenta) using a single 100x100 pixel flashing square at various frequencies in the computer monitor's center. Both participants in this pilot run found the white square easier to focus on than the color squares as well. **Table 3-1** shows the mean power spectrum over both participants for white versus non-white, i.e. the max value over all other colors combined. It is important to point out that studies involving color SSVEP stimuli are typically done using LED stimulating devices, whereas our pilot study used a standard LCD computer monitor for presentation. This may have influenced the decrease in amplitude seen in the initial EEG signal spectral analysis.

	O1	Oz	O2
6Hz, FF, white	0.27	0.3	**0.55**
6Hz, H1, white	0.16	0.43	**0.53**
6Hz, FF, color	**0.43**	0.21	0.16
6Hz, H1, color	0.45	0.54	**0.65**
13Hz, FF, white	**0.37**	0.17	0.22
13Hz, H1, white	**0.73**	0.45	0.38
13Hz, FF, color	**0.16**	0.08	0.13
13Hz, H1, color	**0.38**	0.19	0.09

Table 3-1. A comparison of white to color SSVEP flicker stimuli. Displayed are power spectrum response (in dB) results for three occipital electrodes

(O1, Oz, O2) over the fundamental frequency (FF) and first harmonic (H1) of either a 6Hz or 13Hz stimulus. For 6Hz, white has a higher power in FF, yet color seems to do better in H1. For 13Hz, white evokes a higher spectral response across all harmonics.

3.3.2 Flicker Frequency

As mentioned earlier, frequency selection also plays a vital role in correctly classifying SSVEPs. Zhu's survey of SSVEP BCI papers revealed three bands of commonly used frequency ranges: low (1-12Hz), medium (12-30Hz), and high (30-60Hz). Many of the papers reported use of low-medium frequency pairs with most runs picking one from the 7-9Hz range and the other from the 12-17Hz range. Studies using computer monitors rather than LEDs for stimulus presentation are severely limited in frequency range due to the refresh rate *R* of most LCD monitors being 60Hz, setting a max stimulus frequency of 30Hz, i.e. *R/2*. Even with this 30Hz limit, many SSVEP papers choose frequencies under 15Hz in order to retain high power in the harmonics of each presented stimulus. For our experiments, 10Hz (+/-1Hz) is also avoided due to the ubiquitous alpha rhythm commonly seen when the eyes are closed or when the subject is in a state of wakeful relaxation. This effect was found in all our studies.

In Vialatte and colleagues' 40-year survey of SSVEP, they mention that early vision scientists believed the SSVEP boundaries ranged from 3–50Hz, yet more recent studies showed that SSVEPs can be generated up to 80Hz (Vialatte et al. 2010). It is theorized that the VEP is correlated with phase resetting/alignment to ongoing background EEG as opposed to additive amplitude modulation (Moratti et al. 2007). Thus, repetitive visual stimuli induce a reset of the EEG phase that can be viewed after averaging numerous trials. Vialatte points out that if this theory is true, the SSVEP frequency range is limited by the konio-, magno- and parvocellular pathway capabilities, depending on the type of stimulus presented, i.e. variations in color, motion, or shape will limit the frequency range by triggering different pathways.

Different flicker frequencies can also have varying effects on harmonic responses in the primary visual cortex. An important aspect of classifying SSVEP signals is analysis of a simulation frequency's harmonics. **Figure 3-4** displays the Fast Fourier Transform (FFT) power spectrum for a typical 6Hz trial as well as that of a 13Hz trial. These plots show mean activations for the three primary visual electrodes (O1, Oz, O2) over a 5s trial averaged across ten trials. For the 6Hz signal at the top of **Figure 3-4** it is clear there is a distinct peak at around 6Hz with a declining set of peaks at 12Hz, 18Hz, and 24Hz. The same trend can be seen at the bottom of **Figure 3-4** for 13Hz only with subsequent peaks near 26Hz and 39Hz. One other item to point out is that at least two of the three electrodes show significant activation at the fundamental/stimulating frequency, first harmonic, and second harmonic peaks. Spectral plots for higher flicker frequencies such as 21Hz and 29Hz trials showed the same activation patterns, yet little activation was noticeable above baseline noise in either of the first two harmonics.

Another point of interest in the harmonics domain is the difference in amplitude of various harmonics depending on the flicker frequency presented.

Figure 3-5 shows that the fundamental frequency response for 6Hz trials often dominates the harmonic responses, however, for 13Hz trials (Figure 3; bottom) the first harmonic gives a more robust signal than the fundamental frequency.

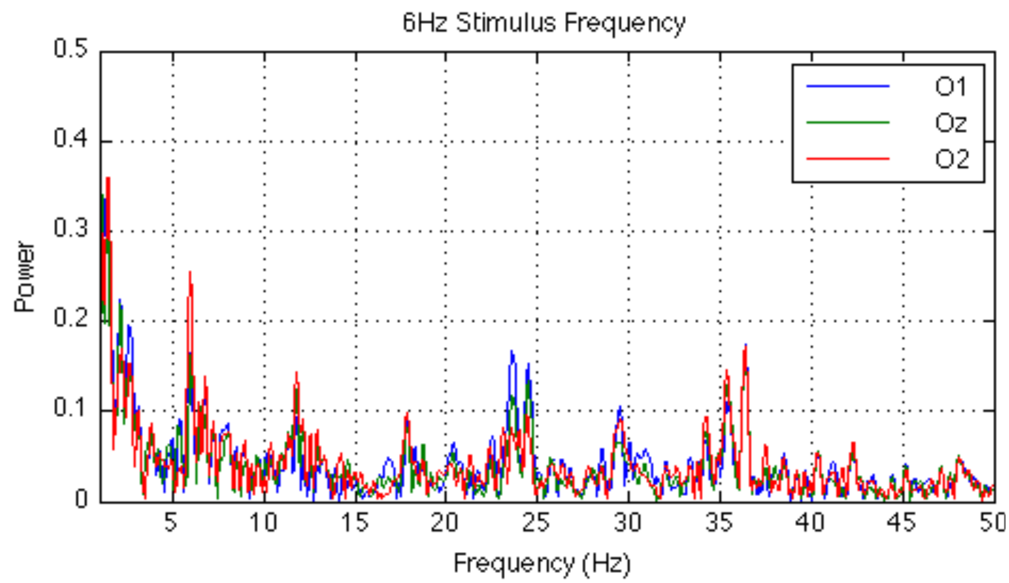

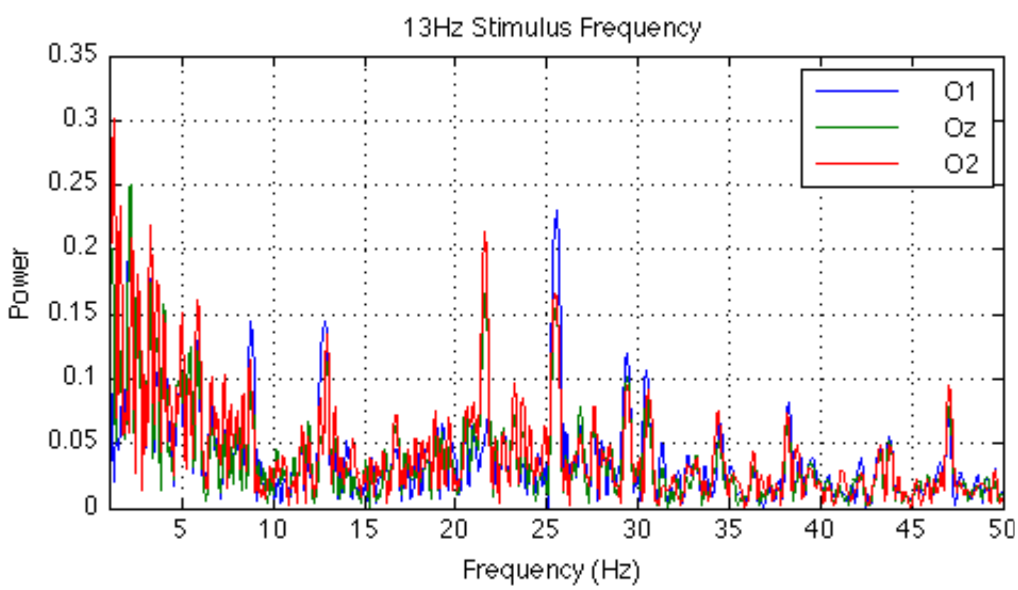

Figure 3-4. Mean power spectrum density plots for 6Hz (top) and 13Hz (bottom) over all trials.

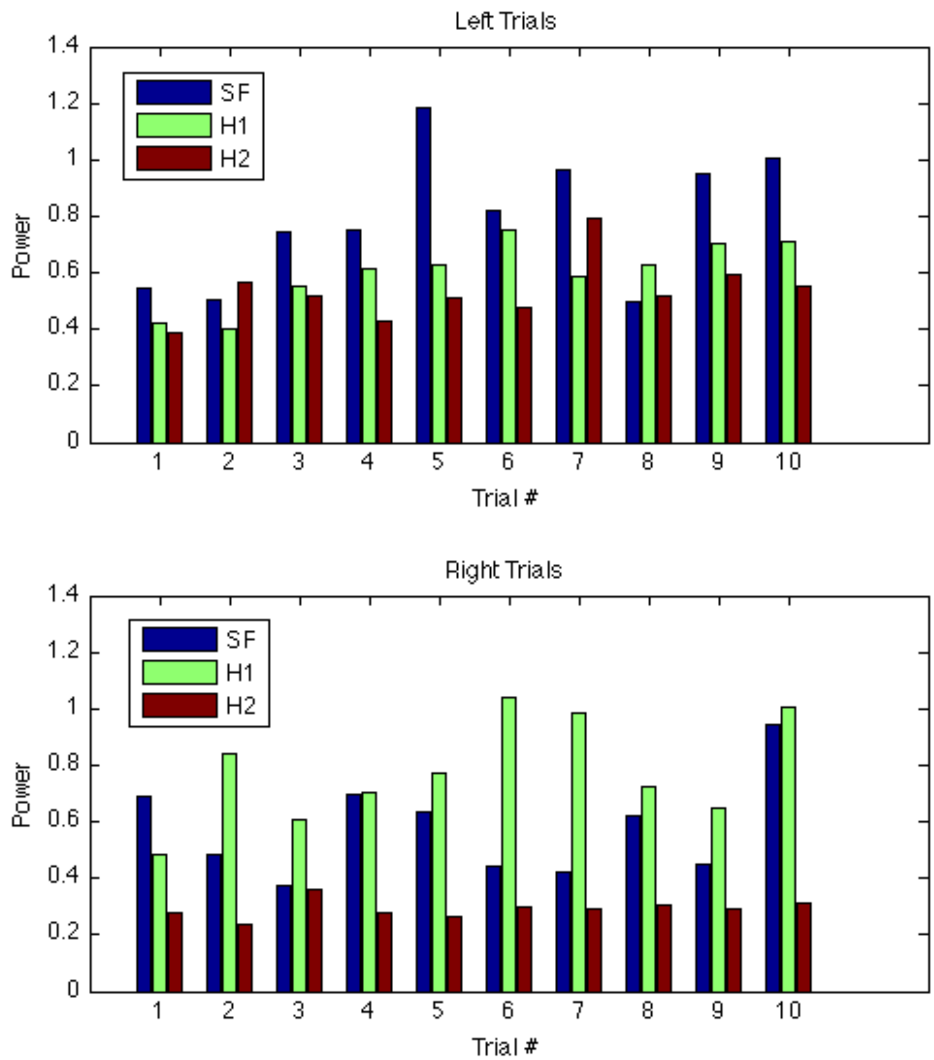

Figure 3-5. Fundamental stimulus frequency (FF), first harmonic (H1) and second harmonic (H2) for all Left (6Hz) and Right (13Hz) trials.

3.3.3 Stimulus Pattern

Stimulus pattern variations such as the ones shown in **Figure 3-6** have been tested in an attempt to bolster SNR. Common patterns include 1) single squares or circles, 2) white/black checkerboards comprised of numerous rows/columns of squares, and 3) LEDs affixed to the sides of a monitor (Morgan, Hansen, and Hillyard 1996). Both single flashing white squares and checkerboard patterns were tested in an initial offline SSVEP pilot study investigating a two-directional BCI system. A more robust SSVEP response was observed in checkerboard pattern stimulus PSD amplitudes from electrodes placed over V1. Sharper spectral peaks were also detected at the stimulating frequency and its harmonics, making for better feature extraction vectors and subsequently higher BCI classification rates.

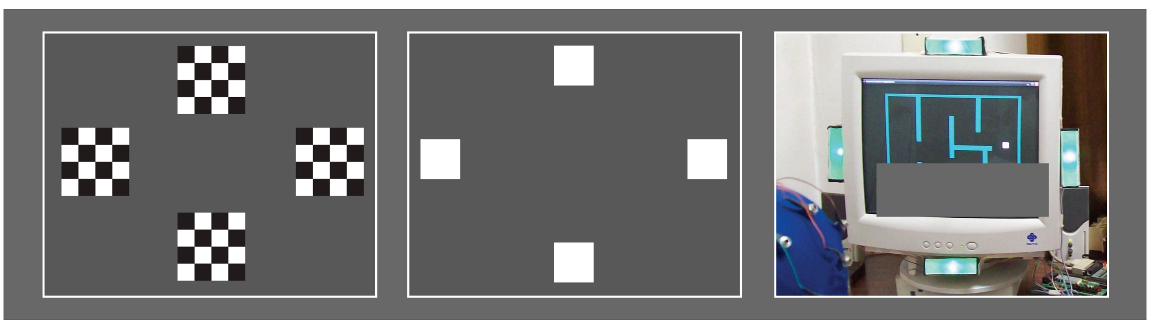

Figure 3-6. SSVEP stimulus variations – checkerboard (left), single square (center), and LEDs (right) are most commonly used in most SSVEP BCI studies. Right image reprinted from (Diez et al. 2011).

Addressing issues of stimulus pattern, size and screen placement can now be easily studied within the Unlock Project API. A researcher can now vary stimulus patterns in Python without needing to worry about the underlying graphics implementation. Instead, a stimulus pattern is simply defined by creating a stimulus instance of the `SSVEPStimulus()` class. This class has a number of parameters:

- **Screen** – the display surface on which the stimulus will be drawn;
- **Flicker rate** – specified in Hz;
- **Anchor position** – what corner of the stimulus acts as the anchor point;
- **Rotation** – counterclockwise rotation (in degrees) about the stimulus center;
- **X/Y Offset** – X and Y offsets from the top left corner of the stimulus;
- **Width/Height** – the width and height (in pixels) of the checkerboard;
- **X/Y Spatial Frequency** – the number of repeating on-off colored box pairs;
- **X/Y Duty Cycle** – the percentage of repeating on-off colored box pairs width/height that is taken up by the "on" box;
- **X/Y Evenness** – specifies whether the last on-off box pair only contains the "on" box; and
- **On-Off Color** – the percentage of the repeating on-off colored box pairs width/height that is taken up by the "on" box.

The ability to change any of these parameters speeds up coding time for researchers and facilitates quick online BCI comparisons across various stimulus pattern types.

3.3.4 On-Off vs. Contrast Reversal

A majority of SSVEP BCIs using checkerboard stimuli use contrast reversal, meaning *every* square in the checkerboard is flipped from either black-to-white or white-to-black at the desired stimulating frequency. Visual psychophysics experiments have shown, on the other hand, that *on-off* checkerboard stimuli elicit twice the VEP amplitudes within the medium frequency range mentioned earlier (Parry, Murray, and Hadjizenonos 1999). Another study showed that pattern reversal SSVEPs had reduced amplitudes that may be due to cancellation of signals dominated by transient and sustained mechanisms (Strasburger, Murray, and Remky 1993). For this reason, the on-off checkerboard stimulus pattern is used for all SSVEP experiments discussed herein.

3.3.5 Light Source

Lastly, characteristics of the light source of the stimulus must be considered. In Zhu's review, 14 papers use checkerboards, 18 use rectangular stimuli on a screen, 24 use LEDs, and the rest used some form of fluorescent or xenon lighting source. To compare SSVEP BCI results across these various light sources, one paper looked at three techniques in particular: LEDs, an LCD screen using timers, and an LCD screen using the vertical refresh rate for synchronizing visual stimuli (Cecotti, Volosyak, and Graser 2010). The latter of these offered the highest classification rates over a number of flicker frequencies due to careful detail paid toward robust and precise flicker presentation. With an LCD display refresh rate of 60Hz, the frequencies best emulated on a screen are 30, 20, 15, 12, and 8.57Hz.

Most SSVEP BCI research groups use a photodiode to test the accuracy of their LCD-based flicker stimulation methods to ensure they are indeed displaying at the correct frequency – as shown in **Figure 3-7** below. For this plot, a photodiode was attached to a Lenovo LCD screen, cycling through four stimulus frequencies (12, 13, 14, and 15Hz) once every 60s. The software used was the Unlock API in Python. It is evident from the results here that our stimulus frequencies are indeed being displayed at the proper flicker rates.

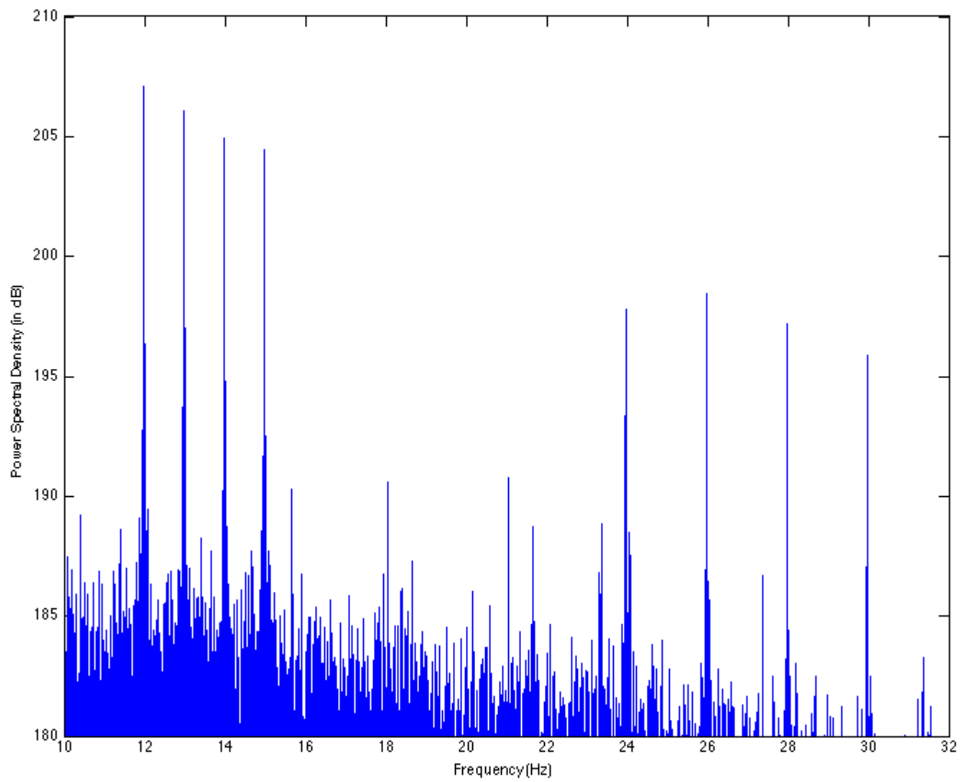

Figure 3-7. Photodiode power spectral density test of flicker frequencies at 12, 13, 14, and 15Hz on a Lenovo laptop running the Unlock API with Python's pygame package.

3.4 Analysis Methods

3.4.1 Spatial Localization

Spatial localization is especially important for BCI frameworks such as motor imagery that tend to require information garnered from a higher number of electrodes. This process is less important for SSVEP BCIs due to the strong localization of neural activity acquired from V1 in the EEG signal; in fact, many studies in the SSVEP BCI literature tend to simply choose one of, or a combination of, the following electrodes: O1, Oz, or O2 With that said, one paper involving electrodes covering the entire scalp has recently suggested a number of common spatial filtering approaches to increase SSVEP detection (Garcia-Molina and Zhu 2011).

To validate the literature consensus in our own data, a number of different spatial localization techniques were performed on offline EEG data from trials of a participant attending to a square white box flickering at 13Hz. Signals collected during the first four seconds of each trial were averaged for each of the 32 electrodes recorded across the scalp. From this averaged trial data, four commonly used techniques were performed: exploratory factor analysis, fuzzy c-means clustering, k-means clustering, and principal component analysis. A 2D topographic map of the scalp is show for each technique in **Figure 3-8**. In a) the exploratory factor analysis hot spots of the fourth factor are shown in red. In b) a fuzzy c-means clustering algorithm output shows the same weighting pattern of explained variance in the EEG data as seen in a). K-means clustering in c) also shows similar trends as c-means clustering, but appears to also include eye blink artifacts clustered in the same cluster as that seen in the visual area SSVEP response. A different result is seen entirely in d) where principal component analysis was used; the third coefficient vector was the closest to the other three methods described here (the first two vectors looked like artifacts).

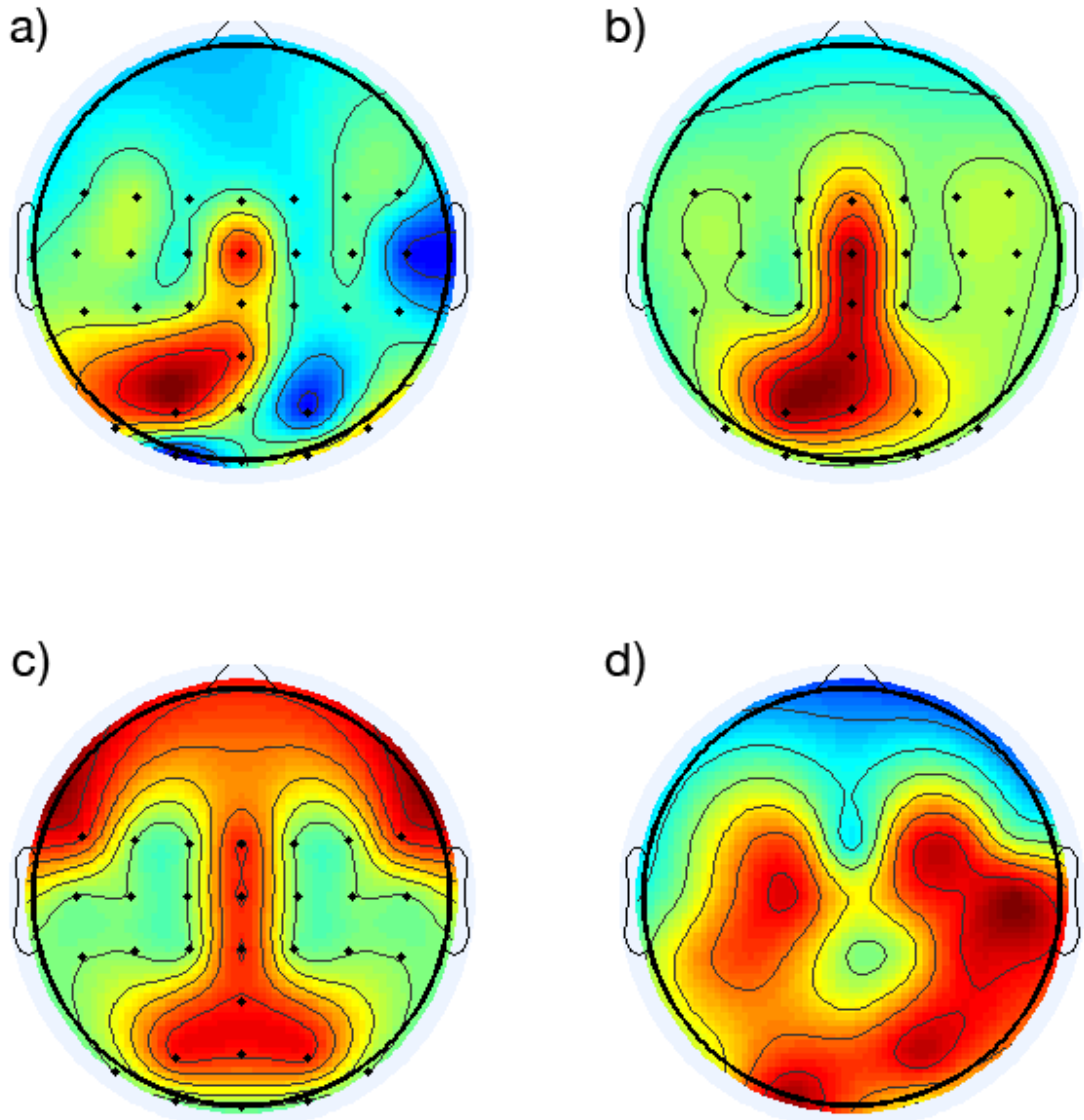

Figure 3-8. Spatial localization of EEG signal during an SSVEP task. For each topographic plot, the colors range from red (high correlations or weights) to blue (low correlations or weights). a) Fourth factor result from exploratory factor analysis; b) First cluster from the final fuzzy partition matrix output; c) First cluster output from k-means clustering using the correlation distance method; and d) Third coefficient vector output from principal component analysis.

A spectral analysis using FFT was also performed on the same dataset as shown in the topographic maps above to verify that O1, Oz, and O2 are the appropriate electrode choices for further SSVEP BCI decoding. The results shown in **Table 3-2** show that, for this particular participant, O2 and Oz were the best choices for a 6Hz flicker whereas PO7 and O1 were optimal for 13Hz. The PSD amplitudes for 6Hz oscillations were far higher in O2 and Oz relative to other surrounding electrodes. What's surprising here is the sharp drop-off in response from O1, whereas O8 over parieto-occipital cortex showed a robust response in the stimulating frequency range. In the 13Hz PSD, however, the opposite effect is seen between O1 and O2. This initial pilot study shows how varied the spatiotemporal outcome can be based on flicker frequency alone. With that said, all of the strongest SSVEP responses still seemed to reside in either primary visual areas or electrodes in higher visual areas making their way up the dorsal or "where" stream in parietal cortex. This result is plausible given that SSVEPs often cause motion artifacts (Bakardjian, Tanaka, and Cichocki 2010), with posterior parietal cortex, V5/MT, and MST being strongly represented in the spectral analysis below.

6Hz	**FCz**	**Cz**	**CPz**	**O1**	**Oz**	**O2**	**PO4**	**PO8**
SF	**0.52**	0.48	0.41	0.27	0.30	**0.55**	0.48	**0.525**
H1	0.29	0.305	**0.32**	0.16	**0.42**	**0.52**	0.195	0.275
H2	0.12	0.11	0.16	0.18	**0.22**	**0.233**	**0.26**	0.16
13Hz	**Pz**	**Cz**	**CPz**	**O1**	**Oz**	**O2**	**PO3**	**PO7**
SF	0.34	0.30	0.33	**0.37**	0.16	0.23	**0.56**	**0.53**

H1	0.10	0.19	0.12	**0.74**	**0.45**	0.38	0.422	**0.425**
H2	0.09	0.078	0.076	**0.29**	0.209	**0.211**	0.19	**0.217**

Table 3-2. Spectral power for both 6Hz and 13Hz stimulus frequency (FF), first harmonic (H1), and second harmonic (H2). *Green* indicates highest spectral amplitude electrode response for that particular spectral band, with *orange* indicating second strongest and *yellow* third strongest. See **Figure 2-1** for a 2D map of electrode 10-20 position nomenclature.

3.4.2 Artifact Detection & Removal

Muscle and eye movements produce large artifacts in EEG signals that, for most BCI decoding paradigms, need to first be identified in a signal, then either removed completely or denoised into a transformed waveform. One advantage of an SSVEP BCI is that minimal artifacts are seen from residual muscle or eye movements via electrodes placed over the primary visual cortex, thus few steps are necessary when removing artifacts from SSVEP-generated EEG signals. Detecting large artifacts such as eye movements, however, is advantageous in that they can be used as binary selection mechanisms (see Section 4.1.7 for implementation details).

Nonetheless, artifact detection and removal can still improve a BCI system by taking into account erratic movements, jaw clenching, large breaths, or eye movements. For the purpose of this dissertation, artifacts were largely eliminated by performing an assortment of preprocessing algorithms on the raw EEG data before feature extraction and classification steps were taken. After some preliminary power spectral density analyses of pilot SSVEP data, it was decided that spatial filtering was not necessary for SSVEP due to the strong concentration of explained signal variance seen over primary visual area electrodes – specifically, O1, Oz, and O2. The current BCI system uses zero-mean trial signal denoising followed by a 4th-order Butterworth bandpass filter spanning the stimulating frequencies their first harmonics. For example, a four-choice system with flicker frequencies of 12, 13, 14, and 15Hz required a bandpass filter ranging from 8Hz to 34Hz, thus a 4Hz padding was applied to both the lower and upper bounds.

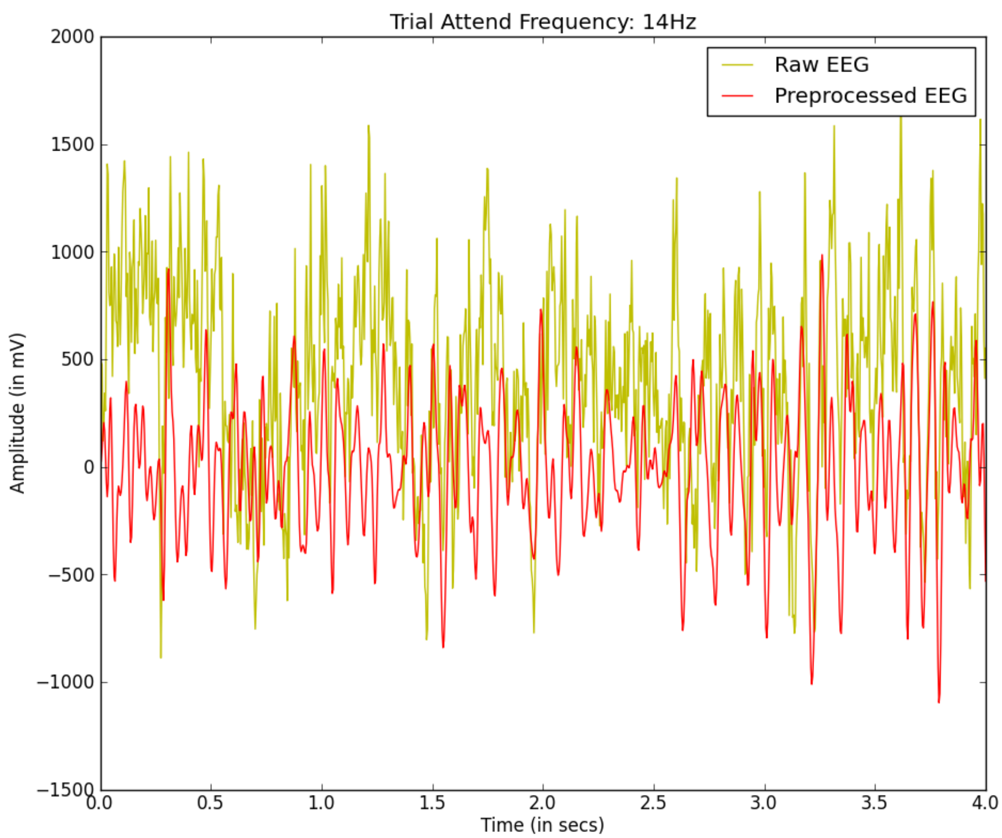

Figure 3-9. Comparison of raw and preprocessed EEG signals for a four-second SSVEP trial with a 14Hz flicker frequency. The signal itself is a mean time trace averaged over O1, Oz, and O2 at each sample within the four-

second trial. The variance among these three electrodes is often small, thus an average of the three signals is justifiable.

Figure 3-9 demonstrates the importance of preprocessing data as a first step. The yellow trace shows far more noise in the signal due to high and low frequency noise in the EEG. The red trace overlaid on the yellow trace shows a much cleaner signal due to a simple zero-mean of the data segment followed by a Butterworth bandpass filter in the ranges mentioned earlier. One added preprocessing/artifact removal step that could be taken would be independent component analysis, or blind source separation, for quick removal of muscle artifacts that are easily discarded in such a process (Vasquez, Bakardjian, and Vallverdu 2008). The ICA method was not used for the system proposed in this dissertation for two reasons: 1) these artifacts tend to have very specific frequency domain signatures that are not in the ranges looked at for PSD-based SSVEP classification, and 2) few artifacts were seen over the visual cortex whereas a majority of artifacts were seen over electrode recordings near the eyes during blinking.

3.4.3 Feature Extraction & Selection

Feature extraction and selection methods depend primarily on whether a *time* or *frequency* domain classifier is being used. For time domain classifiers, canonical correlation analysis (CCA) is a newly popular choice in the SSVEP literature (Bin, Gao, Yan, et al. 2009), as is stimulus-locked inter-trace correlation (SLIC), a technique that takes advantage of the relative timing between the EEG signal and repeated flashing light onsets (Luo and Sullivan 2010; Luo and Sullivan 2010). For SLIC, the mean trace is calculated for each attended/non-attended stimulus, and correlation coefficients can be taken across each stimulus frequency for further classification.

In the frequency domain, the Discrete Fourier Transform (DFT) can be calculated, and coefficients at the SSVEP-stimulated fundamental frequencies and first harmonics subsequently extracted (Lopez-Gordo et al. 2011; Lopez-Gordo et al. 2011). A variant of this is called the harmonic sum decision (HSD) method that sums the harmonic values across all stimulating frequencies displayed on the screen. These values are then normalized before classification. The harmonic sum method was modified in this dissertation for an offline pilot study analysis by taking the mean value of a small window around the fundamental frequencies and their subsequent harmonics. This is done because often times the response frequency is not exactly at, say, 7Hz – a slight jitter could place the maximum value somewhere between 6.9Hz and 7.1Hz, thus a mean (or argmax) value within the 6.9-7.1Hz range renders better results as shown in **Figure 3-10.** In other words, the bandwidth increases in size when jitter is introduced. Dealing with this slight response offset makes for a practical modification when using LCD screens for stimulation. A photodiode power spectrum density can illuminate whether this jitter is due to screen display issues as opposed to physiological origins. Numerous other techniques are also discussed in the literature, but omitted here since they will not be implemented within the proposed BCI system.

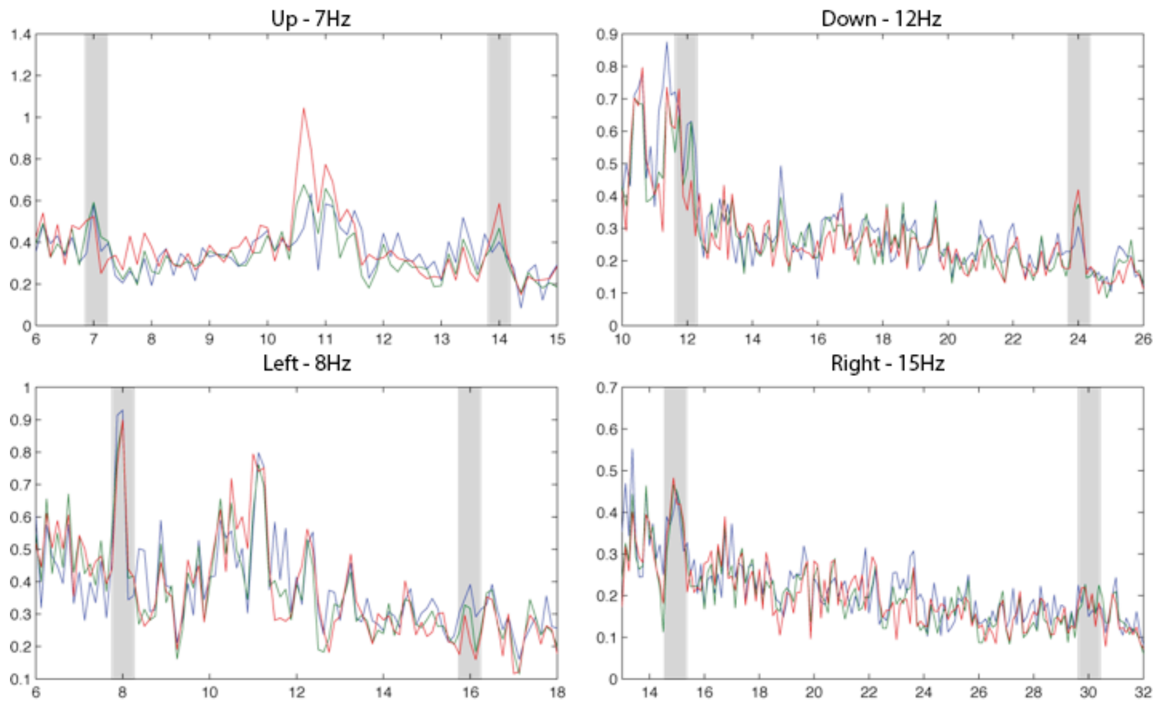

Figure 3-10. Mean trial power spectral density plots over 5s for SSVEP attended stimulus directions – Up (top left), Down (top right), Left (bottom left), and Right (bottom right). The three traces represent O1 (blue), Oz (red), and O2 (green) electrode power spectral density values in the frequency domain. Windows are drawn in gray around each stimulating frequency and its first harmonic to demonstrate the mean harmonic sum window lengths used. Windows are taken across both attended and non-attended stimuli, but only attended stimulus windows are shown here for simplicity. Note that stimulating frequencies avoid the 10Hz, or alpha rhythm, range due to its overshadowing power spectral density amplitudes. This particular subject's alpha rhythm tends to be closer to 11Hz, which may be a result of numerous top-down factors or SSVEP frequency stimulation interaction.

3.4.4 Classification

Once feature vectors have been extracted from the pre-processed EEG signal, a classifier is chosen based on the feature methods used. According to a review of BCI signal processing algorithms by Bashashati and colleagues, linear discriminant analysis (LDA) is far and away the most widely used method for classification (Bashashati et al. 2007). This seems reasonable given LDA's simple yet effective results compared to more complex neural network, support vector machine, k-nearest neighbors or other nonlinear classifiers that deliver comparable accuracies yet are burdened by higher computational overhead. Some of these classifiers become untenable as options in a real-time BCI system where speed is of the essence.[6] LDA methods require a training session in order to learn the weights for further testing sessions and may be paired with slow parameter adaptation for BCI users. Conversely, there are several SSVEP-specific classification methods that do not require training. **Table 3-3** gives a short list of SSVEP-based BCI feature/classifier systems that have been tested on our pilot study data and show promise as viable options.

[6] Such concerns can be overcome, however, with the growing feasibility of cloud data processing. This option may become necessary if EEG data is to be processed in real-time on less computationally robust tablets.

Feature extraction method	Classifier	Source
Spectral power windowing	Max normalized harmonic sum decision	(Müller-Putz et al. 2008)
Common spatial patterns	Boosted regularized LDA	(Parini et al. 2009)
SLIC	LDA	(Luo and Sullivan 2010)
Filtered amplitude waveform signal	CCA	(Bin et al. 2011)
CWT	Support vector machine	(Zhang, Li, and Deng 2010)

Table 3-3. A select list of optimal feature and classifier methods specific to SSVEP BCIs, several of which have been tested as efficient classification options.

In this dissertation, a modified mean window HSD classifier was tested and showed the most promise as being highly reliable for an online BCI. In an initial study, two single square stimuli were flashed – 6Hz on the left side of the screen and 13Hz on the right. Using just 2s of data to compute the power spectral density (via FFT), the system was able to classify with 75%, and up to 90% after 3s for one subject. Changing the stimulation frequencies to 21Hz and 29Hz increased the classification accuracy to 89% and 100% for 2s and 3s, respectively. Rectangular stimuli in an online 4-choice (up-12Hz, down-13Hz, left-14Hz, right-15Hz) SSVEP grid cursor control task showed an average of >95% classification accuracy for one subject with an FFT duration of 4s.

Several factors contributed to the high performance values observed in this pilot study: 1) two workstation computers were used– one for handing stimulus display and the other for acquiring/decoding EEG signal, and 2) Psychtoolbox for MATLAB was used to present SSVEP stimuli. This MATLAB package for vision science research is known for presenting highly precise temporal stimulation presentation due to its CPU optimization techniques. The mobile SSVEP BCI system proposed in Section 4.1 also uses the modified mean window HSD classifier, yet does not render as high classification accuracies.

3.4.5 Confidence Measures

The vast majority of BCI papers to date focus on accuracy results; however, other measures must be considered in order to get at the robustness of a BCI system (Hamadicharef 2010; Millán et al. 2010). With an online, real-world BCI, confidence interval measures can assist with assuring the classified output truly is the correct output to be sent, reducing false positives in the process. For a CCA classifier, Wilks' lambda (likelihood ratio) statistic can be calculated in order to obtain confidence values for choosing one class versus another. Simply put, Wilks' lamba is a test statistic used in multivariate analysis of variance to test difference in means between two groups of data based on a combination of feature vectors. For an HSD classifier, multiclass probabilistic linear discriminant analysis (LDA) posterior probabilities can be used as a real-time confidence measure. LDA is a common machine learning and statistical classifier method that finds linear combinations of features, where the goal is to split groups of data as much possible, i.e. maximize orthogonality. A recent paper has shown that the evaluation criterion quantifying the level of agreement or effect size measure, known as the kappa coefficient, assesses reliability of a predicted class over multiple points in time. Higher subject kappa coefficients have been show to improve BCI performance (Kubler and Müller 2007; Xu et al. 2011).

Adding a voting strategy is another method for increasing accuracy and decreasing false positives. If a classification is made, say, once every 250ms, and a final decision is expected at 2s intervals, eight votes are collected and the mode class could be taken as the winner. Another form of voting could be created between classifiers running in parallel, so that if an HSD classifier produces a final choice with a higher confidence interval than a CCA classifier's confidence interval value, the winner is the HSD output. Unfortunately, this sort of voting schema is limited to the processing power of the hardware running the signal processing algorithms and, depending on the hardware, might only function correctly with two computationally lightweight classifiers.

3.5 Frequency-based Models

Now that the preprocessing, feature extraction, and classification options of constructing an SSVEP BCI have been discussed, *time-based* and *frequency-based* model categories for real-time prediction of neural signals using EEG will be introduced.. The latter of these two categories dominated the majority of real-time SSVEP BCIs for quite some time; however, time-based models are becoming increasingly popular due to their faster classification rates. Both time- and frequency-based models of SSVEP face the same difficult challenges of stimulus presentation method/speed as well as algorithm selection for artifact, feature and classification steps. As will be seen from discussion of the papers in this section, both model categories often use similar methods to approach the problem from two different but complimentary angles.

The Bashashati survey of signal processing algorithms referenced earlier in this dissertation found that a few predominant model designs have emerged (Bashashati et al. 2007). The most popular feature classification methods reported include LDA, threshold detection, or artificial neural networks such as the multi-layer perceptron, radial basis function, fuzzy ARTMAP, etc. It should be noted that this survey was published in 2007 prior to the emergence of the now-numerous time-based models common in the SSVEP BCI literature. This is testament to how quickly the field is moving.

One common SSVEP BCI model uses the minimum energy (ME) approach (Friman, Volosyak, and Graser 2007). This particular algorithm cleans the raw EEG signal of noise and unwanted frequency components by projecting artificial oscillations at the stimulating frequencies plus their harmonics onto their orthogonal EEG signal complements. Equation (0.1) has three parts: first is the evoked SSVEP response signal, second is the set of nuisance signals $z_j(t)$ which are added to each electrode signal and scaled by the $b_{i,j}$ weights, and lastly there is the measurement noise, $e_i(t)$, for each electrode. The end result is the supposed noise itself, which can weight the incoming signal for denoising.

$$y_i(t) = \sum_{k=1}^{N_h} a_{i,k} \sin(2\pi kft + \phi_{i,k}) + \sum_j b_{i,j} z_j(t) + e_i(t) \tag{0.1}$$

SSVEP detection then is performed via a test statistic as shown in Equation (0.2) where $\hat{P}_{k,l}$ is estimated power in a particular harmonic in Equation (0.3).

$$T = \frac{1}{N_s N_h} \sum_{l=1}^{N_s} \sum_{k=1}^{N_h} \frac{\hat{P}_{k,l}}{\hat{\sigma}_{k,l}^2} \tag{0.2}$$

$$\hat{P}_{k,l} = \left\| X_k^T s_l \right\|^2 \tag{0.3}$$

The test statistic, then, calculates the ratio of an SSVEP stimulus being presented or not for all stimulating frequencies over all EEG channels selected. The output is simply a ranked order list of frequencies with the highest SNR.

Another frequency-based model discussed here uses the LDA method, which is quite common in BCI algorithms – especially in motor imagery. To understand LDA's use in SSVEP-based BCIs, Parini et al.'s protocol offers a good example case. In a recent paper, their protocol had three sessions: 1) user-specific frequency selection, 2) training for parameter selection, and 3) testing to validate the chosen parameters (Chadwick et al. 2011; Parini et al. 2009; Friman, Volosyak, and Graser 2007). After eight EEG channels were bandpass filtered around the stimulating frequency and its first two harmonics in 3-second windows, a common spatial filter was used to spatially filter the data into one of two classes, *stimulus* or *nonstimulus* (Equation (0.4). The two covariance matrices, Ω_S and Ω_{NS} , are diagonalized with the eigenvalues summing to one. The particular spatial filter used with the highest eigenvalue is considered as pertinent to the SSVEP signal.

$$\Omega_{\text{class}} = \frac{1}{N_{\text{class}}} \sum_{i=1}^{N_{\text{class}}} X_i X_i^T \text{with (class} \in \{S, NS\}) \tag{0.4}$$

Once a spatial filter is created, feature extraction is performed whereby an amplitude estimation of the SSVEP is obtained by way of Equation (0.5). This states that the standard deviation of the average, time-locked to the *s*th stimulus, is proportional to the standard deviation over the entire data window. Each stimulating frequency, then, has its own normalized feature vector ranging from zero to one.

$$FX(s) = \frac{\sigma(B_s)}{\sigma(X_{\text{win}})} \tag{0.5}$$

From the $FX(s)$ features a 5-class (up, down, left, right, null) normalized LDA classifier is trained upon. Normalized feature vectors comprise a more optimal set of coefficients during the testing session. Using LDA for SSVEP tasks, Parini et al. (2009) were able to obtain an average bit-rate across eleven subjects of 51.47 bit/min.

Lastly, the Graz BCI group in Austria has looked extensively into the impact of harmonic frequency components in SSVEP stimuli. In a 2005 study, the Graz researchers looked at variability in classification rates by including or excluding a range of harmonics taken from DFT bands of the stimulating frequencies (Müller-Putz et al. 2005). For classification in this study, a lock-in analyzer system was used. This particular system relies on sine and cosine values of each stimulating frequency that are multiplied by EEG signals containing the SSVEP in order to boost signal at the proper spectral frequency windows (i.e. the fundamental frequencies and their first two harmonics).

In a subsequent 2008 paper (Müller-Putz et al. 2008) the same researchers compared their lock-in analyzer algorithm to a method that looks at a sum of spectral power at fundamental and harmonic frequencies across each stimulating frequency – a method known as harmonic sum decision (HSD). Participants in the study were shown 6, 7, 8, and 13Hz flicker frequencies for 3.5 seconds. A 1024-point DFT was taken followed by breaking up each stimulating frequency's fundamental frequency, first harmonic and second harmonic (known as H1, H2, H3 here). Since the harmonic sums for 6Hz would typically be larger in the PSD than sums at 13Hz, the DFT bin feature vectors are normalized first prior to classification. The HSD classifier in Equation (3.6) is unassuming yet extremely robust in its simplicity. The BLn^{-1} values are the inverse baseline of each flicker frequency and are derived from the DFT taken from 1.5 seconds of rest interval data. The largest of the four harmonic sums is the winning class. This simple yet effective classifier is the basis for all classification performed in the experiments discussed in Chapter 4.

$$\text{class} = \arg\max \begin{pmatrix} \sum_{i=1}^{3} H_i 6 \cdot BL6^{-1}, \sum_{i=1}^{3} H_i 7 \cdot BL7^{-1}, \\ \sum_{i=1}^{3} H_i 8 \cdot BL8^{-1}, \sum_{i=1}^{3} H_i 13 \cdot BL13^{-1} \end{pmatrix} \tag{3.6}$$

3.6 Time-based Models

In one way or another, all of the SSVEP BCI models in Section 3.5 use a spectral estimation method (typically the DFT) for transforming raw EEG signal into the frequency domain. Time-based models, on the other hand, work with raw EEG signals (or preprocessed time-based EEG signals) to choose from multiple SSVEP flicker frequency classes. There are numerous advantages to using a time-based classifier for SSVEP BCIs. The first and foremost is that time-based models can achieve upwards of 90-100% classification accuracies with as low as 1s of data, whereas frequency-based models require at least 3s or 4s of data to obtain stable estimates of spectral power.

One of the more impressive sets of time-based SSVEP BCI models stems from Guangyu Bin, Xiaorong Goa, and colleagues at Beijing's Tsinghua University (Wennberg et al. 1998; Lin et al. 2007; Voytek et al. 2009; Jia et al. 2011; Y. Li et al. 2010). CCA is a multivariate statistical method used on two data matrices that may or may not share some underlying correlation. CCA measures the linear relationship between two multi-dimensional variables, producing canonical coefficients that act as weight vectors for transformation of the raw EEG signal. The goal in CCA is to maximize the correlations between the so-called canonical variables.

CCA does not constrain the two sets of multidimensional data, *X* and *Y*, unlike other correlation-based exploratory statistical methods such as principal component, independent component or factor analysis. Rather, CCA finds the weight vectors, W_x and W_y that maximize correlations between the linear combinations of *X* and *Y*, i.e. $x = X^T W_x$ and $y = Y^T W_y$. This max canonical correlation, ρ, is calculated as follows:

$$\begin{aligned} \max_{W_x, W_y} \rho(x,y) &= \frac{E[x^T y]}{\sqrt{E[x^T x]E[y^T y]}} \\ &= \frac{E[W_x^T XY^T W_y]}{\sqrt{E[W_x^T XX^T W_x]E[W_y^T YY^T W_y}} \end{aligned} \tag{3.7}$$

Bin et al.'s CCA model is shown below in **Figure 3-11** (Miller et al. 2009; Bin, Gao, Yan, et al. 2009). First, a template reference signal, *Y*, is made for each of the stimulating frequencies; this reference signal (a pure sinusoid) consists of a matrix of the fundamental and harmonic frequencies over time at the same sampling rate as the EEG signal, as well as the same number of time samples in the vector. Each electrode's signal, then, is processed via the CCA algorithm at the reference/EEG buffered signal length and outputs a canonical correlation. The max correlation is considered the winner. Of the twelve participants that tested the online version of this particular setup, the average number of correct hits was 28.6 out of 30. The authors found a similar increase in classification accuracy as the sample buffer length increased over time.

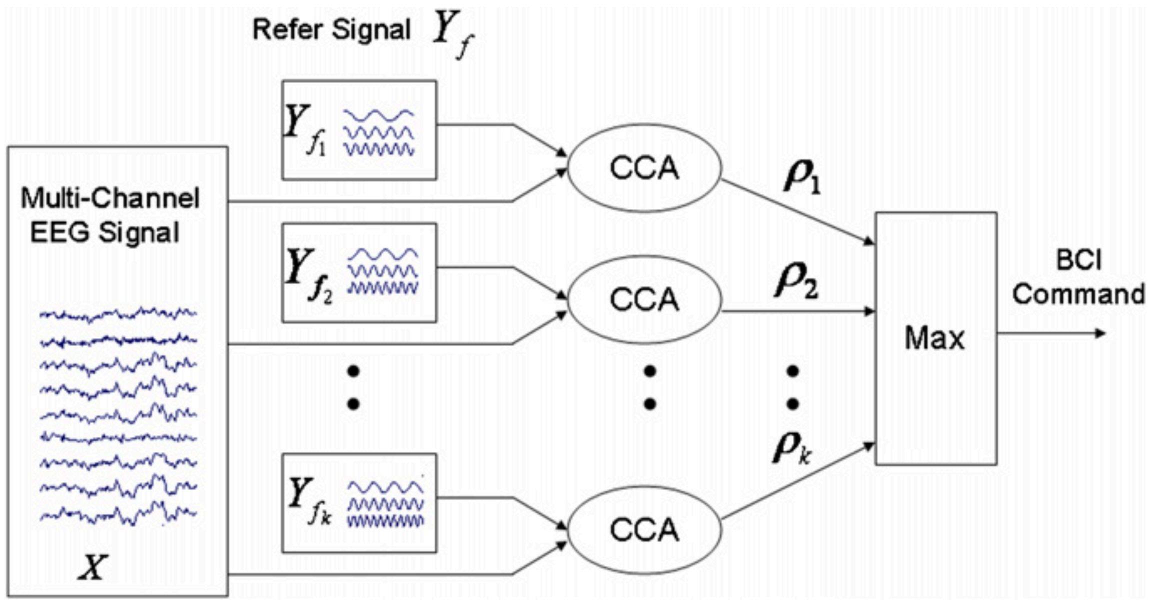

Figure 3-11. Diagram of Bin et al.'s CCA model for an online SSVEP BCI.

Researchers at NeuroSky have also recently tested a time-based classifier based on the work by Muller-Putz and colleagues (Müller-Putz et al. 2008; Luo and Sullivan 2010). Using the SLIC method, SSVEP classifications can be made by computing the correlation between ERPs that are time-locked to the stimulus onset and participant’s known response to a particular flicker frequency. This method requires precise knowledge of stimulus onset to work correctly as well as dedicated stimulus presentation hardware in order to assure accurate correlation of ERPs to flicker timing.

After SLIC features were extracted from one electrode's EEG signal at a predetermined sample length, Four LDAs were performed on the SLIC features to determine whether a particular flicker frequency was attended to or not. The greatest of these four LDA outputs was chosen if it exceeded a certain threshold value; if the threshold is reached a "YES" is given. Lastly, if enough "YES" LDA outputs are collected over a certain amount of time, a decision is made. This same system was used only with frequency-based PSD feature extraction to compare classification accuracies. The group average for SLIC performance for this four-choice task was 87.5% and 82.1% for PSD-based performance.

Another paper has also recently looked at the difference between frequency- and time-based SSVEP models by comparing harmonic frequency detection (using PSD estimation) to CCA detection (Hakvoort and Reuderink 2011). The same CCA methods used in the Bin et al. paper mentioned earlier in this section were compared to a simplified version of the HSD frequency classifier. Similar to Bin et al., the authors found that the CCA method performed anywhere from 10-55% better across a number of stimulating frequencies and across subjects.

Lastly, a very different approach to time-based SSVEP decoding, originally used by Sutter in his 1992 brain response interface paper (see **Figure 3-2**), has become *en vogue* once more. Rather than extremely precise flicker frequency stimuli, one can use something called the m-sequence – also known as a pseudorandom sequence – as a viable SSVEP BCI stimulus. Bin and colleagues have described a visual evoked potential BCI model using m-sequences in a recent IEEE magazine article (Haas 2003; Bin, Gao, Wang, et al. 2009). Briefly, the m-sequence is a binary vector sequence generated using maximal linear feedback shift registers. The binary m-sequence has an autocorrelation that approximates a Dirac delta function, or point process spike, and is nearly orthogonal to its time lag sequence (i.e., versions of the sequence created by shifting one or more bits to the left or right). With regards to stimulus flashing, “1”s turn the flash on while “0”s turn the flash off in a pseudorandom sequence over a fixed time length. This same sequence can be shifted to the left or right, resulting in a time/phase shift by a certain number of frames in order to elicit different time-lagged stimulus onset and offset responses for a large number of spatially separated frame-staggered stimulus options.

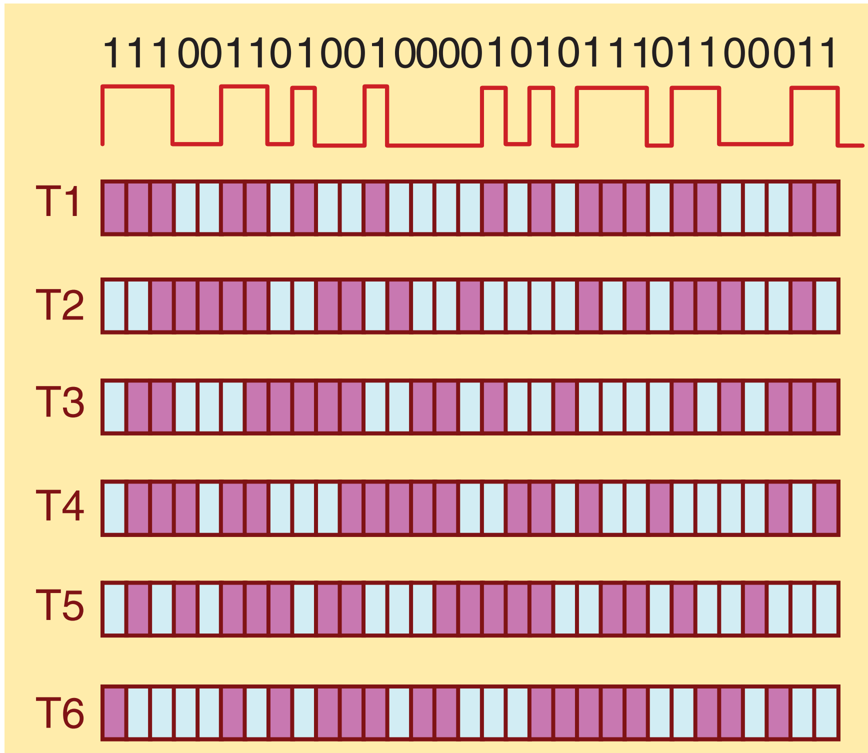

Figure 3-12. Example of a binary m-sequence staggered to the right four frames for six different stimuli (Bin, Gao, Wang, et al. 2009).

In order to identify which m-sequence, frame-staggered stimulus is being attended, a template matching system is required. First, a training session is run whereby the user fixates on one of the flashing targets as a fixed length of EEG data is collected for N stimulation cycles. The template is simply the average of the N cycles, time-locked to the start of the stimulus presentation, of collected EEG data during the training session. With k_0 being the averaged template stimulus, templates for all other stimuli can be obtained by shifting $T(t)$:

$$T_k(t) = T(t - (\tau_k - \tau_{k_0})) \tag{3.8}$$

Equation (3.8) finds the proper time lag between the template and each stimulus shifted around that template target. Next, the correlation coefficient between incoming EEG data, *x*, and template T_k is calculated:

$$\rho_k = \frac{T_k x^T}{\sqrt{(T_k T_k^T)(x x^T)}} \tag{3.9}$$

Lastly, the target template that maximizes ρ_k is considered the class winner. Non-spectral, statistical correlation methods such as the m-sequence correlation algorithm discussed above are powerful time-based SSVEP BCI models that are gaining popularity in the BCI field and show promise for future practical BCI system development.

4 A Practical SSVEP BCI Feasibility Study

Other than a few P300 Speller pilot studies in recent years (Vaughan et al. 2006; Krusienski and Wolpaw 2009), BCI technology has been confined primarily to the laboratory. The primary purpose of this dissertation was to create a BCI that was robust enough to handle real-world, in-home use by individuals with severe motor impairments such as ALS or LIS. There are a number of reasons why practical BCI development is just now becoming feasible:

- **Lack of computing power.** It was inconceivable even a decade ago to run stimulus presentation, EEG acquisition, and algorithm decoding all on one laptop. For this reason, many early BCI studies collected data and analyzed results offline.
- **Lack of portability.** Running BCIs from workstations with fast monitors is not sufficient for everyday use. The same is true for stationary, as opposed to mobile/wireless, EEG systems.
- **Inadequate electrode transmission.** Difficulty getting signals from a portable EEG cap to a computer without requiring tethered wires has been a stumbling block until recently with the advent of Bluetooth data sending capabilities.
- **Algorithm development.** BCI artifact removal, feature extraction, and classification methods have matured and refined dramatically in the past several decades.

- **User needs.** Many studies use healthy controls to test their BCIs, yet tailoring BCIs to individuals with severe motor disabilities requires understanding the user interface needs they require – not just focusing on classification rates and higher bit-rates.

This study aimed to address each of these concerns in order to develop a robust noninvasive EEG-based BCI using the steady-state visual evoked response due to its high bit-rates and lack of long training sessions. The goal of the following experiment was to determine whether or not an SSVEP-controlled BCI is a feasible option for severely motor impaired individual use. A tandem objective is to validate and confirm the Unlock Project system is functioning usefully for both paralyzed and healthy participants.

4.1 Methods

4.1.1 Participants

Control participants were 14 healthy adults (9 women, 5 men; age range = 22 – 65; mean age = 32, SD = 14.41). No visual, motor, or cognitive deficits were reported for any of the individuals in the study. Due to the nature of the SSVEP stimulus presentation method, participants also had no prior history of epilepsy or susceptibility to seizures brought on by flashing light. Paralyzed participants consisted of 5 adults (1 woman, 4 men; age range = 29 – 64; mean age = 46, SD = 14.59). Two paralyzed individuals had traumatic brain injuries resulting in brainstem strokes; two participants had ALS and one individual had a form of

Parkinson's known as Progressive Supranuclear Palsy (PSP). Informed consent was obtained from all control subjects in accordance with the Boston University Institutional Review Board. For paralyzed participants, informed consent was obtained by a caregiver with power of attorney on behalf of the study participant. Paralyzed participants also were asked to communicate assent to study procedures.

4.1.2 Hardware

Recording was performed with the g.Tec MOBIlab+ (Guger Technologies, Graz, AT). Three active electrodes were used for SSVEP – O1, Oz, and O2 – and one active electrode for eye blink detection placed at AF8 over the right lower temple. A passive ground was placed in the center of the forehead at FPz and a reference ear clip was attached to the right ear. EEG signal was acquired at 256 samples per second and sent wirelessly via Bluetooth to a Lenovo ThinkPad running Ubuntu 12.04. A custom wrapper from g.Tec's C++ API to Python was created in order to acquire and modify raw, real-time EEG signals in Python.

4.1.3 Software

The Unlock Project API, as described in Section 2.4.3, was used for raw EEG signal preprocessing, SSVEP stimulation, user neurofeedback, screen display items, artifact detection, feature extraction, and classification. **Table 4-1** gives a brief overview of the software and algorithmic structure used in this initial test run of the Unlock Project API and all its components running at once.

BCI System 1.0	
Computer/OS/Language	Lenovo ThinkPad running Python on Linux OS
SSVEP Stimulation Method	LCD laptop screen with rectangular checkerboards
Artifact Detection Method	Running mean for eye blink detection
Feature Extraction Method	4s FFT with frequency bin averaging
Classification Method	HSD

Table 4-1. Initial BCI study system plan using the Unlock Project API.

4.1.4 Stimulation

The screen refresh rate of the ThinkPad was 75Hz. The experiment presented four on-off checkerboard pattern SSVEP stimuli that were 600 pixels wide by 100 pixels high for the top and bottom stimuli, and a 90-degree rotation (100x600 pixels) for left and right stimuli. Analysis was performed beforehand to ensure that the screen draw refresh rate was at or around 60 frames per second in order to obtain precise enough stimulus presentation for the SSVEP paradigm. The checkerboard was white-black for optimal contrast with the rest of the screen being black, thus the checks that were black remained black in the on-off pattern whereas white checks alternated between white and black. An alternate square 250x250 pixel checkerboard with an x- and y-spatial frequency of 5 (where a “1” is 100px) was also used for comparison to the rectangular stimulus described earlier in order to test variations in stimulus shape and spatial frequency. Lastly, the participant sat approximately 60cm from the screen in order to maximize SSVEP response in V1 for one stimulus direction without interfering with the other three checkerboards on the screen.

4.1.5 Procedure

Frequency Sweep Configuration

Each participant began with an initial SSVEP frequency configuration run whereby the participant was shown a text cue in the screen's center for 2s indicating the direction to attend (Up, Down, Left, Right). The participant was then asked to attend to one of the four SSVEP frequencies flickering for 5s in duration. Participants were told not to move their head and restrict eye movements to a minimum. The flicker frequencies were displayed in random order and chosen from a set of ten possible options: 6.67, 7.0, 7.5, 8.0, 8.57, 12.0, 13.0, 14.0, 15.0, and 16.0 Hz. Each of these ten frequencies was chosen as the trial attend direction target 5 times per frequency, resulting in 50 total trials. These particular frequencies were originally used because they are either integer divisors of 60Hz or commonly used SSVEP stimulating frequencies.

Four-choice SSVEP Online Prediction

For this task, subjects were shown a 2s text cue on the screen's center, instructing them to attend to one of four directions as described above for the frequency configuration run. After the cue presentation, subjects were instructed to hold their fixation on the attended flicker frequency direction for 4s. A fixed set of flicker frequencies (12.0, 13.0, 14.0, and 15.0 Hz, representing up, down, left and right in that order) were used for comparison across all participants. A real-time feedback "thumbs up" was displayed if a correct prediction of the attended direction was made or a "thumbs down" if the BCI algorithm guessed incorrectly. Once the prediction cue disappears, a blank 1s inter-stimulus interval was given before starting the next trial. At least four runs were performed for each subject with each run consisting of 20 total trials – five repetitions per flicker frequency in each of the four attended stimulus directions.

4.1.6 SSVEP Prediction

Preprocessing

The SSVEP decoder acquires data sampled at 256Hz, adding it to a buffer until four seconds (or 1024 samples per channel) of data is buffered. For preprocessing, zero-mean normalization is applied to the four-second segment of data. A Butterworth bandpass filter was initially used but is unnecessary given that higher and lower frequency components are not accounted for using the HSD classifier method. Thus, the bandpass filter was removed to save on computational power. Another preprocessing step that was only used for offline testing in a few participants creates a baseline power spectral FFT vector based on the subject's rest period data. Having the subject stare at a blank screen for twenty seconds was used as a simple calibration run. From this data, the mean can be taken over five four-second data segments, and then an FFT of this average trial segment is used as a baseline power spectral estimate. This method can be used as an alternative to subtracting the 4s trial mean as discussed above.

Feature extraction

After the buffered data is preprocessed for O1, Oz and O2 electrodes, the FFT and absolute value is calculated over each electrode. Since the four stimulating frequencies used are close together in the spectral space, it is assumed that using the magnitude-based FFT is sufficient as opposed to the log10-based FFT. Both variations were analyzed for offline classification purposes and showed similar accuracies, although the magnitude-based FFT seemed to perform slightly higher, thus only the magnitude-based FFT was used for online prediction. For offline analysis, an alternative power spectral estimate using the multi-taper method (MTM) was calculated as a classification comparison with FFT results. Results comparing these two methods are discussed in detail in the results section. Once preprocessed data was converted into the frequency domain, a 0.2Hz window was taken over each of the four stimulating frequencies and their first harmonics. For example, with a 15Hz stimulus all the spectral values between 14.9 to 15.1Hz as well as those between 29.9 to 30.1Hz were extracted.

Classification

Once harmonic windows are found for each of the stimulating frequencies, the mean value within the fundamental frequency (FF) window and first harmonic (H1) window are found for each electrode. The mean value over each electrode is then taken for both the FF and H1 windows. Lastly, these two values are summed. This renders one harmonic sum per flicker frequency, and the *argmax* of these four is considered the attended direction. This process is then once every four seconds (with no overlap of 4s windows).

4.1.7 EOG Selection

For the static and hierarchy grid tasks, the adaptive mean estimation technique used by Vidaurre et al. was implemented in order to detect eye blinks, shown below in Equation (3.10)(Vidaurre et al. 2011). The researchers in this paper found that the optimal update coefficient value, η_μ, is 0.05, thus it was used in our setup as well.

$$\mu_i(t) = (1-\eta_\mu)\cdot\mu_i(t-1)+\eta_\mu\cdot x_i(t) \tag{3.10}$$

Eye blinks create very distinct patterns in the EEG signal and with this simple adaptive mean estimation equation we were able to smooth the incoming samples and set a threshold. This eye blink threshold was different for each subject and was adjusted manually as needed. If two eye blinks were above the threshold and separated by at least 200ms, this was classified as a double eye blink or “1” in the binary switch. This double blink timing parameter was also subject-dependent.

4.2 Results

4.2.1 Frequency Sweep Configuration

Each participant in the study began the session with a configuration run to see which frequencies would be best to use for a four-choice SSVEP decision task. The four best frequency outputs from the algorithm were not used for the task in the following section, since the goal for that study was to compare the same four frequency responses across all participants. **Figure 4-1** shows a typical PSD output of the top four (in blue colors) and bottom four (in orange colors) stimulating frequencies averaged over each of the ten displayed frequencies. It is noteworthy that the top four frequencies tend to have a sharper peak than the bottom four.

After looking at the data across all frequencies, several participants had similar "top four" outputs (see **Figure 4-2**). In other words, this figure looks at how many of the participants had a certain stimulating frequency chosen as the best, second best, etc. from the list of viewed SSVEPs. Both 7Hz and 8Hz were standouts among a majority of participants as being the top two frequencies picked based solely on the sum of fundamental and harmonic amplitude values alone. The log-transformed PSD was used to account for any bias towards lower frequencies in the power spectrum. As for the bottom four choices (see **Figure 4-3**), 15, and 16Hz stimulating frequencies consistently showed lower SSVEP responses. These top and bottom calibration frequency result figures consist of both control and paralyzed participants.

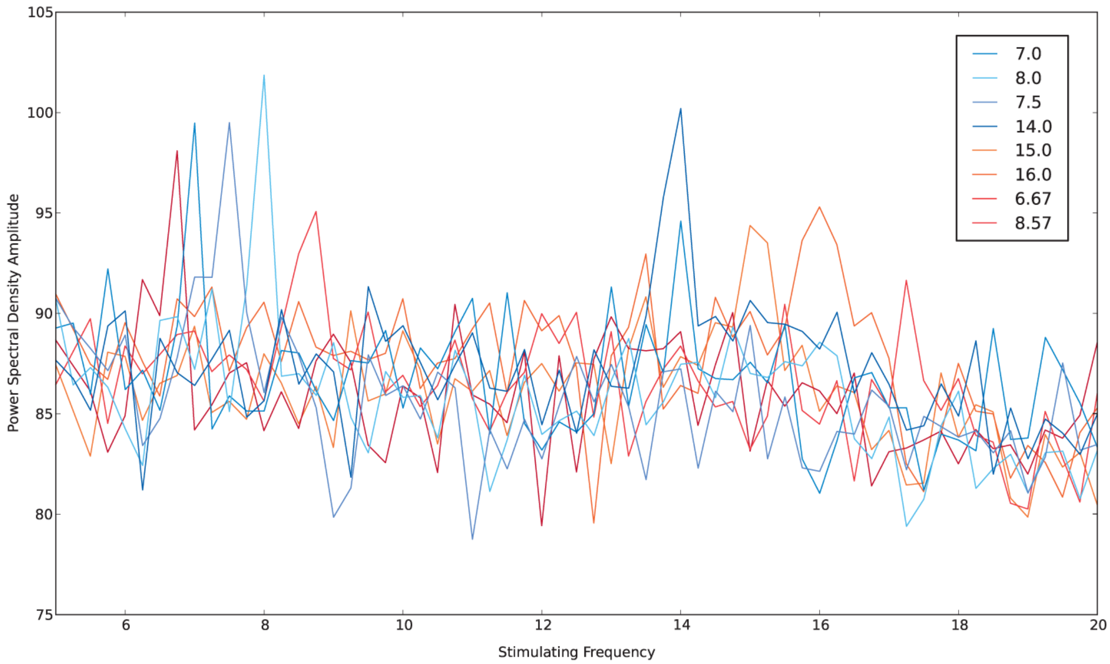

Figure 4-1. Top and bottom four calibration frequencies. The top four frequency PSD amplitudes are shown in blue colors and the bottom four frequency PSD amplitudes are shown in orange colors.

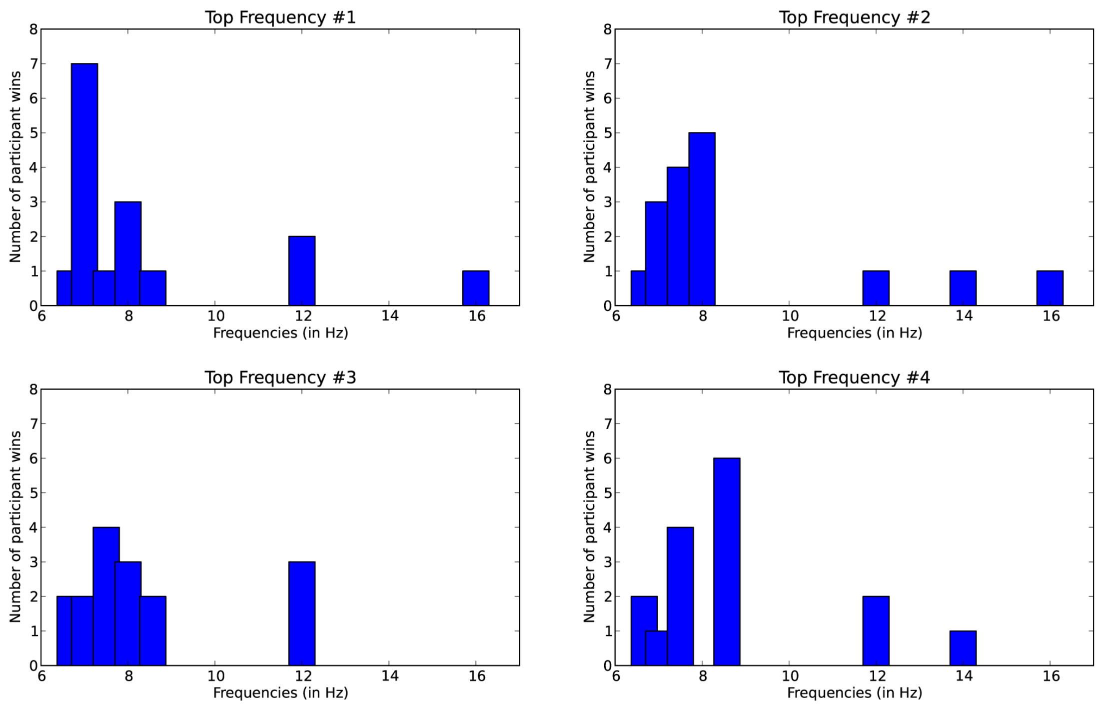

Figure 4-2. Number of times a calibration frequency was in the *top* four frequencies selected for all participants. Top Frequency #1 constitutes the stimulating frequency picked the most number of times during the SSVEP frequency calibration run. In this experiment, 7Hz was "chosen" the most number of times.

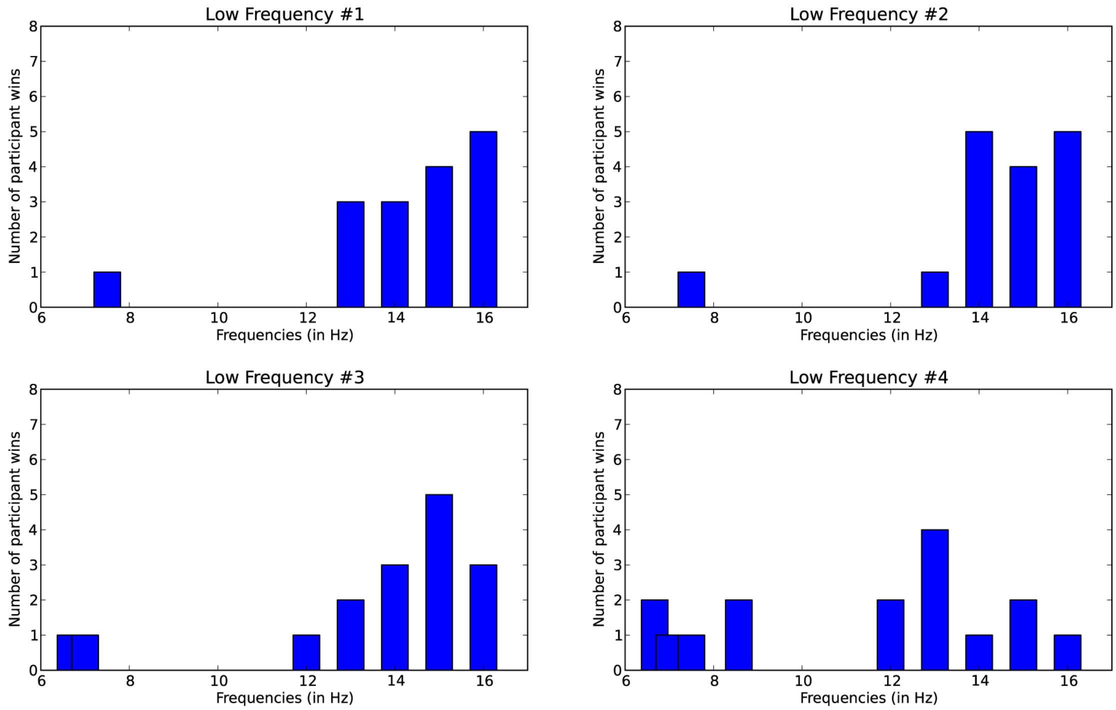

Figure 4-3. Number of times a calibration frequency was in the *bottom* four frequencies selected for all participants. Low Frequency #1 constitutes the frequency least picked by *n* participants' attention to that particular SSVEP flicker rate. In this experiment, 16Hz was the least picked of the group.

4.2.2 Four-Choice SSVEP BCI

Each of the participants in this study performed at least four runs of the four-choice SSVEP task. After two runs using the rectangular checkerboard setup, square checkerboards were then tested with varying spatial frequencies. This was done because certain participants performed better with more dense, square stimuli, whereas others performed drastically worse after this change.

Control group

Figure 4-4 shows average PSDs of a typical control participant run consisting of 40 four-choice SSVEP trials. The top plot shows the stimulating frequency response, and the bottom plot shows the first harmonic response for each direction. Since the HSD classifier sums the response of both the fundamental and first harmonic, it is helpful to have accurate peaks in both PSD frequency ranges. Unfortunately, this is often not the case. The bottom plot of **Figure 4-4** shows a very weak first harmonic response to 12Hz stimuli, whereas for 15Hz stimuli the first harmonic response is much more discriminable from the other three frequencies.

Paralyzed group

As for paralyzed participants, the PSD peak responses were not nearly as discernable as those seen for control participants. The plots shown in **Figure 4-5** are from a participant with locked-in syndrome due to a brain stem stroke nearly a decade ago. Compared to the control participant's SSVEP responses, most severely paralyzed individuals were unable to match the classification accuracies obtained for control participants; this directly correlates to the lack of differentiable PSD peaks across each of the four frequencies displayed. Also, there is a very strong alpha response that could be interfering with selection of the attended stimulating frequency.

Despite the lower accuracies seen in the severely motor-impaired group, each of these five participants was able to control at least one or two of the four

SSVEP attend directions as shown in **Table 4-2**. Participant SSVEP-P-001 had ALS and was able to attend to each SSVEP direction without any problems, and this is reflected in his higher accuracies across all directions. Participant SSVEP-P-002 also had ALS and was able to control both Up and Down directions. His accuracies dropped for right trials in particular due to difficulty seeing clearly through his right eye. Left trials were also difficult for him because of the angle of the screen relative to his reclined wheelchair position. Participant SSVEP-P-003 suffered from a traumatic brain injury (TBI) and was unable to keep his head positioned straight ahead in his wheelchair. To accommodate his needs, we positioned the laptop running the SSVEP BCI on a tray to his left side so that he could rest his head comfortably to one side. This positioning may have caused difficulties for this subject to see all four SSVEP stimuli clearly, and could be why only left and up directions showed accuracies above chance. Participant SSVEP-P-004 had Progressive Supranuclear Palsy (PSP) and squinted through a majority of the SSVEP trials due to blurry visions brought on by her condition. She was also unable to see anything underneath her, which is why her Down trials all had 0% accuracy. Lastly, participant SSVEP-P-005 suffered from a TBI and reported no particular visual deficiencies, however, he did acknowledge having difficulty attending to the SSVEP stimuli for long periods of time and grew tired after only a few runs. This particular participant also had very limited eye movement as well as eye blinking abilities that may have made it difficult for him to attend anywhere other than Up (as noted by his high accuracy only in this direction).

Subject ID	Total % Correct	Up % Correct	Down % Correct	Left % Correct	Right % Correct
SSVEP-P-001	50.42	**67.5**	**45**	**41.67**	**47.5**
SSVEP-P-002	41.67	**41.67**	**83.33**	25	16.67
SSVEP-P-003	20	**40**	0	**75**	10
SSVEP-P-004	31.25	**40**	0	**75**	10
SSVEP-P-005	31.25	**70**	25	15	15

Table 4-2. Total, and individual attend direction, percent correct accuracies for all five paralyzed participants. Accuracies high enough to possibly be used for control are shown in bold, larger fonts.

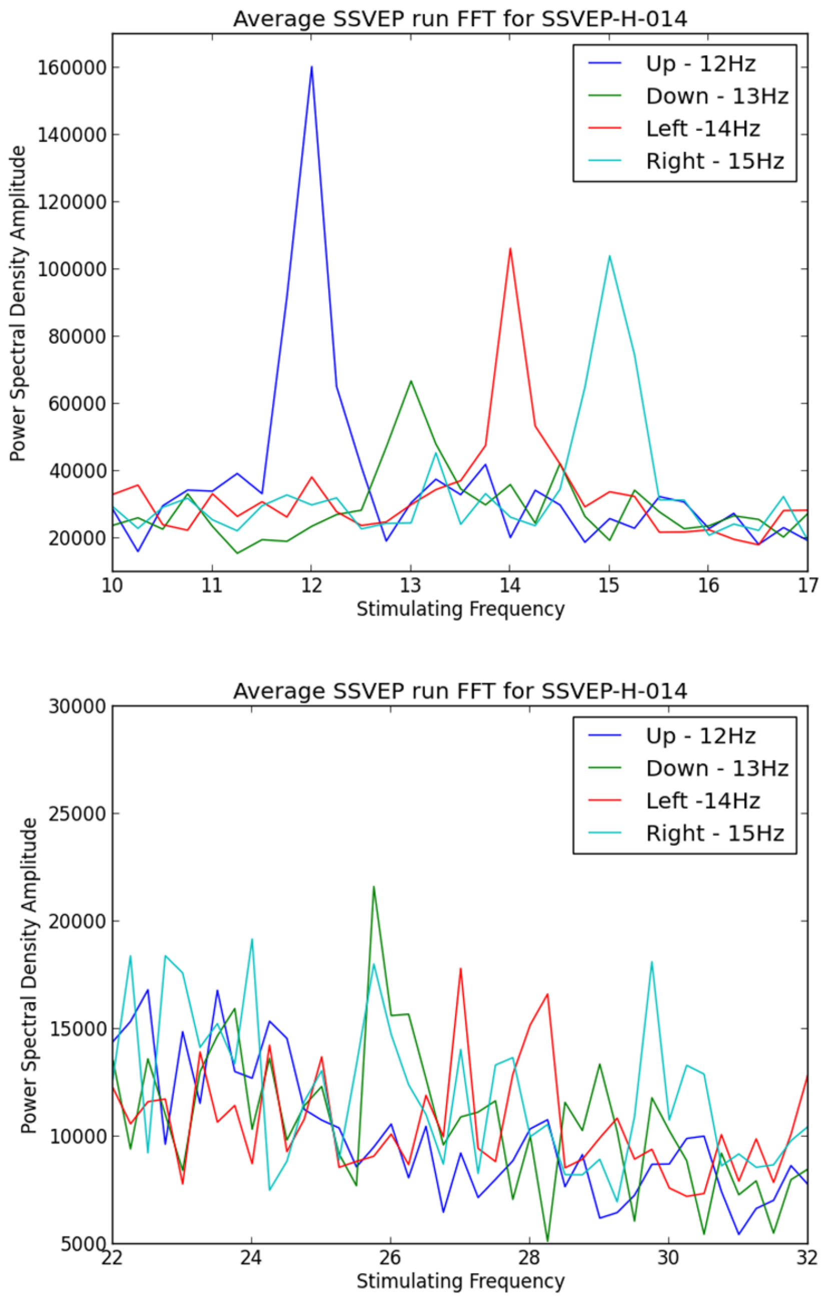

Figure 4-4. Average SSVEP Up, Down, Left, Right PSD values for a control participant. The participant was shown 12, 13, 14, and 15Hz stimulating frequencies. (Top) Fundamental frequency amplitudes for each of the four SSVEP directions. (Bottom) First harmonic amplitudes for each of the four SSVEP directions in the same run.

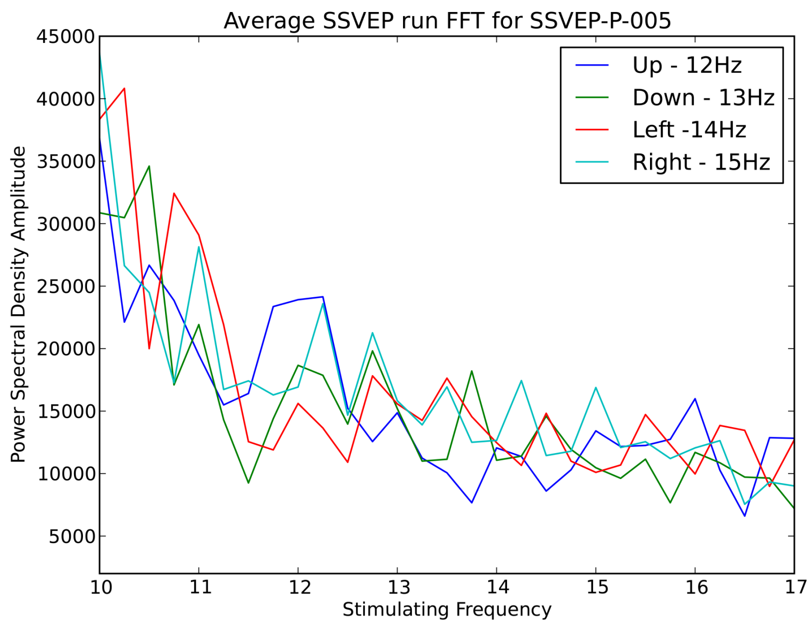

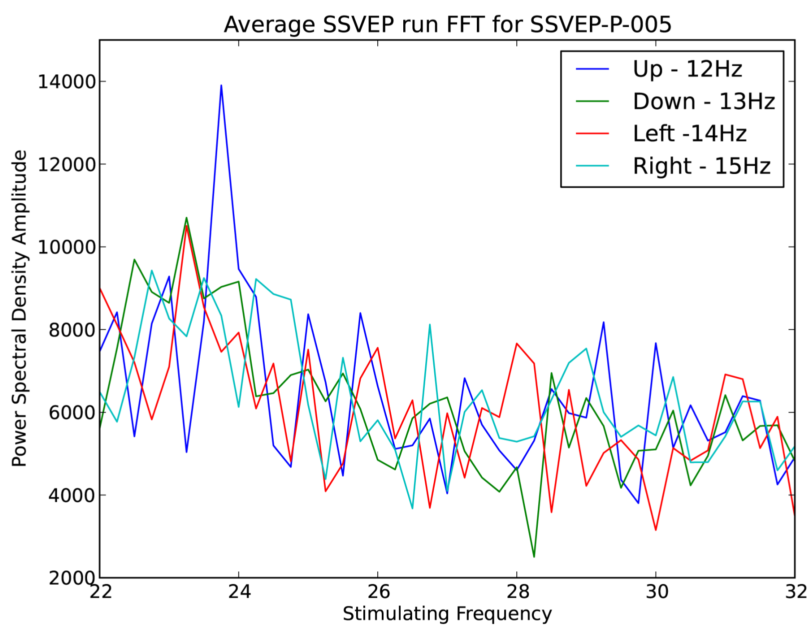

Figure 4-5. Average SSVEP Up, Down, Left, Right PSD for a locked-in brain stem stroke participant. The participant was shown 12, 13, 14, and 15Hz stimulating frequencies. Fundamental frequency amplitudes for each of the four SSVEP directions (Top). First harmonic amplitudes for each of the four SSVEP directions in the same run (Bottom).

An analysis of maximal PSD amplitudes was also performed in order to discern differences across the fundamental frequency and first harmonic responses for each attended direction. **Figure 4-6** shows the average maximum PSD response for a control participant across all runs. First, it is obvious from this figure that the UP attended frequency, which was 12Hz here, had a far greater response for this particular participant than the other three frequencies. Were the frequency sweep configuration outputs used for this task, the max PSD amplitudes may have been more homogenous and also rendered higher classification rates overall. Also worth noting is the trend towards increased max PSD amplitudes after each run. This increased amplitude response trend was similar across a number of participants, a tendency that supports the claim that more exposure to SSVEP stimuli can increase classification accuracies.

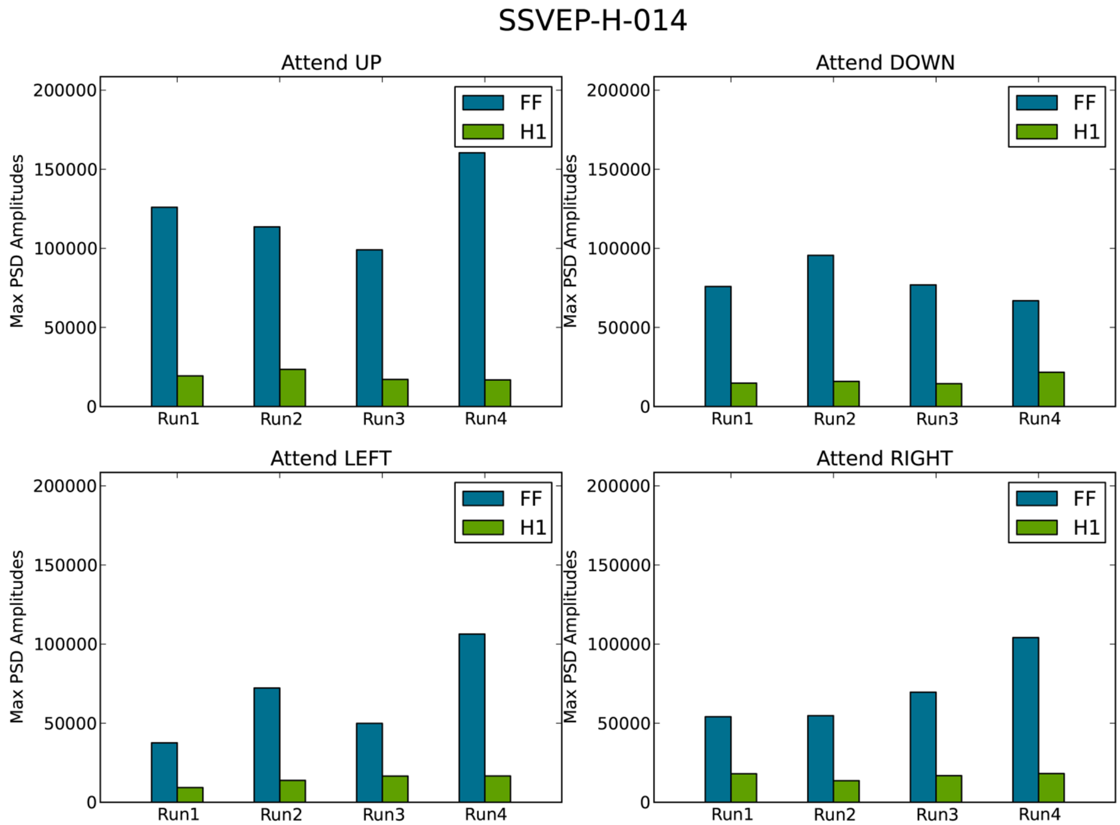

Figure 4-6. Maximum PSD Amplitudes over all SSVEP Up, Down, Left, Right runs for a control participant. For each attended direction, the average maximum PSD value was calculated over all trials within a run. The fundamental frequency (FF) max response is show in blue; the first harmonic (H1) max response is shown in green.

Figure 4-7 shows the same results and trends as the prior figure only for a paralyzed participant. One differentiating factor between the control and paralyzed groups was a decrease in the fundamental frequency response for paralyzed participants. Lastly, with regards to PSD harmonic frequency response, **Figure 4-8** simply gives another way of viewing fundamental and harmonic frequency data from all participants in the study. For this figure, each participant is represented as either a blue circle (control) or a green square (paralyzed). The max PSD amplitude values from **Figure 4-6** and **Figure 4-7** are used to plot x-y points. This was done in order to see if any noticeable clusters emerged between the two groups, yet no discernable group differences were seen in this respect.

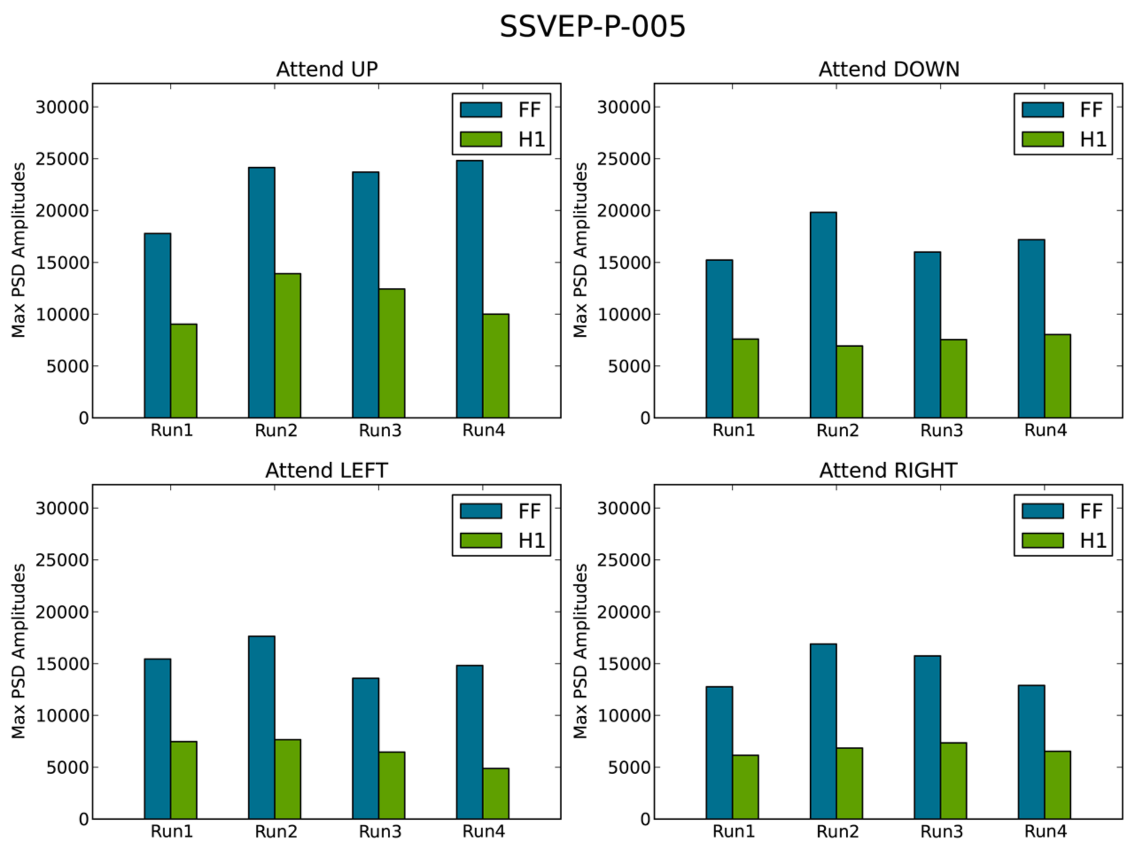

Figure 4-7. Maximum PSD Amplitudes over all SSVEP Up, Down, Left, Right runs for a locked-in brain stem stroke participant. For each attended direction, the average maximum PSD value was calculated over all trials within a run. The fundamental frequency (FF) max response is show in blue; the first harmonic (H1) max response is shown in green.

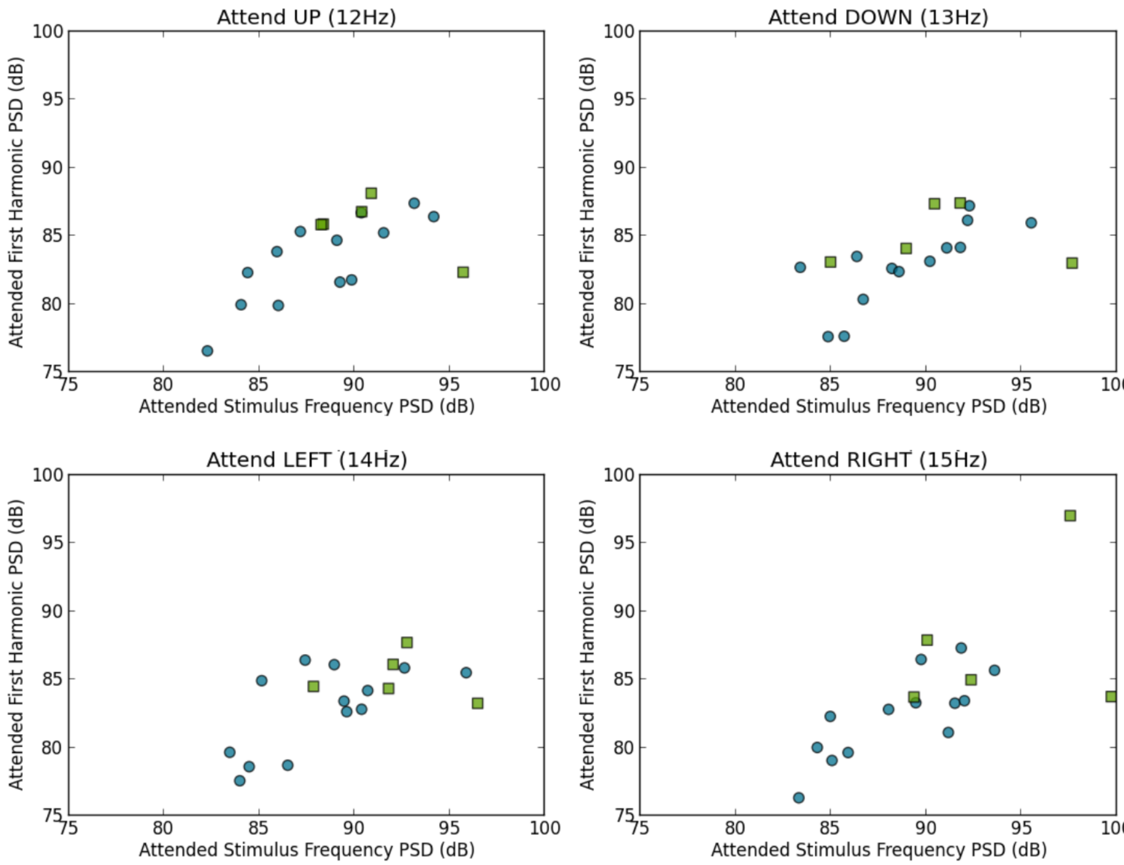

Figure 4-8. Average attended SSVEP direction stimulus frequency and first harmonic for Up, Down, Left, Right in both control and paralyzed participant groups. Both the x- and y-axes are power spectral density values in decibels. Control participants are shown as blue circles and paralyzed participants in green squares.

Although there were no PSD clustering differences between the two groups, there was a notable split seen for classification accuracies as seen in **Figure 4-9**. Overall, paralyzed participants (shown in blue) performed worse than those in the control group (shown in green). The two higher functioning participants in the paralyzed group both had ALS yet were able to communicate via either an eye gaze tracker or having a loved one lip-read. Both of these participants were locked-in yet highly attentive and cognitively aware individuals, and thus performed much better during the four-choice SSVEP task than the other more low-functioning severely motor-impaired individuals in this study.

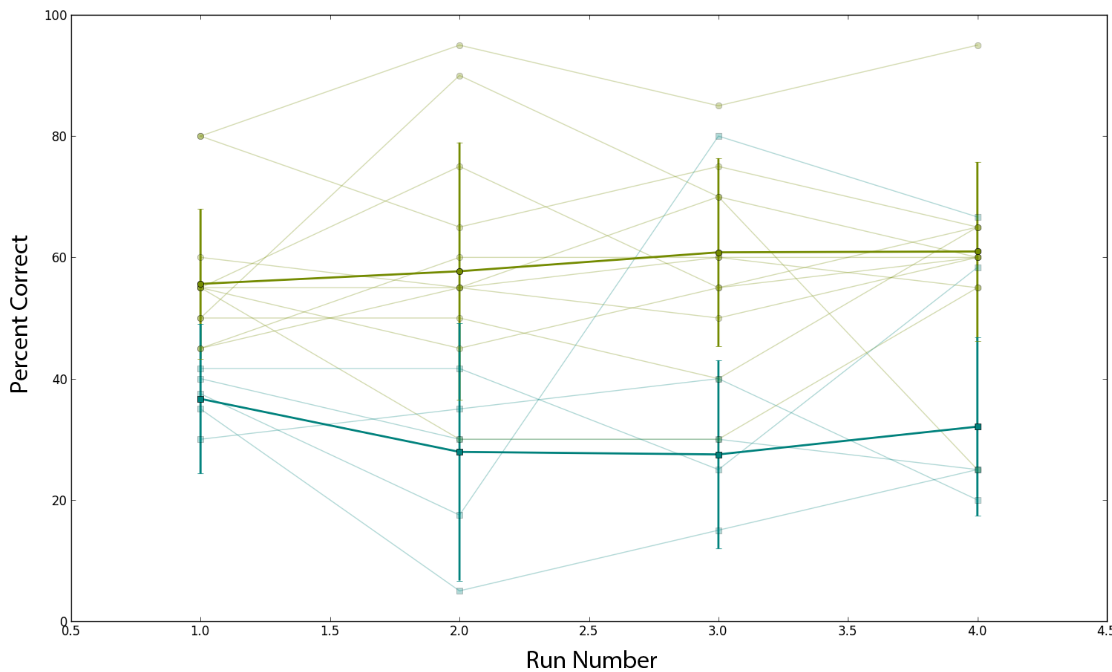

Figure 4-9. Mean classification percent accuracy results over four runs for both control (green) and paralyzed (blue) participant groups. Individual results for controls are shown in light green and those for the motor-impaired group are shown in light blue.

Figure 4-10 clearly demonstrates the differences in percent correct across all runs for the two groups. This result was confirmed quantitatively via a one-way analysis of variance (ANOVA) for class accuracies comparing the two groups: control versus paralyzed. The ANOVA analysis revealed a main effect of subject group ($p < 0.001$) which indicates the two groups showed statistically significant differences in classification accuracies.

In order to test whether or not these low classification accuracies in the paralyzed group were due to the feature estimation method used, three variations of calculating the PSD were compared before running the HSD algorithm (see **Figure 4-11**). For both groups, the percent correct scores shifted slightly – for better and worse – but there was no significant advantage seen for one PSD calculation method over the others for either population group. To validate this result, a one-way ANOVA was run across the three groups: HSD-FFT-Magnitude, HSD-FFT-Log10, and HSD-MTM-Magnitude. There were no significant main effects of PSD method ($p = 0.1154$), thus the null hypothesis could not be rejected. No particular method variation tested here was statistically different in obtaining higher accuracies than the other two.

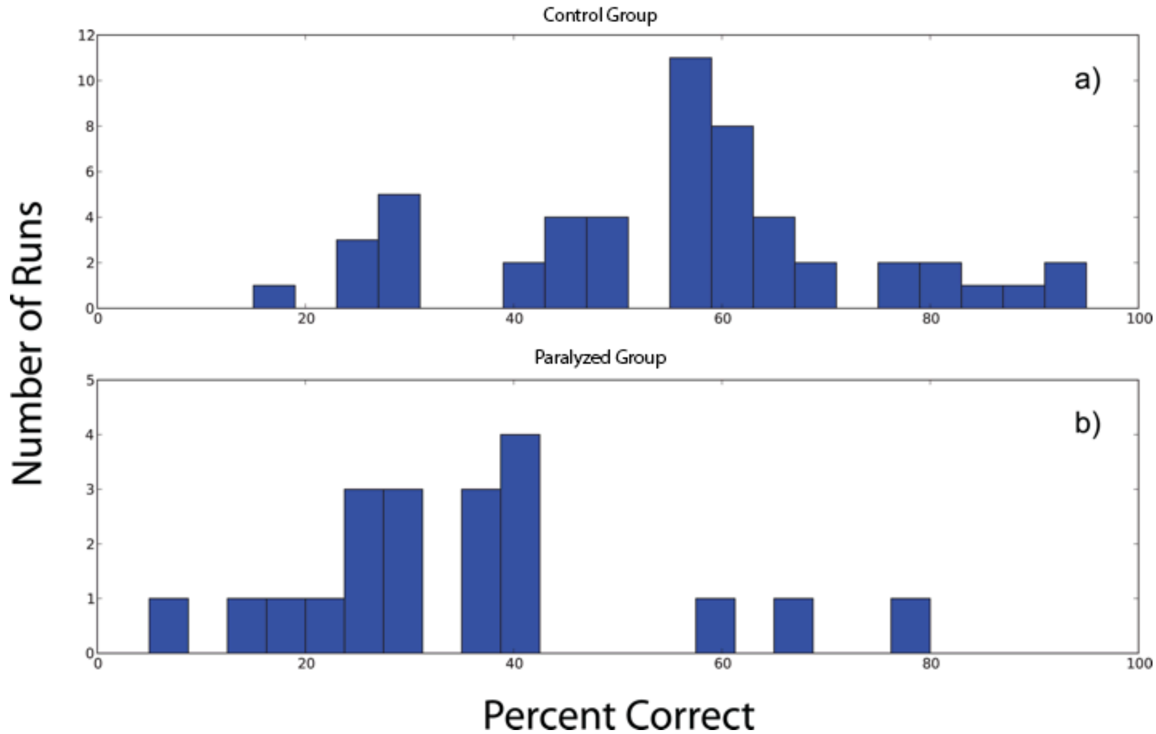

Figure 4-10. Classification percent correct histogram between a) control and b) paralyzed participant groups. Each participant performed four runs of the four-choice SSVEP experiment.

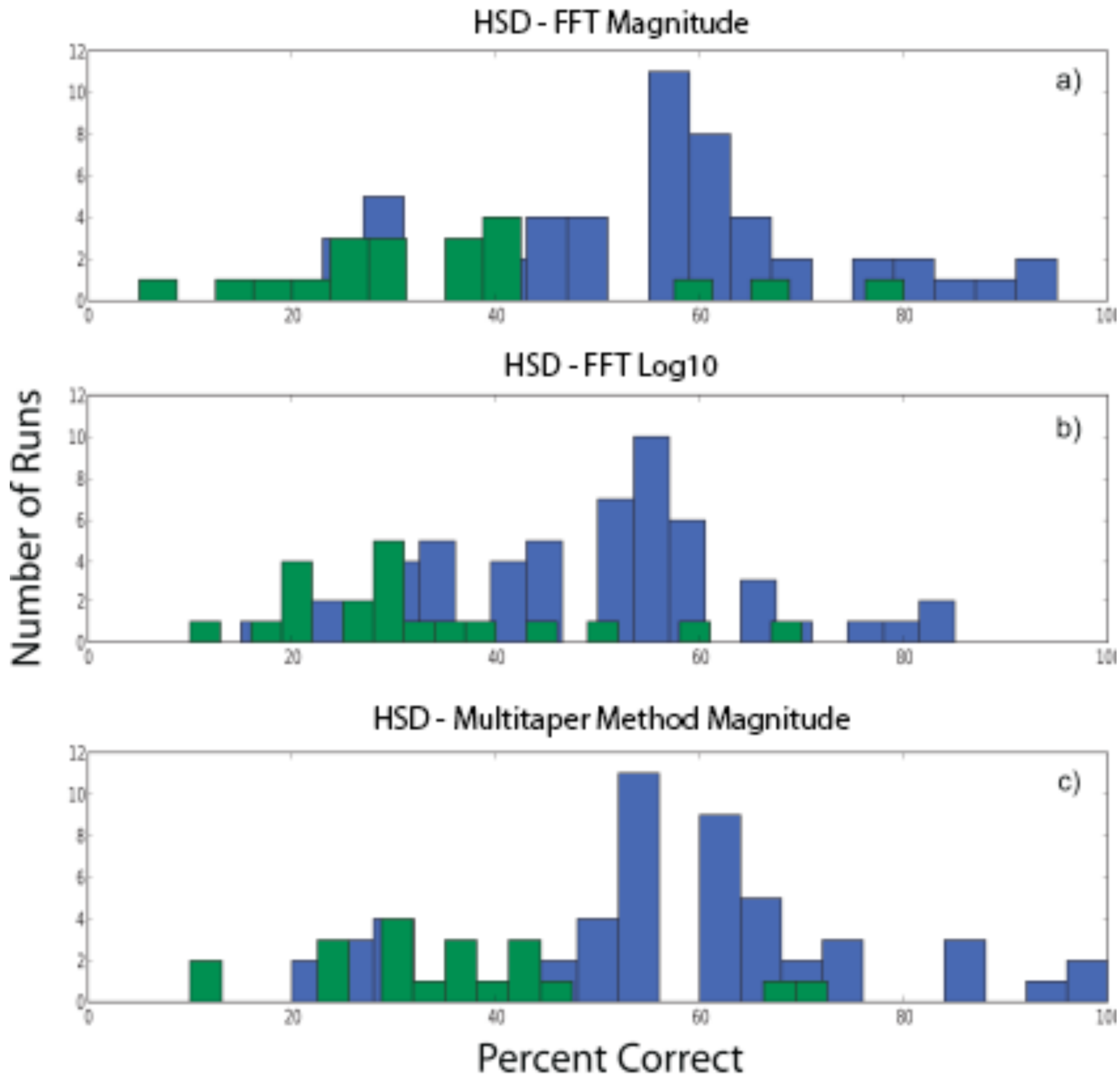

Figure 4-11. Comparison of three different HSD power spectrum analysis techniques across control (blue) and paralyzed (green) participant groups. a) HSD with FFT magnitude was used; b) HSD with FFT log10 was used; and c) HSD with MTM magnitude was used.

4.2.3 Alpha Response

An alpha response task was also performed halfway through the study on several control participants. The results, shown below in **Figure 4-12**, demonstrate the viability of the closed eyes alpha response as a binary switch. Most of the participants that ran the alpha response task saw peaks in the typical alpha oscillation range of 8-12Hz. This task also shows that after only 1s of closed eyes the alpha response is significantly different than background noise in the EEG signal, making it a potentially quick selection mechanism. This significance was tested using a one-way ANOVA separately comparing the six eye close segment times as groups (0.5s, 1.0s, 1.5s, 2.0s, 2.5s and 3.0s) to a PSD baseline value. This baseline was derived by taking the mean PSD value across 0Hz to 20Hz in all trials. To be conservative, 20Hz (rather than a higher PSD range) was used in order to create as high of a baseline noise level as possible. With this higher baseline estimate, the ANOVA analysis revealed a main effect of subject group ($p < 0.001$), showing that even only half of a second could be used to predict a change in alpha from baseline. As is evident in **Figure 4-12**, this change from baseline increases with every half-second interval in which the user closes his or her eyes.

This same task was tested on several paralyzed participants, however, the trials and interstimulus intervals within the run were far too short for these individuals to open and close their eyes in time, thus the data collected was unusable from these individuals. Were future experiments to be performed testing the alpha response in severely motor-impaired individuals, a more thoughtful paradigm setup should be considered that allows for increased effort and time required to open and close one's eyes. This also illustrates the need for individualized BCI setup and comprehensive assessment/evaluation.

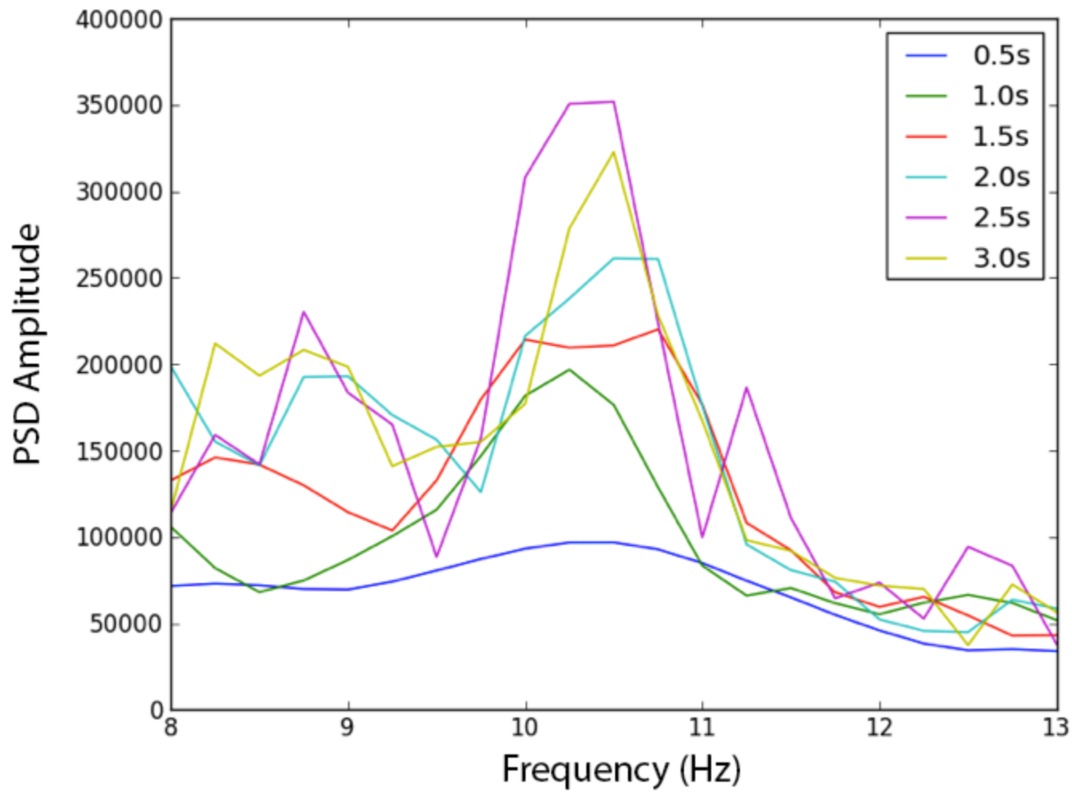

Figure 4-12. Participant SSVEP-H-005 average PSD amplitude response to "close eyes" prompts ranging from 0.5 – 3.0s. The x-axis shows this response ranging from 8 to 13Hz.

4.3 Discussion

In this study both healthy and severely motor-impaired individuals tested a number of practical SSVEP-based BCI system variations in order to increase classification accuracies for potential in-home use. A good portion of control individuals obtained 60-70% correct accuracies (low compared to the studies discussed in Chapter 3), and the classification accuracies were even lower for most paralyzed participants. There are numerous reasons for this dip in accuracy. First, attending to an SSVEP stimulus can be tiring from a cognitive standpoint, especially if eye movement control is severely impaired, and the LIS individuals reported a much faster fatigue rate when performing these tasks compared to control participants. Second, four of the five paralyzed participants in this study suffered from visual deficits in one form or another. One individual was unable to see anything below them in their foveated vision whereas two others had completely unreliable eye movements to the left and right. The inability to focus on the SSVEP stimulus due to blurriness or direct attention could be a cause for less robust neural activation in the primary visual cortex. These V1 neural responses can also drop when a user has poor peripheral vision or is unable to foveate toward the target SSVEP stimulus.

Issues such as these illustrate the fact that, were an SSVEP BCI to be practically useful for severely paralyzed individuals, to the degree possible, stimulus location on a screen should be tailored to each user's particular attention and/or eye control constraints. Also, more sophisticated decoding methods are needed, particularly those that take into consideration individual-specific patterns of response to the flashing stimuli and compare a user's response pattern during BCI use with a baseline pattern specific to that individual in order to detect directional commands. Another option is to change the classifier used. CCA is a promising technique that is gaining momentum in SSVEP BCI research, and warrants further exploration. Initial studies were performed with CCA in the lab, yet displaying SSVEP stimuli on a laptop can show inconsistencies in flicker rates that make CCA untenable. For this method to be useful, LEDs would most likely need to be attached to the edges of the laptop screen in order to eliminate the potential issues of computational processing power and screen refresh rates. In some cases a four-choice SSVEP BCI may not be viable but a two-choice option could be coupled with other non-BCI selection mechanisms to create a working alternative system. Adding EOG or alpha rhythm responses are other viable alternatives that deserver further exploration.

Although classification accuracies may have been low for several individuals, nearly all participants in the study demonstrated increases in accuracy for a four-choice SSVEP task over time. Given that the SSVEP stimulus was novel to all the participants in this study, it is hoped that regular exposure to such stimuli by paralyzed users would increase accuracies over time.

Lastly, with regards to the hierarchy and static grid tasks, the switch from cued attend direction to free movement in a grid poses a number of problems. One key issue is developing a strategy for knowing where your target is on the screen while doing your best to relax and focus on the stimulus frequency of the box to be advanced. In order to reduce cognitive strain and frustration from incorrect SSVEP movements, smaller grid sizes should make movement through a discrete grid of choices an easier task. For example, a grid composed of letters along with ten extra characters (such as space, delete, backspace, period, etc.) can be represented with a few extra characters in just a 6x6 grid. The results from this SSVEP BCI study helped shape the user interface design of the communication application discussed in the next chapter.

5 Intelligent User Interface VOCA Design

5.1 Intelligent User Interface Overview

Human-computer interaction (HCI) is an interdisciplinary field that unites concepts taken from computer science, neuroscience, cognitive psychology, graphic design and other fields, building new ways for people and computers to interact. More specifically, a relatively new subfield of research, intelligent user interface (IUI) design, has emerged in order to address HCI techniques by merging artificial intelligence methods into the HCI corpus (Lopez Jaquero et al. 2009). IUIs, then, are human-machine interfaces that should improve efficiency, effectiveness, and the natural interaction between user and device. By including the domain of artificial intelligence into the equation, IUIs fuse knowledge of cognitive science with all the areas traversing this wide, interdisciplinary field – vision, speech and language processing, planning, reward, spatial attention, learning and memory, among other fields..

There are also numerous cognitive (e.g., perceptual, attention, and memory) principles discussed in the HCI literature that will inevitably need to be addressed when creating practical BCIs. These methods are beyond the scope of this dissertation but should be a helpful foundation in building user-centered BCI apps. For example, according to a foundational paper by Mark Maybury (one of the early IUI design advocates), well designed intelligent interfaces, and traditional interfaces for that matter, should be three things: learnable, usable, and transparent (Maybury 1999)

Maybury also provides a simple diagram in this paper of what an IUI would entail as shown in **Figure 5-1**. Despite the rapid change in computing power since the writing of that article nearly 15 years ago, the principles of IUI design remain largely the same today as they did then. The main three sections of this diagram involve:

1. *Presentation* as represented by input processing and output rendering;
2. *Dialog control* as an overlap between the media analysis/design subareas with the interaction management modules; and
3. *Application interface* that represents models, such as those seen on the bottom of **Figure 5-1**, supporting intelligent interaction.

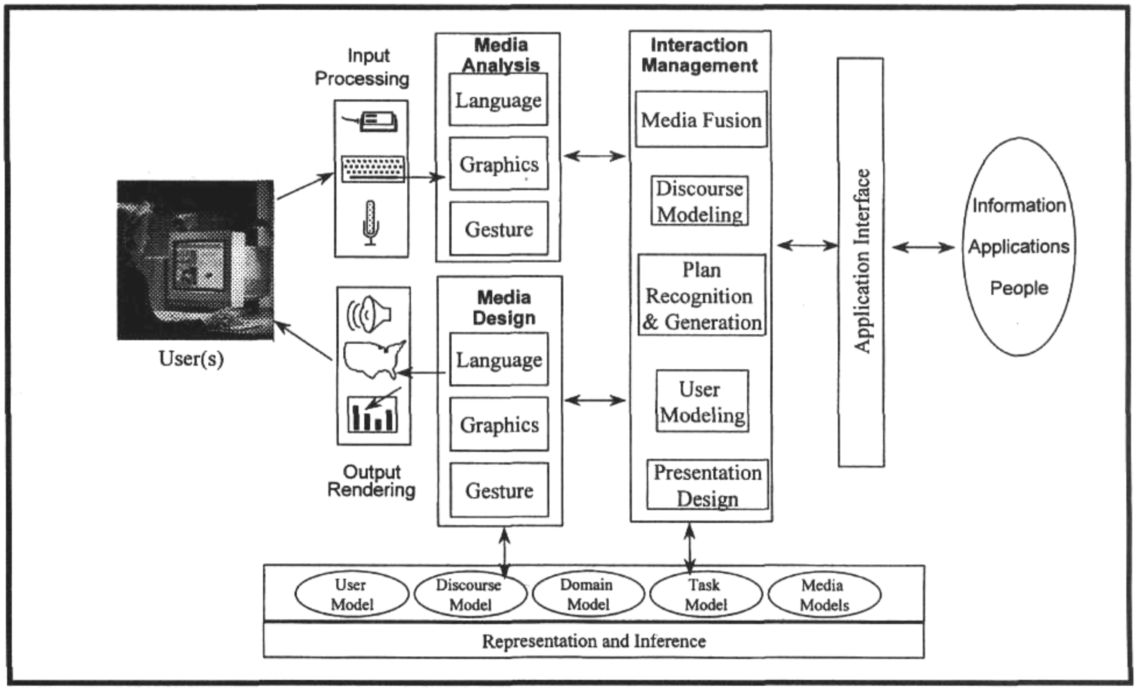

Figure 5-1. Maybury's 1998 architecture of a sample intelligent user interface.

Traditional user interfaces dealt only with presentation, dialog and application in a simple input/output manner, whereas intelligent interfaces take into account variability across users and move beyond canned text, sounds, or images. One difficulty with this merging of multimedia components is knowing how to coordinate mouse clicks, voice recognition commands, keyboard presses and other computer inputs in a holistic and meaningful way. For example, with regards to the IUI being constructed in this dissertation it was difficult to merge sensor data such as global positioning system (GPS) coordinates and facial recognition with text-based natural language processing (NLP) prediction outputs. For this reason, fusion of these two elements was considered beyond the scope of this dissertation and is being pursued as a future direction.

A key asset to resolving some of these issues is the context-sensitive augmentative and alternative communication (AAC) device work begun by Rupal Patel and colleagues in the MIT Media Lab and Northeastern University. An early goal was to combine multimodal sensing of a user via haptic, visual, and auditory inputs with machine learning techniques (Patel 1998). Once the system is trained, a user would make some form of salient behavior that the algorithm recognizes to perform a given action or task. For individuals with severe speech impairment, a teachable interface that uses multimodal cues may be more efficient and reliable than traditional mouse/keyboard setups. A context-aware interface can receive real-time feedback from a user in order to adapt to the individual's specific intentions. Further, in Patel's 1998 paper, the system's goal was to translate unintelligible vocal sounds into either computer-guided actions or speech synthesizer outputs.

In a later study, GPS was used as a context-aware input sensor for a communication aid (Dominowska, Roy, and Patel 2002). Traditional AAC devices rely on static layouts to display vocabulary, a method that can make communication a long, tedious process in everyday scenarios. An adaptive communication display, on the other hand, can dynamically change the layout of symbols based on the needs of the individual, taking into account geographic location in a similar way to that proposed in Section 5.4.1. Dominowska and colleagues created a chat room interface that loaded location-specific vocabulary to use GPS as contextual cues to vocabulary choices. This work was taken one step further (Patel 2007) by improving access to situational vocabulary via GPS to predict vocabulary.

5.2 Qualitative User Report Summary

Building BCI algorithms is only the first half of developing a successful real-world application – BCI user experience and feedback must also be addressed. Each paralyzed BCI user in our study reacted to the Unlock Project system in a unique way. Thus a qualitative AAC BCI survey (see Appendix A) of user experience was administered to obtain information about the protocol and relevant HCI considerations (Chin, Diehl, and Norman 1988). This questionnaire helped refine the system and tailor it to user needs in future iterations.

The qualitative survey probed participants with severe speech and motor impairments about impact of the shape, screen position placement and frequency as well as issues of cognitive strain or task difficulty. Independent of comments regarding the SSVEP stimulus itself, several questions in the survey delved into individual communication methods, reading capacity, willingness to learn a new form of communication, and preference for what type of interaction they would have with the computer.

This last question regarding interaction preference with the application prompted a complete rethinking of the ContextSpeak communication application constructed in this dissertation. The original idea was to create a corpus of canned phrases that ALS/LIS users would most likely "say" during the course of daily life. A set of eight different high-level categories such as *urgent requests*, *medical* or *feelings & emotions* were created, and each of these categories contained 24 phrases pertaining to that particular topic. For example, in *feelings & emotions* there were phrases including: "I am feeling happy" or "I don't like that." A separate questionnaire was also created in order to refine this list of phrases by asking the caregivers of each subject to list common things they'd expect their patient or loved one to say in various scenarios throughout the day.

This particular questionnaire was to be filled out after the BCI experiment session, yet none of our participants completed this portion of the experimental paradigm. We learned from most (if not all) of the paralyzed subjects that canned phrases were *highly undesirable* as a form of communication! One of the ALS subjects still had excellent eye gaze control and preferred communicating via his DynaVox system that efficiently spelled out full sentences. When asked about the proposed ContextSpeak phrases, his speech synthesizer speakers resonated a strong "no". With regards to context-specific adaptive spelling, however, this same individual became very excited at the prospect of increasing his eye gaze-controlled typing speed. Even for users unable to communicate well with an existing VOCA system, phrases were not preferable. Knowing this helped shape the context-based IUI for BCI use that is discussed in Section 5.4 (Reich 2005; Glennen and DeCoste 1997; Schlosser and Wendt 2008).

5.3 VOCA Devices for the Severely Motor-Impaired

The American Speech-Language-Hearing Association estimated in 1991 that more than two million individuals in the United States alone were unable to communicate using speech or had other severe communication issues (Reich 2005; Glennen and DeCoste 1997; Schlosser and Wendt 2008). VOCAs have been developed in order to help this population interact with their environment. In general, AAC systems include *unaided* methods such as gesturing and sign language as well as *aided* options such as picture symbol boards and computer systems with synthesized speech (i.e., VOCAs). Before discussing the Unlock Project approach to VOCA user interface design, we first look at current technology in both traditional AAC hardware and the more recent trend towards tablet-based communication aids.

5.3.1 Traditional VOCAs

The pool of companies producing dedicated VOCA hardware is relatively small considering the relatively large number of people that rely on this technology to adequately communicate with others. **Figure 5-3** shows four common VOCAs available for individuals searching popular AAC options. As one can see from these four systems, they all look and feel remarkably similar and have similar technical specifications as well.

Figure 5-2. Popular VOCA devices currently available on the market. a) DynaVox Vmax+; b) PRC Accent 1200; c) Saltillo NOVA Chat 10; d) Words+ Conversa.

According to recent academic paper reviews of AAC adaptation among ALS users, the largest technological advancement centers on the addition of eye gaze tracking (Coyle et al. 2004; Beukelman, Fager, and Nordness 2011; Beukelman et al.

2007; Fried-Oken et al. 2006). This addition to commercially available VOCAs marked a significant advancement in helping individuals with severe motor impairment to select speech items on a screen for synthesizer output. Despite this advance in hardware, many of the VOCAs shown above remain fairly static with regards to software development.

5.3.2 Tablet Apps

Dedicated VOCA hardware systems can be expensive, bulky, and difficult to travel with effectively, and software development for these systems may be limited due to the restrictive screen or sensor capabilities of these systems. Some of these issues have been bypassed thanks to the boom in tablet app creation for devices like the Apple iPad or Android-based systems such as the Samsung Galaxy. The website AppsForAAC.net updates an ever-growing list of apps available for the iPhone/iPod, the iPad or both. In their "Symbol Grid System" and "Text To Speech" categories there were well over 20-30 apps of each type, with some overlap between the two.

A sample representation of what currently is available in tablet apps can be seen in **Figure 5-3**. Despite its simplistic GUI, the Intellipad iPad app is highly rated due to its inclusion of word prediction and a minimal interface. Simple design considerations such as this allow users to focus on what matters – communicating quickly and efficiently. Another app of note is the Verbally iPad VOCA that offers a choice of either *word* or *phrase* conversation tabs along with a robust *next word* prediction feature. From this list it is obvious that app-based VOCAs are the way of the future for AAC technology.

Figure 5-3. A sample set of tablet VOCA apps. a) KType; b) Assistive Chat; c) Intellipad; and d) Verbally.

5.3.3 The Unlock Project Approach

Systems such as the popular Vmax+ by DynaVox Technologies use a portable, dedicated Windows-based touch screen system requiring special hardware that can be cumbersome for severely motor impaired users, yet a simple tablet device can be used instead. Although the brain-computer communication device hypothesized here, ContextSpeak, is being developed in Python on a Linux-based laptop computer, a future goal of the Unlock Project is to make the API compatible with both iOS and Android platforms.

Many current VOCA applications/devices are still organized as simple grids with symbols, pictures, or text displayed separately, which may not adhere to IUI principles such as prompt type optimization or navigation accuracy based on cognitive variation among LIS individuals compared to those with higher motor capabilities (Birbaumer and Cohen 2007; Wallace, Hux, and Beukelman 2010). An adaptive, dynamic user interface, on the other hand, can increase communication speed as well as connect preceding and upcoming words for more fluid speech output. GUI aesthetics also play an important role. A number of VOCAs, both traditional and app-based, use stick figures, neon colors, and antiquated clip art (approved by the AAC research community) in a grid structure with too many selection elements on the screen at one time. Combining user feedback with well-planned input/output flow, reducing displayed options, and presenting only items selected by IUI agents are key aspects of efficient interaction between user and computer. Each of these components should be considered required elements for building effective BCI systems in the real world.

One difficulty with using an SSVEP-based laptop (or tablet) BCI is the amount of display space reserved for display of the flickering stimuli as shown in **Figure 5-4**. Flickering SSVEPs could theoretically take up to half the screen space if such a setup worked best for a particular user. One solution is to use LEDs for stimulation rather than display-drawn checkerboards as discussed in Section 3.3.5; LEDs could be clipped to the outer edges of a monitor or tablet, leaving far more space for application use. Allocating as much space as possible for application display is especially important for motor-impaired users that have vision problems, and may be unable to read text or see graphics clearly when below a certain pixel size.

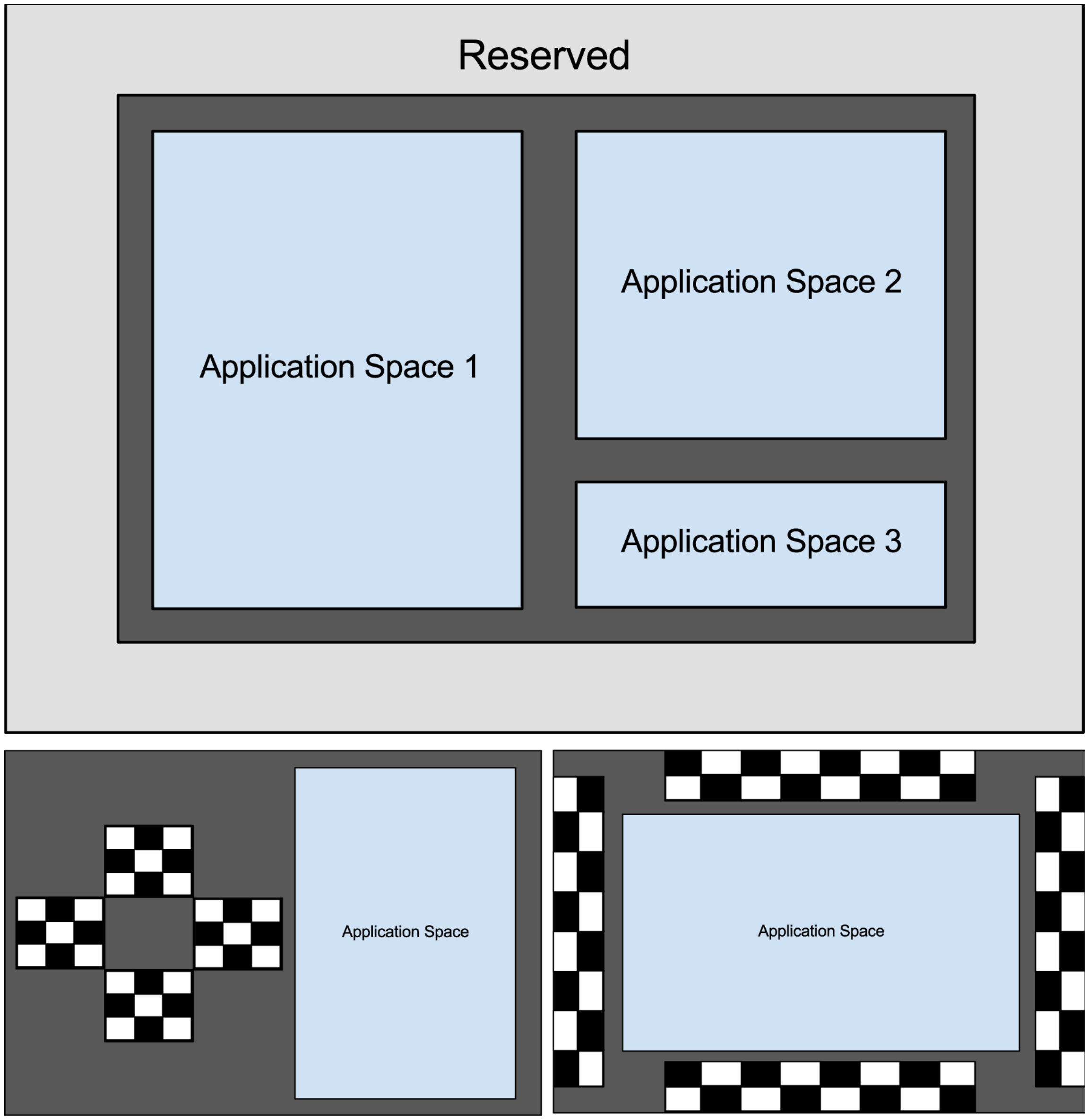

Figure 5-4. Examples of graphical layouts that can be implemented using the proposed framework. (Top) A general description of visual layouts. A section of the screen (e.g. the border in this example) is reserved for stimuli and the remaining area is partitioned for multiple apps, or displays. (Bottom) Example layouts employed in existing framework applications: Screen border SSVEP layout with four different stimuli and a single application space (right); split-screen SSVEP layout, again with four stimuli and a half-screen application space (left).

5.4 Context-based IUIs for BCI Use

Most BCIs up until this point have focused primarily on better SNR, higher classification rates, and faster bit-rates. All of these are extremely important pieces towards building a BCI that could be used one day by severely motor-impaired individuals on a daily basis – yet this is only the beginning. How do we move beyond bit-rates? How do we build a BCI device that takes the user into account? The VOCA devices and apps discussed in this chapter are stepping-stones.

With the advent of smartphone and tablet technology, however, far greater possibilities are waiting to be explored. Arguably the largest leaps forward will stem from the arena of context-aware computing. Sensor data is readily available in just about every mobile computing device on the market today, data that can be accessed and processed in real-time aboard these devices with little effort. Smartphone users will be able to get more relevant feedback and prediction from Bluetooth-enabled heart rate monitors, sports activity accelerometers, wearable sensors, and apps with user "likes" and preferences. Combining user data from their smartphone coupled with incoming data from the increasing number of wireless sensors being used to monitor daily activities can help discover data trends, offer task-related suggestions, or make predictions that would've otherwise gone unnoticed.

Three context-related IUI items were developed for purposes of this dissertation. First, an IUI model for processing context-related input/output structures was developed for the app. Second, a preliminary VOCA app GUI was designed based upon basic human-computer interaction principles. Lastly, specific NLP and sensor-specific algorithms were selected based on available sensors housed on a current tablet or laptop computer.

5.4.1 IUI Model & GUI

With the addition of sensor inputs such as an accelerometer, wi-fi, and audio input in just about every consumer computing device today, IUI principles are quickly becoming essential as more data streams bombard computer users looking for information in a streamlined manner.[7] IUI principles can be applied to real-world BCI systems as well, moving beyond reported bit rates for BCI output selection and towards BCI choices being one of many sensor inputs for user selection. The IUI system developed here relies upon computer inputs from:

- **Wi-fi** – for GPS-like access to location-specific commands;
- **Clock** – for recording internal time of day events;
- **Audio In** – for doing speech-to-text translation;
- **Bluetooth** – for receiving EEG/EOG BCI-specific selection commands; and
- **Video** – for facial recognition from built-in cameras.

The initial model had to be completely revised due to feedback from our paralyzed participants. The original goal was to display only four context-

[7] See introduction of Apple's Siri as an example of a simple yet well-constructed IUI consumer input data integration device.

dependent *phrases* on the screen (**Figure 5-5**), letting the user return to a larger set of phrase options should their choice not be displayed as one of the predicted our selections. The primary issue with this approach is that every user that was asked did not like the idea of choosing from predefined phrases. No matter how paralyzed the individual, people like to feel like they're in full control of what they say.

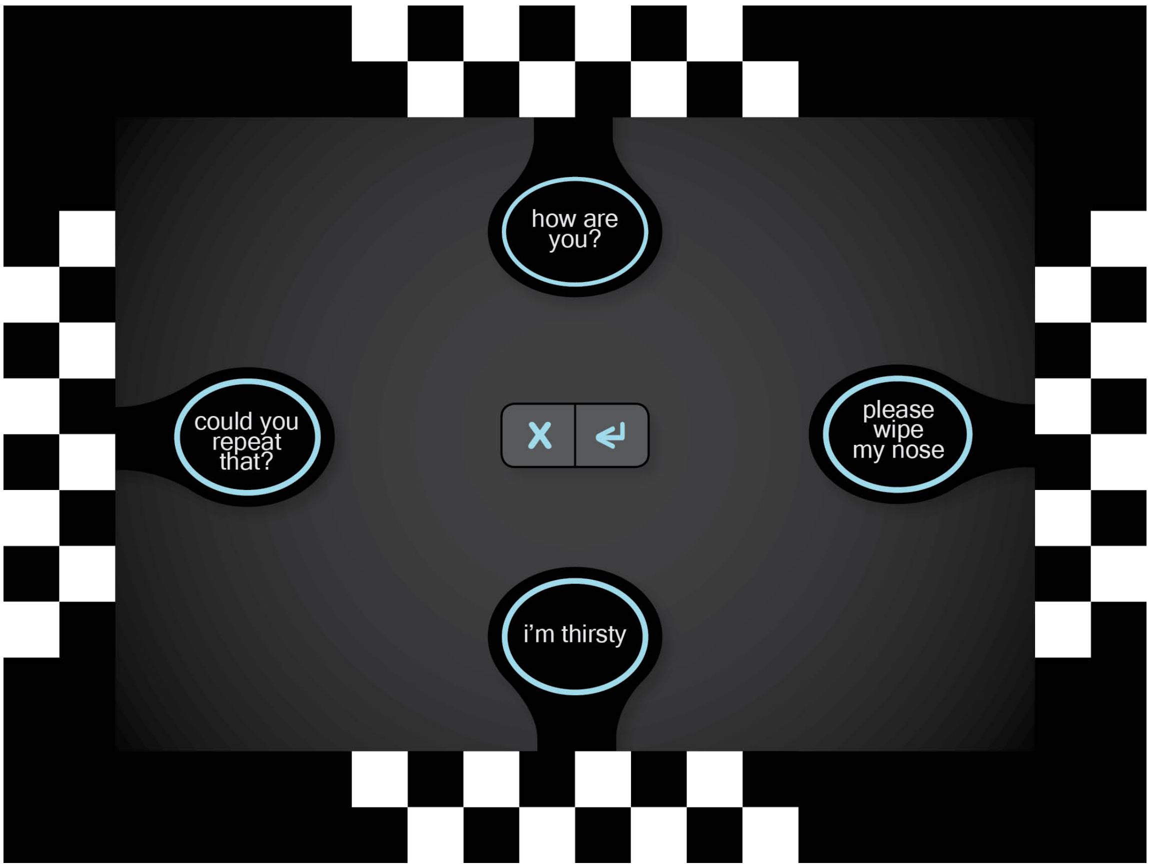

Figure 5-5. The original four-choice phrase prediction user interface. Users can select using the SSVEP BCI from one of four predicted phrases, or use alpha wave-based selection in the middle to either turn the system off "X" or select from a more grid of phrases using the back arrow.

Another problem was finding the appropriate phrases that matched certain context-specific scenarios. We asked caregivers of severely motor-impaired individuals to fill out an online form that inquired what their loved one or patient might want to say in certain situations such as “At Home in the Morning” or “At the Hospital in front of the Doctor”. This task proved difficult for most caregivers since the range of phrases their loved one would want to choose from didn’t match just one category. Thus, creating a phrase corpus specific to ALS or LIS users became a nearly impossible task that was eventually abandoned.

The next approach taken was to predict one letter, word, phrase or sentence at a time in a progressive fashion, allowing the user to select at which point in the prediction chain to stop and begin a new BCI choice. **Figure 5-6** shows the complete model comprising the user interface, NLP algorithms, and sensor acquisition and processing. The left side of the diagram shows the user interface with the current prediction shown at the top and the grid of choices below it. The four colors in the prediction output area are as follows:

- **WHITE** for the user-selected letter;
- **RED** for the Next Letter prediction;
- **BLUE** for the Full Word prediction of the currently spelled word; and
- **GREEN** for prediction of the Next Word.

If the user approves of the next letter, the “NL Ok” can be picked, whereas “FW Ok” for full word and “NW Ok” for next word predictions can be made in order to speed up navigation through the grid.

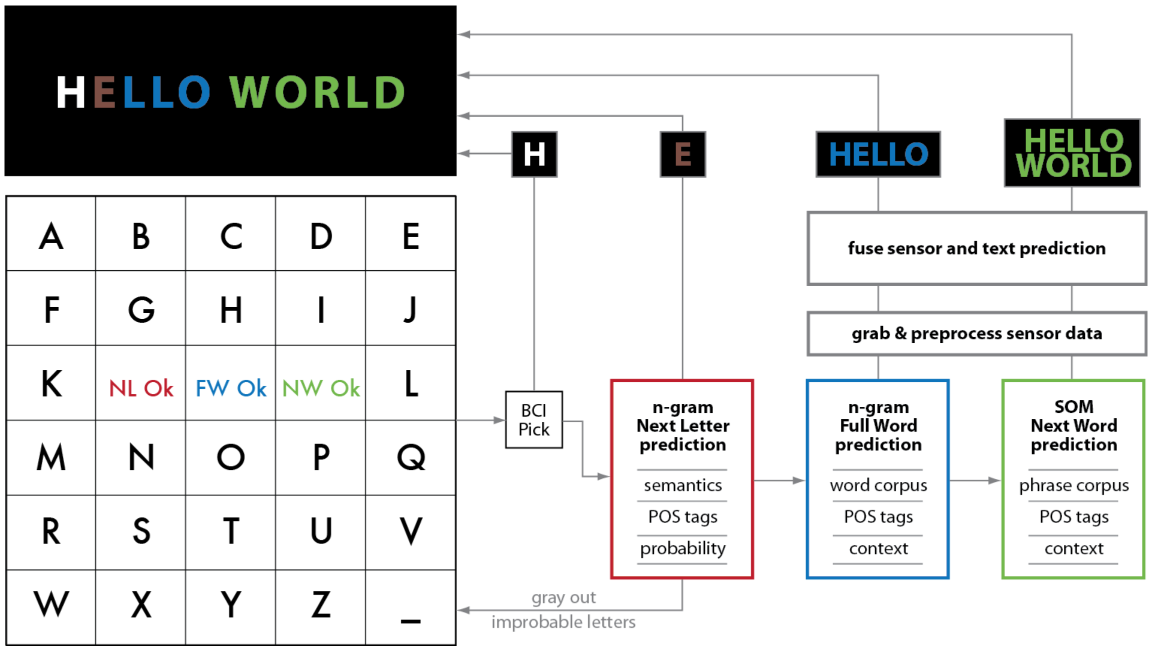

Figure 5-6. Context-based communication app model. A basic concept of the GUI is represented on the left, with NLP units shown in the bottom right. Full word and next word predictions then feed into all available sensors before fusing and modifying prediction before sending output to the screen.

To begin the process, a user selects a letter via the BCI. This letter is fed to the n-gram model for next letter prediction, the details of which are discussed in Section 5.4.2. After a next letter is chosen, all improbable letters are then grayed out, making it easier for users to skip over any letters that would not get picked. For example, after “H” and “E” are displayed, the letters “G”, “Q”, “Z”, etc. would turn gray. If the cursor resets to “FW Ok” after each selection, and the user wanted to navigate to “A” next, the cursor would skip over the “G” after discrete movements towards the “A”. One potential issue with this method is that improbable but correct next letter choices cannot be selected in this particular framework. Simple considerations like this can reduce time-to-target, a necessary feature when each move can take several seconds. Once a BCI letter selection is made, this selection then triggers the available sensors to start processing any data in their buffers since the last selection.

Next, the full word and next word n-gram predictions are made in parallel before sending their outputs to the sensor fusion stage. If the user's camera is turned on and sees a familiar face via the facial recognition algorithm, then the name of the identified person is paired with the next letter/word outputs to hone the estimates based on contextual information. The same pairing process holds true for the GPS, speech-to-text, and clock system inputs..

As an example of an everyday scenario, say an SSVEP-based ContextSpeak user is at home in the morning and his mother says "Good morning." In this situation, the user might want to respond with "Hello, Mom." To do so, first the SSVEP system is turned on (possibly with an alpha/eye blink combination), and then a BCI selection of "H" is made. This is where the NLP algorithms begin their predictions in order to find likely outputs. If facial recognition, GPS location, time of day, and speech-to-text are all on and receiving sensor data, an array consisting of `[mom, home, morning, 'good morning']` would be created. This array will help to make more robust NLP outputs for both the full word and next word predictions due to heavy weighting of context-specific options. For example, should "Hello" be chosen as the first word, a natural next choice could easily have been

"Dad" yet the introduction of context-specific cues makes this choice less probable because Mom is standing right there, not Dad.

As for the GUI, **Figure 5-7** shows a preliminary design that maximizes the space for display of the letter selections along with the currently spelled output. Unlike traditional AAC device applications, no drop-down menus or nested lists are used here; rather, the focus is on communicating effectively and masking the intelligent user interface processing underneath. Obviously use of SSVEP takes up a significant amount of space, yet this could change were LEDs used in future versions. To the right of the currently spelled output is an icon that lets the user speak the finished phrase or sentence via a specified binary selection mechanism such as eye blinks or alpha detection.

For purposes of this dissertation, the NLP algorithms and sensor input processing details (discussed further in Sections 5.4.2) were both implemented separately in Python, but were not fused together. These algorithms were also not fully integrated into GridSpeak using the GUI shown in **Figure 5-6** via the Unlock Project API. Fusing these elements together into a working GridSpeak app that can be refined with user feedback represents a future direction work in progress.

Figure 5-7. The ContextSpeak communication app GUI for an SSVEP-based BCI. The current cursor position is shown with a black key and white text.

5.4.2 IUI Algorithm Description

Natural language processing

Natural language understanding by a computer has been a fruitful research area encompassing the fields of computer science and linguistics, among others for over 60 years (Bates 1995). We take for granted the numerous NLP algorithms running in our word processors, text messages, and Internet searches. Most NLP systems today attempt to tackle one or more of the following issues: *lexicon* selection and/or reduction (Qiu et al. 2011), *syntax*, (Solan et al. 2005), *semantics* (Royer et al. 2010; Farahat and Kamel 2011; Zheng, Kang, and Kim 2009), and *discourse/pragmatics* (Neuper et al. 2009; Cristea, Postolache, and Pistol 2005). Each of these issues has rendered highly interesting results, and pieces of each problem have been addressed using the somewhat simple, yet very robust *n*-gram model.

N-gram models, a commonly used class of NLP models, are used for everything from "tab complete" sentence prediction (Birbaumer 2006; Bickel, Haider, and Scheffer 2005) to determining whether or not a sentence is worthy of "that's what she said" status (Kiddon and Brun 2011). In order to complete such NLP tasks, we need to estimate the probability of a string of words that are presented as input to a noisy channel (Brown et al. 1992). Particularly, in an *n*-gram model two probability histories are treated equally if they end in the same n – 1 words. This assumes that for $k \geq n$, $\Pr\left(w_k \mid w_1^{k-1}\right)$ is equal to $\Pr\left(w_k \mid w_{k-n+1}^{k-1}\right)$ where w is a string of word (or letters) within a corpus. The parameters for an *n*-gram model are determined during a training run in a predetermined text corpus, commonly using a statistical technique known as sequential maximum likelihood estimation. In general an *n*-gram of size 1 is known as a unigram, size 2 *n*-gram a bigram, size 3 *n*-gram a trigram and so on.

For the model shown in **Figure 5-6**, an *n*-gram of size 4 was sufficient to predict realistic sentences. Python's Natural Language Toolkit (NLTK) is a powerful package that includes an *n*-gram model class with a number of feature options (Brumberg et al. 2010; Loper 2004; Bird, Klein, and Loper 2009). Two separate *n*-gram models were trained on the commonly used Brown corpus[8] – one for letter prediction in the Next Letter module and one for word prediction used in the Full Word and Next Word modules. Preprocessing techniques such as part-of-speech tagging were performed in order to associate a part of speech with every word in the corpus. For example, the word "cool" can be tagged as a noun, verb or adjective. The part-of-speech tagger looks at the use of each word in the context of the words before and after it. Different string smoothing parameters were also tested according to recommendations by Chen and Goodman (Chen and Goodman 1996).

One important problem in NLP is the choice of corpus. Depending on the target application and the training text corpus, results of an *n*-gram model algorithm will vary dramatically. For example, let's say you want to create a website that helps physics students find the right forum answer to their problem. Training an NLP model with text from 50 sports blogs will assuredly find worse matches than a model trained on physics textbook inputs. Rather than use a generic set of text input sentences such as the Brown Corpus, an attempt was made to find corpora more specific to words, phrases, and sentences employed more frequently by AAC users (Iida and Campbell 2001; Vertanen and Kristensson 2011; Patel 2007). The corpus created by Vertanen and Kristensson used Amazon's Mechanical

---

[8] http://icame.uib.no/brown/bcm.html

Turk service[9] to enlist hundreds of random individuals to create a fictional collection of AAC phrases. Their corpus was available online and was used as a comparison case against the Brown corpus; unfortunately, the AAC corpus model proliferated far more nonsensical sentence structures than those in the Brown training model. Having looked at the raw AAC corpus data, it was clear that many of the "mechanical turks" did not take the task seriously and simply wrote gibberish sentences in order to get paid. Another issue is that, unless actual AAC users or caregivers create the corpus, it is doubtful that such a corpus could be considered accurate.

Sensor processing

Figure 5-6 only illustrates sensor data as an abstract input module, yet for prototyping purposes, algorithms for *facial recognition*, *speech-to-text translation*, *geolocation*, and *time of day* were implemented. For facial recognition, the Python interface for OpenCV, a highly popular code library focused primarily on real-time computer vision, was used. Specifically, the Haar Feature-based Cascade Classifier for Object Detection OpenCV function[10] was used to train on a database of human frontal view faces. Using a built-in laptop camera, the algorithm was easily able to detect and track multiple faces within its field of view. Once a face is detected, it

[9] https://www.mturk.com/mturk

[10] http://opencv.willowgarage.com/documentation/python/objdetect_cascade_classification.html

then captures an image of the face and compares it to a database of previously stored faces – or "favorites". If the cross correlation of the captured and a stored image is above a certain threshold value, it results in a match. Thus, if mom walks in the room, the facial recognition algorithm will detect and capture an image of her face then compare it to the stored favorites of [dad, mom, nurse] and output "mom".

For speech-to-text translation, the `speech` package for Python was chosen[11]. Unfortunately, this particular package only runs on Windows machines due to its integration with the Microsoft Speech Kit; however, other cross-platform software such as Dragon[12] could used in future versions. The implementation here turns on the speech listener when the program starts, then translates any human speech it picks up over the laptop audio input port. The translated speech is converted to a string that can be used as a feature vector input to the system.

Geolocation on a laptop is a somewhat more difficult task since one would need an external GPS device in order to get proper latitude-longitude coordinates. If a wifi network is available on the laptop, a workaround is possible. First, the Google Maps API[13] allows developers to write JavaScript code within an HTML page to get geolocation coordinates. Unfortunately, the latitude and longitude JavaScript outputs do not translate easily to Python, so other methods were tested. Currently, the geolocation algorithm determines the laptop user's public IP address, and then

---

[11] http://pypi.python.org/pypi/speech/
[12] http://www.nuance.com/for-developers/dragon/index.htm
[13] https://developers.google.com/maps/

gets geolocation information from an open-source database of stored IP address locations at hostip.info. Once the latitude-longitude coordinates are found, they are compared to a “favorite locations” list set by the user. If the current geolocation is within a small enough range of one of the stored favorites, then the BCI system chooses that location from the list and prints the output.

Lastly, time of day was used as another sensor input to the system. Currently, only the current day of the week and current hour are used as feature vector, yet other time information such as month, season or year could be used. Knowing time-based information is often relevant. Discussions of breakfast, for example, usually take place in the morning, and discussions about the weather are dependent on what season it currently is.

5.5 Future Directions in Context-Dependent BCIs

Once we have a number of preprocessed sensor features, one of the more difficult tasks entails knowing how to merge this data with natural language processing outputs to better refine text prediction. As was mentioned in the previous section, fusing sensor and NLP data was not performed for this dissertation, yet executing this task is vital and far from trivial.

The ContextSpeak prototype discussed above barely scratches the surface of what context-aware computing can offer to both BCI- *and* VOCA-based human-computer interactions. Apple’s Siri and Android’s Robin smartphone applications are indicative of where next-generation technology is heading. As processing power increases on smaller devices, the ability to find correlations among numerous sensors, app data, and user inputs will become commonplace. Context-aware integration will allow users to weed away the chaff of data overload, focusing instead on information they need more quickly and discovering possible new items of interest based on current location and past preferences.

Context-dependent BCIs should consider other content such as calendar schedule details, Yelp favorite restaurants, Netflix queue info, prior sentence selections based on available sensor configurations, etc. With regards to ContextSpeak, in particular, building a corpus specific to severely motor-impaired individuals is tantamount in importance to creating context-based outputs. As more ContextSpeak users add to the database of selected words, phrases and sentences, better predictions can be made across all users.

6 Conclusion

This dissertation presented research that led to creation of a fully mobile SSVEP-based BCI for severely motor-impaired individuals. Furthermore, a novel approach to moving beyond bit-rates in BCI accuracies by adding intelligent user interface principles was discussed as a future direction for development of fast, robust BCI-driven VOCAs. Lastly, an experiment was performed, for both healthy and paralyzed participants, testing the portable BCI developed in this dissertation. The results of this experiment helped shape theoretical design of a communication app, ContextSpeak, for The Unlock Project and provided insight into modifications required for creation of a more robust in-home SSVEP-based BCI.

In Chapter 2, an introduction to the field of BCI as a whole was provided. First, invasive recording methods, such as the Utah Array and ECoG, as well as common BCI-related invasive paradigms performed were discussed. Advantages and disadvantages of invasive BCIs were compared to noninvasive approaches such as EEG, fNIRS or MEG, recording techniques that exchange signal to noise ratio (in the form of noisier neural signals) for ease of use. Next, noninvasive EEG activations used in BCI research –such as the P300 evoked response, motor imagery, and SSVEP – were discussed in detail in order to get a landscape for BCI paradigms currently being explored. EEG hardware that could be used for practical BCI applications was then discussed along with BCI software tested in this dissertation, the culmination of which was the Neural Prosthesis lab's creation of The Unlock Project API for quick BCI app building.

This broad BCI overview was narrowed to focus on SSVEP-based BCI research and methods in Chapter 3. In order to better understand what SSVEPs are and how they are generated, a brief history of psychophysical SSVEP studies was given along with an overview of the human visual system and how it processes visual evoked potentials flashing at repetitive intervals, i.e. in a steady state. In order to generate maximal SSVEP responses, SSVEP stimulus presentation parameters such as size, color, spatial frequency, flicker frequency, shape, and hardware optimization are discussed. Preliminary results testing all of these variations showed that choice of flicker frequency and stimulus checkerboard shape can influence power spectral density harmonics in unique ways. After stimulus creation was discussed, analysis methods including spatial localization, artifact detection and removal, feature extraction and selection, classification options, and false positive reduction were compared in the SSVEP BCI literature. This chapter concluded by comparing time- and frequency-based models, giving a thorough quantitative description of harmonic sum decision in particular.

Chapter 4 sought to compile the information discussed in the prior two chapters by testing a fully portable SSVEP-based BCI using a four-choice system. The primary goal of The Unlock Project is to provide a fully functional BCI system to severely motor-impaired users, thus five paralyzed participants from Boston, MA and Duluth, GA willingly tested our BCI. The data collected from these five participants were compared to fourteen healthy controls in order to gain an understanding of how well the system performed for each user group. Before running the four-choice SSVEP BCI task, users completed a frequency calibration run in order to find which four (of ten) frequencies were optimal for each individual. The results of this study also demonstrated that the control group was able to control the SSVEP BCI with far higher classification accuracy than the paralyzed group as a whole. Furthermore, classification accuracies varied drastically among the paralyzed users, with performance seeming to correlate directly with visual attention capacity. Individuals with increasingly impaired vision had a more difficult time controlling the BCI whereas those participants with more robust vision performed similarly to control group users.

Finally, Chapter 5 switched gears completely by discussing practical motivations for development of a context-aware VOCA for severely motor-impaired users built upon the theoretical principles of intelligent user interface design. An overview of the HCI and IUI research fields was given as prerequisite information for creation of any future BCIs targeting in-home application. For this reason a qualitative user summary was concocted based on paralyzed participant feedback from the study performed in Chapter 4. This information was then used to modify an initial context-aware communication app model in order to take into account user needs and concerns. Research on existing VOCA devices using traditional hardware, as well as more recent tablet apps, were reviewed to provide a feel for what VOCAs currently existed on the market. A GUI mockup for ContextSpeak was then designed based on research conducted across the VOCA market. Lastly, details of constructing sensor data and natural language processing outputs was touched upon within the context of a model that uses information such as time of day, current location, facial recognition, and speech-to-text to make better text prediction outputs for SSVEP-based BCI users.

Now that a fully mobile SSVEP-based BCI, practical BCI development framework, and intelligent user interface model has been created specifically for the purposes of helping severely speech- and motor-impaired individuals, there are a few primary factors that need to be addressed next. First, SSVEP accuracies need to be boosted for these individuals in a way that makes the app usable on a day-to-day routine. Exploration of LED options that use the CCA algorithm, adding better confidence measures, creating a BCI hybrid model to take advantage of any remaining motor control such as eye blinks (or another BCI paradigm altogether), or simply selecting frequencies that a particular user responds best to are just a few improvements that can be made to the system.

Second, in ContextSpeak, processed sensor information such as facial recognition, geolocation, and speech-to-text needs to be fused with natural language processing model outputs in order to refine potential speech predictions for the user. Getting to this point requires a more user-centric database of existing phrases pertinent to severely motor-impaired users. Building such a database of words, phrases, and sentences will take time and effort; this information can begin to be amassed by ContextSpeak users once they've been able to interact with the app on a daily basis. Once a large enough set of word databases is correlated with sensor data, prior decisions can also be integrated into the system along with adaptive natural language processing algorithms that learn to output a word or phrase based on past observations. Doing so may reduce communication output time by orders of magnitude in order to move beyond BCI accuracies and bit-rates towards applied, practical use of a BCI using context from the world around us.

The results from Chapter 4 proved that there is still a long way to go in developing a practical SSVEP-based BCI that could be used by severely motor-impaired individuals, yet progress has been made in development of a portable system that could be used in homes in the near future. No matter what the end BCI product may be, it should be clear from the research discussed here that classification rates are only the beginning of practical BCI creation. Taking into account user interaction with a BCI device, feedback from these users, and adding context-aware computing to the mix will quicken app development for severely speech- and motor-impaired individuals hoping to communicate with the outside world once again.

APPENDIX A

CONTEXT-SPECIFIC LIS SPEECH PHRASE CORPUS

Locked-In Speech Phrase Survey

Below are 36 speaking scenarios that have up to three different conditions: 1) the time of day, 2) the person being addressed, and 3) geographical location. For each scenario, list AT LEAST 3 speech phrases that someone without speech capabilities would wish to say in that particular situation. Be sure to hit the RETURN button for each new speech phrase. For example, the "Morning" scenario might have the following phrases: I am hungry. Good morning. How are you today? etc. Let's begin! Be sure to hit the SUBMIT button when you reach the bottom.

* Required

Enter your first and last name: *

1.

Morning. *

2. Morning.
Family. *

3. Morning.
Caretaker. *

4. Morning.
Home. *

5. Morning. Doctor's
Office. *

6. Morning. Family.
Home. *

7. Morning. Family. Doctor's Office. *

8. Morning. Caretaker. Home. *

9. Morning. Caretaker. Doctor's Office. *

10. Afternoon. *

11. Afternoon.
Family. *

12. Afternoon.
Caretaker. *

13. Afternoon.
Home. *

14. Afternoon. Doctor's
Office. *

15. Afternoon. Family.
Home. *

16. Afternoon. Family. Doctor's Office. *

17. Afternoon. Caretaker. Home. *

18. Afternoon. Caretaker. Doctor's Office. *

19. Evening. *

20. Evening.

Family. *

21. Evening.

Caretaker. *

22. Evening.

Home. *

23. Evening. Doctor's

Office. *

24. Evening. Family.

Home. *

25. Evening. Family. Doctor's
Office. *

26. Evening. Caretaker.
Home. *

27. Evening. Caretaker. Doctor's
Office. *

28.
Night *

29. Night.

Family *

30. Night.

Caretaker. *

31. Night.

Home. *

32. Night. Doctor's

Office. *

33. Night. Family.

Home. *

34. Night. Family. Doctor's Office. *

35. Night. Caretaker. Home. *

36. Night. Caretaker. Doctor's Office. *

REFERENCES

Bakardjian, Hovagim, Toshihisa Tanaka, and Andrzej Cichocki. 2010. “Optimization of SSVEP Brain Responses with Application to Eight-Command Brain-Computer Interface..” *Neuroscience Letters* 469 (1) (January 18): 34–38. doi:10.1016/j.neulet.2009.11.039.

Bashashati, Ali, Mehrdad Fatourechi, Rabab K Ward, and Gary E Birch. 2007. “A Survey of Signal Processing Algorithms in Brain-Computer Interfaces Based on Electrical Brain Signals.” *Journal of Neural Engineering* 4 (2) (June 1): R32–57. doi:10.1088/1741-2560/4/2/R03.

Bates, M. 1995. “Models of Natural Language Understanding..” *Proceedings of the National Academy of Sciences of the United States of America* 92 (22) (October 24): 9977–9982.

Beukelman, David R, Susan Fager, Laura Ball, and Aimee Dietz. 2007. “AAC for Adults with Acquired Neurological Conditions: a Review..” *Augmentative and Alternative Communication* 23 (3) (September): 230–242. doi:10.1080/07434610701553668.

Beukelman, David, Susan Fager, and Amy Nordness. 2011. “Communication Support for People with ALS..” *Neurology Research International* 2011: 714693. doi:10.1155/2011/714693.

Bickel, S., P. Haider, and T. Scheffer. 2005. “Predicting Sentences Using N-Gram Language Models.” *Proceedings of the Conference on Human Language Technology and Empirical Methods in Natural Language Processing*: 193–200.

Bin, Guangyu, Xiaorong Gao, Y Wang, B Hong, and Shangkai Gao. 2009. “VEP-Based Brain-Computer Interfaces: Time, Frequency, and Code Modulations [Research Frontier].” *Computational Intelligence Magazine, IEEE* 4 (4): 22–26.

Bin, Guangyu, Xiaorong Gao, Yijun Wang, Yun Li, Bo Hong, and Shangkai Gao. 2011. “A High-Speed BCI Based on Code Modulation VEP..” *Journal of Neural Engineering* 8 (2) (April): 025015. doi:10.1088/1741-2560/8/2/025015.

Bin, Guangyu, Xiaorong Gao, Zheng Yan, Bo Hong, and Shangkai Gao. 2009. “An Online Multi-Channel SSVEP-Based Brain-Computer Interface Using a Canonical Correlation Analysis Method..” *Journal of Neural Engineering* 6 (4) (August): 046002. doi:10.1088/1741-2560/6/4/046002.

Birbaumer, Niels. 2006. “Breaking the Silence: Brain-Computer Interfaces (BCI) for Communication and Motor Control.” *Psychophysiology* 43 (6) (November 1): 517–532. doi:10.1111/j.1469-8986.2006.00456.x.

Birbaumer, Niels, and Leonardo G Cohen. 2007. “Brain-Computer Interfaces: Communication and Restoration of Movement in Paralysis..” *The Journal of Physiology* 579 (Pt 3) (March 15): 621–636. doi:10.1113/jphysiol.2006.125633.

Bird, Steven, Ewan Klein, and Edward Loper. 2009. *Natural Language Processing with Python*. Sebastopol, CA: O'Reilly Media, Inc.

Boly, Melanie, Christophe Phillips, Evelyne Balteau, Caroline Schnakers, Christian Degueldre, Gustave Moonen, Andre Luxen, et al. 2008. “Consciousness and

Cerebral Baseline Activity Fluctuations." *Human Brain Mapping* 29 (7) (July 1): 868–874. doi:10.1002/hbm.20602.

Brown, P.F., P.V. Desouza, R.L. Mercer, V.J.D. Pietra, and J.C. Lai. 1992. "Class-Based N-Gram Models of Natural Language." *Computational Linguistics* 18 (4): 467–479.

Brumberg, J, A Nieto-Castanon, P Kennedy, and Frank H Guenther. 2010. "Brain-Computer Interfaces for Speech Communication." *Speech Communication* 52 (January 1): 367–379.

Brumberg, J, and Frank H Guenther. 2010. "Development of Speech Prostheses: Current Status and Recent Advances.." *Expert Review of Medical Devices* 7 (5) (September): 667–679. doi:10.1586/erd.10.34.

Brunner, C, B Z Allison, C Altstätter, and Christa Neuper. 2011. "A Comparison of Three Brain-Computer Interfaces Based on Event-Related Desynchronization, Steady State Visual Evoked Potentials, or a Hybrid Approach Using Both Signals.." *Journal of Neural Engineering* 8 (2) (March 24): 025010. doi:10.1088/1741-2560/8/2/025010.

Brunner, P, S Joshi, S Briskin, Jonathan R Wolpaw, H Bischof, and G Schalk. 2010. "Does the 'P300' Speller Depend on Eye Gaze?." *Journal of Neural Engineering* 7 (5) (October 1): 056013. doi:10.1088/1741-2560/7/5/056013.

Cecotti, Hubert, I Volosyak, and A Graser. 2010. "Reliable Visual Stimuli on LCD Screens for SSVEP Based BCI." *18th European Signal Processing Conference (EUSIPCO-2010)*.

Chadwick, E K, D Blana, J D Simeral, J Lambrecht, S P Kim, A S Cornwell, D M Taylor, L R Hochberg, J P Donoghue, and R F Kirsch. 2011. "Continuous Neuronal Ensemble Control of Simulated Arm Reaching by a Human with Tetraplegia.." *Journal of Neural Engineering* 8 (3) (June): 034003. doi:10.1088/1741-2560/8/3/034003.

Chen, S.F., and J. Goodman. 1996. "An Empirical Study of Smoothing Techniques for Language Modeling." *Proceedings of the 34th Annual Meeting on Association for Computational Linguistics*: 310–318.

Cheng, M, Xiaorong Gao, Shangkai Gao, and D Xu. 2001. "Multiple Color Stimulus Induced Steady State Visual Evoked Potentials." In, 2:1012–1014. doi:10.1109/IEMBS.2001.1020359.

Chin, JP, VA Diehl, and KL Norman. 1988. "Development of an Instrument Measuring User Satisfaction of the Human-Computer Interface." *CHI '88 Conference Proceedings: Human Factors in Computing Systems*.

Clark, V.P., and S Hillyard. 1996. "Spatial Selective Attention Affects Early Extrastriate but Not Striate Components of the Visual Evoked Potential." *Journal of Cognitive Neuroscience* 8 (5): 387–402.

Coyle, Shirley, Tomás Ward, Charles Markham, and Gary McDarby. 2004. "On the Suitability of Near-Infrared (NIR) Systems for Next-Generation Brain-Computer Interfaces.." *Physiological Measurement* 25 (4) (August): 815–822.

Cristea, D., O. Postolache, and I. Pistol. 2005. "Summarisation Through Discourse

Structure." *Computational Linguistics and Intelligent Text Processing*: 632–644.

Davidson, RJ, DC Jackson, and CL Larson. 2000. "Human Electroencephalography." In *Handbook of Psychophysiology*, ed. GG Bernston, LG Tassinary, and JT Cacioppo, 27–52. Cambridge: Cambridge University Press.

Di Russo, Francesco, Sabrina Pitzalis, Teresa Aprile, Grazia Spitoni, Fabiana Patria, Alessandra Stella, Donatella Spinelli, and Steven A Hillyard. 2007. "Spatiotemporal Analysis of the Cortical Sources of the Steady-State Visual Evoked Potential.." *Human Brain Mapping* 28 (4) (April): 323–334. doi:10.1002/hbm.20276.

Dieters, E I, S H Hidding, M Kalisvaart, and E G Mik. 2011. "Near Infrared Spectroscopy: an Asset to the Diagnosis and Treatment of Traumatic Brain Injury." *Erasmus Journal of Medicine* 1 (2) (January 13).

Diez, Pablo F, Vicente A Mut, Enrique M Avila Perona, and Eric Laciar Leber. 2011. "Asynchronous BCI Control Using High-Frequency SSVEP.." *Journal of Neuroengineering and Rehabilitation* 8: 39. doi:10.1186/1743-0003-8-39.

Dominowska, E, D Roy, and Rupal Patel. 2002. "An Adaptive Context-Sensitive Communication Aid." In, 1–4. Proceedings of the 17th Annual International ….

Farahat, A.K., and M.S Kamel. 2011. "Statistical Semantics for Enhancing Document Clustering." *Knowledge and Information Systems* 28 (2): 365–393. doi:10.1007/s10115-010-0367-z.

Fazel-Rezai, Reza, Brendan Z Allison, Christoph Guger, Eric W Sellers, Sonja C Kleih, and Andrea Kubler. 2012. "P300 Brain Computer Interface: Current Challenges and Emerging Trends.." *Frontiers in Neuroengineering* 5: 14. doi:10.3389/fneng.2012.00014.

Felleman, D J, and D C Van Essen. 1991. "Distributed Hierarchical Processing in the Primate Cerebral Cortex.." *Cerebral Cortex (New York, NY : 1991)* 1 (1) (January): 1–47.

Fried-Oken, Melanie, Lynn Fox, Marie T Rau, Jill Tullman, Glory Baker, Mary Hindal, Nancy Wile, and Jau-Shin Lou. 2006. "Purposes of AAC Device Use for Persons with ALS as Reported by Caregivers.." *Augmentative and Alternative Communication* 22 (3) (September): 209–221. doi:10.1080/07434610600650276.

Friman, Ola, Ivan Volosyak, and Axel Graser. 2007. "Multiple Channel Detection of Steady-State Visual Evoked Potentials for Brain-Computer Interfaces.." *IEEE Transactions on Bio-Medical Engineering* 54 (4) (April): 742–750. doi:10.1109/TBME.2006.889160.

Garcia-Molina, Gary, and D. Zhu. 2011. "Optimal Spatial Filtering for the Steady State Visual Evoked Potential: BCI Application." *Neural Engineering (NER), 2011 5th International IEEE/EMBS Conference on*: 156–160.

Georgopoulos, A P, A B Schwartz, and R E Kettner. 1986. "Neuronal Population Coding of Movement Direction.." *Science (New York, NY)* 233 (4771) (September 26): 1416–1419.

Georgopoulos, Apostolos P, Frederick J P Langheim, Arthur C Leuthold, and

Alexander N Merkle. 2005. “Magnetoencephalographic Signals Predict Movement Trajectory in Space..” *Experimental Brain Research Experimentelle Hirnforschung Expérimentation Cérébrale* 167 (1) (November): 132–135. doi:10.1007/s00221-005-0028-8.

Glennen, SL, and Denise DeCoste, eds. 1997. *The Handbook of Augmentative and Alternative Communication*. San Diego, CA: Singular Publishing Group, Inc.

Grosse-Wentrup, Moritz, Bernhard Schölkopf, and Jeremy Hill. 2011. “Causal Influence of Gamma Oscillations on the Sensorimotor Rhythm..” *NeuroImage* 56 (2) (May 15): 837–842. doi:10.1016/j.neuroimage.2010.04.265.

Guenther, Frank H, J Brumberg, E Joseph Wright, Alfonso Nieto-Castanon, Jason A Tourville, Mikhail Panko, Robert Law, et al. 2009. “A Wireless Brain-Machine Interface for Real-Time Speech Synthesis..” *PLoS ONE* 4 (12): e8218. doi:10.1371/journal.pone.0008218.

Guger, Christoph, Gunter Edlinger, and Gunther Krausz. 2011. “Hardware/Software Components and Applications of BCIs.” In *Recent Advances in Brain-Computer Interface Systems*, ed. Reza Fazel-Rezai. InTech.

Haas, L F. 2003. “Hans Berger (1873-1941), Richard Caton (1842-1926), and Electroencephalography..” *Journal of Neurology, Neurosurgery & Psychiatry* 74 (1) (January): 9.

Hakvoort, G, and B Reuderink. 2011. “Comparison of PSDA and CCA Detection Methods in a SSVEP-Based BCI-System.”

Hamadicharef, B. 2010. “AUC Confidence Bounds for Performance Evaluation of Brain-Computer Interface.” In, 5:1988–1991. doi:10.1109/BMEI.2010.5639671.

Hendry, S H, and R C Reid. 2000. “The Koniocellular Pathway in Primate Vision..” *Annual Review of Neuroscience* 23: 127–153. doi:10.1146/annurev.neuro.23.1.127.

Iida, A., and N. Campbell. 2001. “A Database Design for a Concatenative Speech Synthesis System for the Disabled.” *4th ISCA Tutorial and Research Workshop (ITRW) on Speech Synthesis*.

Jia, Chuan, Xiaorong Gao, Bo Hong, and Shangkai Gao. 2011. “Frequency and Phase Mixed Coding in SSVEP-Based Brain--Computer Interface..” *IEEE Transactions on Bio-Medical Engineering* 58 (1) (January): 200–206. doi:10.1109/TBME.2010.2068571.

Kellis, Spencer, Kai J Miller, Kyle Thomson, Richard Brown, Paul House, and Bradley Greger. 2010. “Decoding Spoken Words Using Local Field Potentials Recorded From the Cortical Surface.” *Journal of Neural Engineering* 7 (5) (September 1): 056007. doi:10.1088/1741-2560/7/5/056007.

Kiddon, C, and Y. Brun. 2011. “That’S What She Said: Double Entendre Identification.” *Proceedings of the 49th Annual Meeting of the Association for Computational Linguistics: Human Language Technologies*: 89–94.

Kim, SP, JD Simeral, Leigh R Hochberg, John P Donoghue, Gerhard M Friehs, and MJ Black. 2007. “Multi-State Decoding of Point-and-Click Control Signals From Motor Cortical Activity in a Human with Tetraplegia.” *Neural Engineering, 2007.*

CNE '07. 3rd International IEEE/EMBS Conference on: 486–489.
Krusienski, Dean J, and Jonathan R Wolpaw. 2009. "Brain-Computer Interface Research at the Wadsworth Center Developments in Noninvasive Communication and Control.." *International Review of Neurobiology* 86: 147–157. doi:10.1016/S0074-7742(09)86011-X.
Krusienski, Dean J, E W Sellers, Dennis J McFarland, T M Vaughan, and Jonathan R Wolpaw. 2008. "Toward Enhanced P300 Speller Performance." *Journal of Neuroscience Methods* 167 (1) (January 15): 15–21. doi:10.1016/j.jneumeth.2007.07.017.
Kubler, Andrea, and Klaus-Robert Müller. 2007. "An Introduction to Brain-Computer Interfacing." In *Toward Brain-Computer Interfacing*, ed. Guido Dornhege, José del R Millán, Thilo Hinterberger, Dennis J McFarland, and Klaus-Robert Müller, 1–27. The MIT Press.
Li, Yun, Guangyu Bin, Bo Hong, and Xiaorong Gao. 2010. "A Coded VEP Method to Measure Interhemispheric Transfer Time (IHTT).." *Neuroscience Letters* 472 (2) (March 19): 123–127. doi:10.1016/j.neulet.2010.01.069.
Lin, Zhonglin, Changshui Zhang, Wei Wu, and Xiaorong Gao. 2007. "Frequency Recognition Based on Canonical Correlation Analysis for SSVEP-Based BCIs." *IEEE Trans Biomed Eng* 54 (6): 1172–1176. doi:10.1109/TBME.2006.889197.
Loper, E. 2004. "NLTK: Building a Pedagogical Toolkit in Python." *PyCon DC 2004*.
Lopez Jaquero, V., F Montero, J P Molina, and P. Gonzalez. 2009. "Intelligent User Interfaces: Past, Present and Future." In *Engineering the User Interface*, ed. M Redondo, C Bravo, and M Ortega. Springer London.
Lopez-Gordo, M A, A Prieto, F Pelayo, and C Morillas. 2011. "Customized Stimulation Enhances Performance of Independent Binary SSVEP-BCIs.." *Clinical Neurophysiology : Official Journal of the International Federation of Clinical Neurophysiology* 122 (1) (January): 128–133. doi:10.1016/j.clinph.2010.05.021.
Luo, An, and Thomas J Sullivan. 2010. "A User-Friendly SSVEP-Based Brain-Computer Interface Using a Time-Domain Classifier.." *Journal of Neural Engineering* 7 (2) (April): 26010. doi:10.1088/1741-2560/7/2/026010.
Maybury, M. 1999. "Intelligent User Interfaces: an Introduction." *IUI '99 Proceedings of the 4th International Conference on Intelligent User Interfaces*.
Maynard, E M, C T Nordhausen, and R A Normann. 1997. "The Utah Intracortical Electrode Array: a Recording Structure for Potential Brain-Computer Interfaces.." *Electroencephalography and Clinical Neurophysiology* 102 (3) (March): 228–239.
McFarland, Dennis J, L M McCane, S V David, and Jonathan R Wolpaw. 1997. "Spatial Filter Selection for EEG-Based Communication." *Electroencephalography and Clinical Neurophysiology* 103 (3) (September 1): 386–394.
Millán, J D R, R Rupp, Gernot R Müller-Putz, R Murray-Smith, C Giugliemma, M Tangermann, C Vidaurre, et al. 2010. "Combining Brain-Computer Interfaces and Assistive Technologies: State-of-the-Art and Challenges." *Frontiers in*

Neuroscience 4 (January 1). doi:10.3389/fnins.2010.00161.
Miller, Kai J, S Zanos, E E Fetz, M den Nijs, and J G Ojemann. 2009. “Decoupling the Cortical Power Spectrum Reveals Real-Time Representation of Individual Finger Movements in Humans..” *Journal of Neuroscience* 29 (10) (March 11): 3132–3137. doi:10.1523/JNEUROSCI.5506-08.2009.
Moratti, Stephan, Brett A Clementz, Yuan Gao, Tomás Ortiz, and Andreas Keil. 2007. “Neural Mechanisms of Evoked Oscillations: Stability and Interaction with Transient Events..” *Human Brain Mapping* 28 (12) (December): 1318–1333. doi:10.1002/hbm.20342.
Morgan, S T, J C Hansen, and S Hillyard. 1996. “Selective Attention to Stimulus Location Modulates the Steady-State Visual Evoked Potential..” *Proceedings of the National Academy of Sciences of the United States of America* 93 (10) (May 14): 4770–4774.
Müller-Putz, Gernot R, Evelin Eder, Selina C Wriessnegger, and Gert Pfurtscheller. 2008. “Comparison of DFT and Lock-in Amplifier Features and Search for Optimal Electrode Positions in SSVEP-Based BCI..” *Journal of Neuroscience Methods* 168 (1) (February 15): 174–181. doi:10.1016/j.jneumeth.2007.09.024.
Müller-Putz, Gernot R, Reinhold Scherer, Christian Brauneis, and Gert Pfurtscheller. 2005. “Steady-State Visual Evoked Potential (SSVEP)-Based Communication: Impact of Harmonic Frequency Components..” *Journal of Neural Engineering* 2 (4) (December): 123–130. doi:10.1088/1741-2560/2/4/008.
Neuper, Christa, Reinhold Scherer, Selina Wriessnegger, and Gert Pfurtscheller. 2009. “Motor Imagery and Action Observation: Modulation of Sensorimotor Brain Rhythms During Mental Control of a Brain-Computer Interface..” *Clinical Neurophysiology : Official Journal of the International Federation of Clinical Neurophysiology* 120 (2) (February): 239–247. doi:10.1016/j.clinph.2008.11.015.
Parini, Sergio, Luca Maggi, Anna C Turconi, and Giuseppe Andreoni. 2009. “A Robust and Self-Paced BCI System Based on a Four Class SSVEP Paradigm: Algorithms and Protocols for a High-Transfer-Rate Direct Brain Communication..” *Computational Intelligence and Neuroscience*: 864564. doi:10.1155/2009/864564.
Parry, N R, I J Murray, and C Hadjizenonos. 1999. “Spatio-Temporal Tuning of VEPs: Effect of Mode of Stimulation..” *Vision Research* 39 (21) (October): 3491–3497.
Patel, Rupal. 1998. “Teachable Interfaces for Individuals with Dysarthric Speech and Severe Physical Disabilities.” In.
Patel, Rupal. 2007. “Enhancing Access to Situational Vocabulary by Leveraging Geographic Context.” *Assistive Technology Outcomes and Benefits*.
Pfurtscheller, Gert, Brendan Z Allison, Clemens Brunner, Gunther Bauernfeind, Teodoro Solis-Escalante, Reinhold Scherer, Thorsten O Zander, Gernot Mueller-Putz, Christa Neuper, and Niels Birbaumer. 2010. “The Hybrid BCI..” *Frontiers in Neuroscience* 4: 30. doi:10.3389/fnpro.2010.00003.
Pollen, Daniel A. 1999. “On the Neural Correlates of Visual Perception.” *Cerebral*

Cortex (New York, NY : 1991) 9 (1) (January 1): 4–19.
Qiu, Qinru, Qing Wu, D.J Burns, M.J Moore, R.E Pino, M Bishop, and R.W Linderman. 2011. "Confabulation Based Sentence Completion for Machine Reading." *Computational Intelligence, Cognitive Algorithms, Mind, and Brain (CCMB), 2011 IEEE Symposium on*: 1–8. doi:10.1109/CCMB.2011.5952109.
Ray, Supratim, Nathan E Crone, Ernst Niebur, Piotr J Franaszczuk, and Steven S Hsiao. 2008. "Neural Correlates of High-Gamma Oscillations (60-200 Hz) in Macaque Local Field Potentials and Their Potential Implications in Electrocorticography.." *Journal of Neuroscience* 28 (45) (November 5): 11526–11536. doi:10.1523/JNEUROSCI.2848-08.2008.
Regan, D. 1966. "Some Characteristics of Average Steady-State and Transient Responses Evoked by Modulated Light.." *Electroencephalography and Clinical Neurophysiology* 20 (3) (March): 238–248.
Reich, Gabriele. 2005. "Near-Infrared Spectroscopy and Imaging: Basic Principles and Pharmaceutical Applications.." *Advanced Drug Delivery Reviews* 57 (8) (June 15): 1109–1143. doi:10.1016/j.addr.2005.01.020.
Renard, Yann, Fabien Lotte, Guillaume Gibert, Marco Congedo, Emmanuel Maby, Vincent Delannoy, Olivier Bertrand, and Anatole Lécuyer. 2010. "OpenViBE: an Open-Source Software Platform to Design, Test, and Use Brain–Computer Interfaces in Real and Virtual Environments." *Http://Dx.Doi.org/10.1162/Pres.19.1.35*.
Royer, A, A Doud, M Rose, and B He. 2010. "EEG Control of a Virtual Helicopter in 3-Dimensional Space Using Intelligent Control Strategies." *Neural Systems and Rehabilitation Engineering, IEEE Transactions on* PP (99): 1–1.
Schalk, Gerwin, Dennis J McFarland, Thilo Hinterberger, Niels Birbaumer, and Jonathan R Wolpaw. 2004. "BCI2000: a General-Purpose Brain-Computer Interface (BCI) System.." *IEEE Transactions on Bio-Medical Engineering* 51 (6) (June): 1034–1043. doi:10.1109/TBME.2004.827072.
Schilit, B, N Adams, and Roy Want. 1994. "Context-Aware Computing Applications." *… Systems and Applications*.
Schlosser, Ralf W, and Oliver Wendt. 2008. "Effects of Augmentative and Alternative Communication Intervention on Speech Production in Children with Autism: a Systematic Review.." *American Journal of Speech-Language Pathology / American Speech-Language-Hearing Association* 17 (3) (August): 212–230. doi:10.1044/1058-0360(2008/021).
Sellers, Eric W, Dean J Krusienski, Dennis J McFarland, Theresa M Vaughan, and Jonathan R Wolpaw. 2006. "A P300 Event-Related Potential Brain-Computer Interface (BCI): the Effects of Matrix Size and Inter Stimulus Interval on Performance.." *Biological Psychology* 73 (3) (October): 242–252. doi:10.1016/j.biopsycho.2006.04.007.
Sitaram, Ranganatha, Andrea Caria, Ralf Veit, Tilman Gaber, Giuseppina Rota, Andrea Kuebler, and Niels Birbaumer. 2007. "FMRI Brain-Computer Interface: a Tool for Neuroscientific Research and Treatment.." *Computational Intelligence*

and Neuroscience: 25487. doi:10.1155/2007/25487.

Slotnick, S D, S A Klein, T Carney, E Sutter, and S Dastmalchi. 1999. "Using Multi-Stimulus VEP Source Localization to Obtain a Retinotopic Map of Human Primary Visual Cortex.." *Clinical Neurophysiology : Official Journal of the International Federation of Clinical Neurophysiology* 110 (10) (September 1): 1793–1800.

Solan, Zach, David Horn, Eytan Ruppin, and Shimon Edelman. 2005. "Unsupervised Learning of Natural Languages.." *Proceedings of the National Academy of Sciences of the United States of America* 102 (33) (August 16): 11629–11634. doi:10.1073/pnas.0409746102.

Srinivasan, R. 1999. "Methods to Improve the Spatial Resolution of EEG." *International Journal of Bioelectromagnetism* 1 (1): 102–111.

Srinivasan, Ramesh, F Alouani Bibi, and Paul L Nunez. 2006. "Steady-State Visual Evoked Potentials: Distributed Local Sources and Wave-Like Dynamics Are Sensitive to Flicker Frequency.." *Brain Topography* 18 (3): 167–187. doi:10.1007/s10548-006-0267-4.

Strasburger, H., I J Murray, and A. Remky. 1993. "Sustained and Transient Mechanisms in the Steady-State Visual Evoked Potential: Onset Presentation Compared to Pattern Reversal." *Clinical Vision Sciences* 8: 211–211.

Sutter, E. 1992. "The Brain Response Interface: Communication Through Visually-Induced Electrical Brain Responses." *Journal of Microcomputer Applications* 15 (1): 31–45.

Turner, J N, W Shain, D H Szarowski, M Andersen, S Martins, M Isaacson, and H Craighead. 1999. "Cerebral Astrocyte Response to Micromachined Silicon Implants.." *Experimental Neurology* 156 (1) (March): 33–49. doi:10.1006/exnr.1998.6983.

Vanacker, Gerolf, José del R Millán, Eileen Lew, Pierre W Ferrez, Ferran Galán Moles, Johan Philips, Hendrik Van Brussel, and Marnix Nuttin. 2007. "Context-Based Filtering for Assisted Brain-Actuated Wheelchair Driving.." *Computational Intelligence and Neuroscience*: 25130. doi:10.1155/2007/25130.

Vasquez, Pablo Martinez, H Bakardjian, and M Vallverdu. 2008. "Fast Multi-Command SSVEP Brain Machine Interface Without Training." *Artificial Neural Networks ….*

Vaughan, Theresa M, Dennis J McFarland, Gerwin Schalk, William A Sarnacki, Dean J Krusienski, Eric W Sellers, and Jonathan R Wolpaw. 2006. "The Wadsworth BCI Research and Development Program: at Home with BCI.." *IEEE Transactions on Neural Systems and Rehabilitation Engineering : a Publication of the IEEE Engineering in Medicine and Biology Society* 14 (2) (June): 229–233. doi:10.1109/TNSRE.2006.875577.

Vertanen, K., and P.O. Kristensson. 2011. "The Imagination of Crowds: Conversational AAC Language Modeling Using Crowdsourcing and Large Data Sources." *Proceedings of the Conference on Empirical Methods in Natural Language Processing*: 700–711.

Vialatte, François-Benoît, Monique Maurice, Justin Dauwels, and Andrzej Cichocki. 2010. "Steady-State Visually Evoked Potentials: Focus on Essential Paradigms and Future Perspectives.." *Progress in Neurobiology* 90 (4) (April): 418–438. doi:10.1016/j.pneurobio.2009.11.005.

Vidal, J.J. 1977. "Real-Time Detection of Brain Events in EEG." In, 65:633–641. doi:10.1109/PROC.1977.10542.

Vidaurre, Carmen, Claudia Sannelli, Klaus-Robert Müller, and Benjamin Blankertz. 2011. "Co-Adaptive Calibration to Improve BCI Efficiency.." *Journal of Neural Engineering* 8 (2) (April): 025009. doi:10.1088/1741-2560/8/2/025009.

Voytek, Bradley, Lavi Secundo, Aurelie Bidet-Caulet, Donatella Scabini, Shirley I Stiver, Alisa D Gean, Geoffrey T Manley, and Robert T Knight. 2009. "Hemicraniectomy: a New Model for Human Electrophysiology with High Spatio-Temporal Resolution." *Journal of Cognitive Neuroscience* (November 19). doi:10.1162/jocn.2009.21384.

Völlm, Birgit A, Alexander N W Taylor, Paul Richardson, Rhiannon Corcoran, John Stirling, Shane McKie, John F W Deakin, and Rebecca Elliott. 2006. "Neuronal Correlates of Theory of Mind and Empathy: a Functional Magnetic Resonance Imaging Study in a Nonverbal Task." *NeuroImage* 29 (1) (January 1): 90–98. doi:10.1016/j.neuroimage.2005.07.022.

Wallace, Sarah E, Karen Hux, and David R Beukelman. 2010. "Navigation of a Dynamic Screen AAC Interface by Survivors of Severe Traumatic Brain Injury.." *Augmentative and Alternative Communication* 26 (4) (December): 242–254. doi:10.3109/07434618.2010.521895.

Wang, Y, Y T Wang, and T-P Jung. 2010. "Visual Stimulus Design for High-Rate SSVEP BCI." *Electronics Letters* 46 (15): 1057–1058. doi:10.1049/el.2010.0923.

Wennberg, R, F Quesney, A Olivier, and T Rasmussen. 1998. "Electrocorticography and Outcome in Frontal Lobe Epilepsy.." *Electroencephalography and Clinical Neurophysiology* 106 (4) (April): 357–368.

Wolpaw, Jonathan R, and Dennis J McFarland. 2004. "Control of a Two-Dimensional Movement Signal by a Noninvasive Brain-Computer Interface in Humans." *Proceedings of the National Academy of Sciences of the United States of America* 101 (51) (December 21): 17849–17854. doi:10.1073/pnas.0403504101.

Wolpaw, Jonathan R, Dennis J McFarland, and T M Vaughan. 2000. "Brain-Computer Interface Research at the Wadsworth Center.." *IEEE Transactions on Rehabilitation Engineering : a Publication of the IEEE Engineering in Medicine and Biology Society* 8 (2) (June): 222–226.

Wolpaw, Jonathan R, Niels Birbaumer, Dennis J McFarland, Gert Pfurtscheller, and Theresa M Vaughan. 2002. "Brain-Computer Interfaces for Communication and Control." *Clinical Neurophysiology : Official Journal of the International Federation of Clinical Neurophysiology* 113 (6) (June 1): 767–791.

Xu, Peng, Ping Yang, Xu Lei, and Dezhong Yao. 2011. "An Enhanced Probabilistic LDA for Multi-Class Brain Computer Interface.." *PLoS ONE* 6 (1): e14634. doi:10.1371/journal.pone.0014634.

Zhang, Zimu, Xiuquan Li, and Zhidong Deng. 2010. "A CWT-Based SSVEP Classification Method for Brain-Computer Interface System." In, 43–48. doi:10.1109/ICICIP.2010.5564336.

Zheng, H.T., B.Y. Kang, and H.G. Kim. 2009. "Exploiting Noun Phrases and Semantic Relationships for Text Document Clustering." *Information Sciences* 179 (13): 2249–2262.

Zhu, Danhua, Jordi Bieger, Gary Garcia-Molina, and Ronald M Aarts. 2010. "A Survey of Stimulation Methods Used in SSVEP-Based BCIs.." *Computational Intelligence and Neuroscience*: 702357. doi:10.1155/2010/702357.

CURRICULUM VITAE

Sean Lorenz

Department of Cognitive Neural Systems
Boston University
677 Beacon Street, Boston, MA 02215
email: lorenz@neurala.com
web: http://neurala.com
cell: 617 256 0026

EDUCATION

PhD, Cognitive and Neural Systems
Boston University, Boston, Massachusetts, 2007-2013
Dr. Frank Guenther, advisor
Thesis entitled: "Development of a Practical and Mobile Brain-Computer Communication Device for Profoundly Paralyzed Individuals"

Masters in Theological Studies in Science, Philosophy & Religion
Boston University, Boston, Massachusetts, 2005-2007
Thesis entitled: "Global Workspace Theory and Synthetic Phenomenology"

Bachelor of Arts in Religion & Philosophy
Oral Roberts University, Tulsa, Oklahoma, 1994-1998

RESEARCH EXPERIENCE

2012 **The Unlock Project, Boston University**
Managed undergraduates and graduate students involved in creation of apps and algorithms.

2010-2012 **Doctoral Research, Boston University**
Working to build an adaptive EEG-enabled brain-computer user interface for locked-in syndrome patients.

02/2010-12/2010 **Doctoral Research, Boston University**
Investigated use of structural equation model and fMRI for comparing control to autism group analysis.

WORK EXPERIENCE

July 2009-present Neurala – *Chief Design Officer*
Work to develop massively parallel, brain-based algorithms for various government, private company, and technology applications.

2008 Introduction to Computational Models of Brain and Behavior, Boston University
Helped develop course lab materials and assignments for a new undergraduate course.

2008-2009 Center of Excellence for Learning in Education, Science, and Technology (CELEST) Project, Boston University
Created and maintained an extensive online, database-driven computational modeling code and paper repository/website.

2003-2008 Four Yard Media – *Founder* of graphic design firm.

2001-2003 The Mishra Group – *Public Relations Executive* for Boston-based tech firms.

POSTERS

1. "Adaptive tablet application design for a mobile EEG brain-computer interface." 8th Annual Conference and Expo on Emerging Technologies for a Smarter World, 2011. Long Island, NY.
2. "Adaptive tablet application design for a mobile EEG brain-computer interface." MIT Sloan BioInnovations 2012. Cambridge, MA.
3. "Adaptive tablet application design for a mobile EEG brain-computer interface." Boston University Science & Engineering Day, 2012. Boston, MA.
4. "Adaptive tablet application design for a mobile EEG brain-computer interface." BU CTSI's Third Annual Translational Research Symposium. Boston, MA.

PUBLICATIONS

1. Brumberg, Jonathan, Sean Lorenz, Byron Galbraith, Frank Guenther. 2012. "The Unlock Project: A Python-Based Framework for Practical Brain-Computer Interface Communication 'app' Development." *Proceedings of the 2012 Annual International Conference of the IEEE Engineering in Medicine andBiology Society (EMBC 2012)*. San Diego, California.

2. Lorenz, S., Ames, H., Versace, M. (2010). "Consciousness & Neuromorphic Chips: a case for embodiment." *Proceedings of the 2010 Interdisciplinary Graduate Conference on Consciousness*. Boston, Massachusetts.

AWARDS

1. BCI 2010 Conference Student Scholarship
2. Winner of "Most Disruptive" award at the 2012 Hacking Medicine @ MIT Conference for the ParkinSync startup company
3. Won 2nd place poster award at MIT Sloan BioInnovations conference
4. Won best poster award for "Neural Technology" at the BU Science & Engineering Day
5. Chosen to present research in the BU Research Showcase at BIO 2012.

SKILLS

- Knowledge of computer programming languages (in order of expertise): MATLAB & Simulink, Python, C++, Qt
- Academic software: AFNI, SPSS, LISREL, OpenVibe, Psychtoolbox, Amos
- Business software: Microsoft (Word, Excel, PowerPoint, Visual Studio)
- Design software: Adobe (Photoshop, Illustrator, InDesign, Acrobat, Dreamweaver, Flash, Premiere), AutoDesk Combustion, Final Cut Pro
- Web software/development: PHP, ExpressionEngine, MySQL, HTML, CSS